THE OLFACTORY SYSTEM OF THE EMBRYONIC COMMON CUTTLEFISH, *SEPIA OFFICINALIS*

by

Alexia Scaros

Submitted in partial fulfilment of the requirements

for the degree of Master of Science

at

Dalhousie University

Halifax, Nova Scotia

August 2017

This thesis is dedicated to Stephen.

Table of Contents

List of Tables

List of Figures

Abstract

Olfactory systems across the animal kingdom have several inter-phyletic similarities, such as glomeruli, which have been well studied in some vertebrates and arthropods. Comparisons in a third taxon, such as the large-brained cephalopods, could help to elucidate the evolution of these commonalities. I used immunohistochemistry and *in situ* hybridization on embryos of *Sepia officinalis*, the common cuttlefish, to map the organization of their olfactory system. I first demonstrated that histamine is a neurotransmitter in a class of olfactory sensory neurons by examining staining from anti-histamine and a custom histidine decarboxylase mRNA probe. To update classic descriptions of the cephalopod brain, I used antibodies and riboprobes against FMRFamide, serotonin, APGWamide, acetylated α-tubulin, and synaptotagmin, in addition to structural stains including phalloidin and DiI. My findings cast doubt upon the hypothetical presence of glomeruli in all molluscs and clarify our understanding of how the sense of olfaction evolved.

List of Abbreviations and Symbols Used

α	alpha
α-tubulin	alpha-tubulin
AcTub	acetylated α-tubulin
°	degree
%	percent
µL	microliter
µm	micrometer
5-HT	serotonin
AP	alkaline phosphatase
APGWa	APGWamide
BB	blocking buffer
BCIP	5-bromo-4-chloro-30-indolyphosphate p-toluidine salt
BLAST	basic local alignment search tool
BLASTn	BLAST protein to translated nucleotide
BLASTp	BLAST protein
BLASTx	BLAST translated nucleotide to protein
BOREA	Biologie des Organismes et Ecosystemes Aquatiques
BSA	bovine serum albumin

cDNA	complementary DNA
C	Celsius
CNRS	Center National de la Recherche Scientifique
CNS	central nervous system
CUBIC	clear, unobstructed brain/body imaging cocktails and computational analysis
DAB	3,3′-diaminobenzidine
DAPI	4',6-diamidino-2-phenylindole
DIG	digoxigen
DiI	(2Z)-2-[(E)-3-(3,3-dimethyl-1-octadecylindol-1-ium-2-yl) prop-2-enylidene]-3,3-dimethyl-1-octadecylindole; perchlorate
DEPC	diethyl pyrocarbonate
dH_2O	distilled water
DMSO	dimethyl sulfoxide
DNA	deoxyribonucleic acid
EDAC	1-ethyl-3(3-dimethyl-aminopropyl)-carbodiimide
EDTA	ethylenediaminetetraacetic acid

EMBL-EBI	European Molecular Biology Laboratory-European Bioinformatics Institute
F-actin	filamentous actin
FMRFa	FMRFamide (Phe-Met-Arg-Phe)
FaRPs	FMRFamide-related peptides
GABA	gamma-Aminobutyric acid
GPCR	G-protein coupled receptor
GnRH	gonadotropin-releasing hormone
GR	granular cells
H_2O	dihydrogen monoxide
HA	histamine
HDC	histidine decarboxylase
hr	hour
IRD	Institut de Recherche pour le Developpement France
IR	ionotropic receptor
ISH	*in situ* hybridization
LIR	like immunoreactivity
LOT	lateral olfactory tract

LNs	local interneurons
M	mole
MABT	maleic acid buffer containing Tween 20
min	minute
mL	milliliter
mM	millimole
M/T	mitral and tufted (neuron)
MNHN	Museum National d'Histoire Naturelle
mRNA	messenger RNA
nm	nanometer
NCBI	National Center for Biotechnology Information
NSERC	Natural Sciences and Engineering Research Council of Canada
OB	olfactory bulb
OE	olfactory epithelium
OSN	olfactory sensory neurons
OR	olfactory receptor
PBS	phosphate buffer saline

PBS-Tx	phosphate buffer saline with Triton X-100
PCR	polymerase chain reaction
PFA	paraformaldehyde
PG	periglomerular cells
PTW	PBS with 1% Tween 20
PNs	projection neurons
RNA	ribonucleic acid
RNase	ribonuclease
sec	second
SDS	sodium dodecyl sulfate
SSC	sodium chloride/sodium citrate
tRNA	transfer RNA
TRIS	tris(hydroxymethyl)aminomethane
UV	ultraviolet
wt%	% by weight
wt/vol	weight/volume %

Glossary

Definitions and interpretations from Nixon and Young (2003).

Anterior basal lobe- Lies along the anterior border of the optic tract; part of the motor control pathway.

Dorsal-basal lobe- Composes the posterior region of the supraesophageal mass; maintains complex connectivity, including input from the olfactory and optic lobes.

Dorsal-lateral lobe- A small lobe separated from the dorsal-basal lobe by the optic commissure is part of the posterior basal region. It is continuous with olfactory lobule one.

Inferior frontal lobe- Important in the control of attack behavior; next to the supraesophageal mass and vertical lobes.

Lateral-basal lobe- A slight swellings on the posterior face of the supraesophageal mass; neuropil is continuous with the basal mass; control muscles of chromatophores and skin.

Magnocellular lobe- Far lateral lobes thought to be part of the ancestral cephalopod nervous system; interconnect with almost all other parts of the brain and are responsible for protective and defensive actions.

Medial-basal- Part of the posterior basal region of the supraesophageal mass; confluent with the lateral-basal lobe.

Olfactory lobe- A lateral extension of the posterior basal lobes; composed of three lobules (posterior, middle, anterior, or lobule one, two, and three respectively).

Olfactory nerve- Connects the olfactory organ to olfactory lobule one.

Optic commissure- Also known as the optic tract; contains dorso-lateral lobe, olfactory lobe, peduncle lobe, and optic gland.

Optic gland- Lateral to the dorsal-lateral lobe on the dorsal surface of the olfactory lobe; assumed to be an endocrine organ and is heavily associated with reproduction and olfaction.

Optic lobe- Visual information from the eye is passed through the optic nerve to the optic lobe. Forms most of the total brain volume.

Palliovisceral- Thought to control mantle contractions through the stellate ganglion; interconnects with many other lobes.

Peduncle commissure- Also known as the olfactory commissure; it is disproportionately large compared to the lobe.

Peduncle lobe- Found between the optic lobe and olfactory lobe along the optic tract; receives input from the optic lobes and projects to motor areas including the supraesophageal mass and pedal lobes. Thought to be analogous to the cerebellum of vertebrates.

Posterior magnocellular- Lateral to the palliovisceral lobe; controls jet propulsion.

Posterior pedal lobe- A lateral region of the oculomotor center; dorsal to the magnocellular lobe; most likely responsible for the direction of swimming by regulating positioning of the funnel.

Subesophageal mass- The ventral brain mass below the esophagus; contains palliovisceral mass, chromatophore, pedal, fin, and funnel lobes.

Subpedunculate- Found above the medial-basal lobe; receives input from the optic nerve.

Superior frontal lobe- Forms as a band across the supraesophageal mass; important for the control of attack behavior.

Supraesophageal mass- Dorsal brain mass above the esophagus; laterally connected to the optic lobes via the optic tract; contains the basal-lobes, pericommissural lobes, sub-pedunculate lobes, and vertical lobe system.

Vertical- Important for the establishment of visual and tactile memories in coleioids. Receives input from the superior frontal lobe.

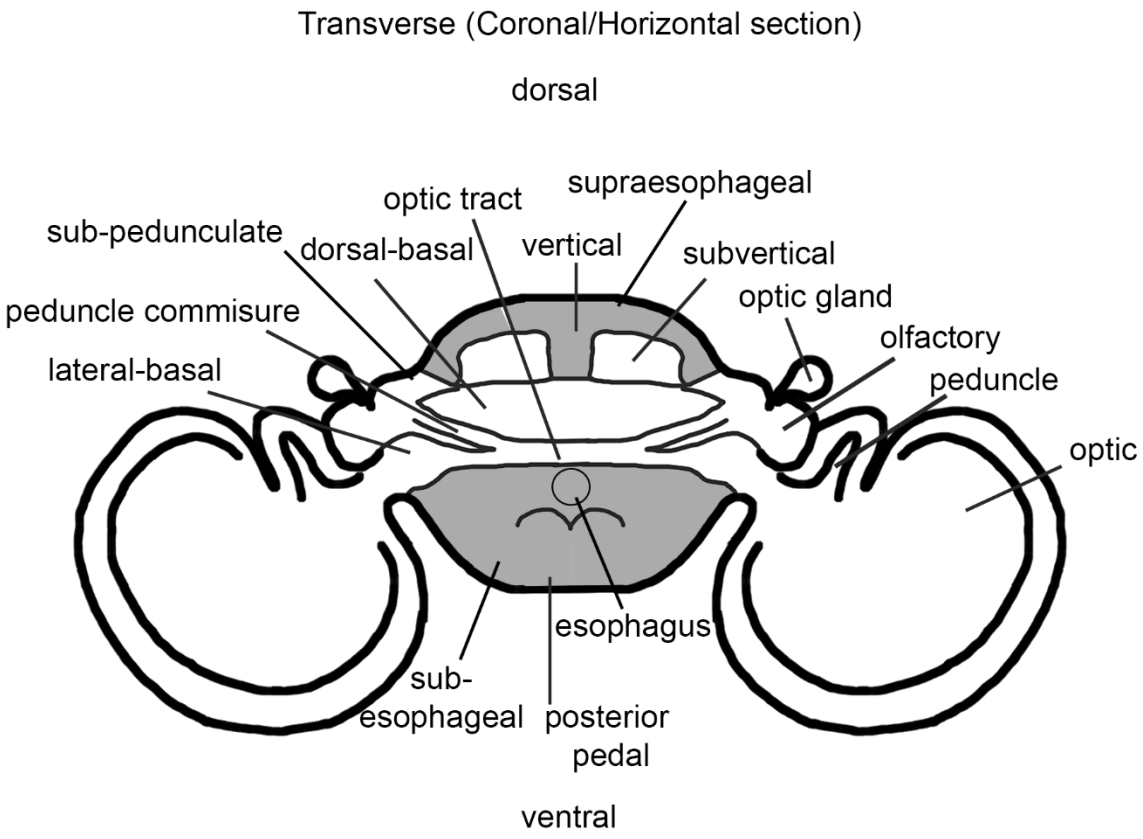

Acknowledgements

First, I would like to thank the organizations and programs that funded my research, including the Natural Sciences and Engineering Research Council of Canada, Laboratoire Biologie des Organismes et Ecosystemes Aquatiques in Paris (CNRS UMR 7208, MNHN, IRD 207, UPMC), the France Canada Research Fund (2013), the Mitacs Globalink Research Program for funding my stay in Paris (2015), the province of Nova Scotia for the Graduate Scholarship (2017), and Dalhousie University for the International Differential Fee Scholarship (2017).

I would also like to thank Dalhousie University for providing the opportunity to work within this amazing program. In addition, I would like to thank the wonderful faculty, staff, and technicians that I interacted with for their help, patience, and guidance.

I am so grateful to the BOREA team in Paris for hosting me for six months to learn *in situ* hybridization, cryosection techniques, and the French language. Particularly Drs. Aude Andouche, Laure Bonnaud, Yann Bassaglia; and Boudjema Imarazene and Antoine Rio-Cabello. Of course, a special thank you also goes to our hosts at La Station Marine de Concarneau for accepting us back year after year, particularly Drs. Stephanie Auzoux-Bordenave and Aicha Badou for their welcoming hospitality.

I owe another thank you to my fellow lab members, particularly Jillian Doyle, Neil Merovitch, Arnaud Gaudin, Griffin Beach, Matt Stoyek, and all the undergraduate volunteers whose comradery and advice always made me look forward to going to the lab.

I am so unbelievably lucky to have had the best supervisory committee, Drs. Alex Quinn, Paivi Torkkeli, and Shelley Adamo. I owe them a huge thank you for all their time, guidance, and advice. I would also like to thank my external examiner, Dr. Alan Fine, for agreeing to read and critique my thesis.

Another thank you goes to my parents and my brother for all their love and constant support, and to Stephen, who has loved and supported me every step (and draft) along the way.

Finally, the greatest thanks go to my two supervisors, Drs. Sébastien Baratte and Roger Croll. Their unwavering confidence, constant support, and seemingly endless revisions made this thesis possible. While in thesis publications, it is custom to use the word "I" instead of "we" to describe our results, this project has very much been a team effort. I owe credit and thanks to both Dr. Baratte for continuing the *in situ* hybridization experiments that we started together, and to Dr. Croll for continuing immunohistochemistry and fixation procedure while I was in Paris. I am incredibly fortunate to have had their help and guidance, and I owe them a lifetime of gratitude.

Chapter 1: Introduction

1.1 What is Olfaction?

Chemoreception, the ability to detect and respond to chemical stimuli, is one of the oldest senses and can be found as early in evolutionary history as the prokaryotes in the form of bacterial chemotaxis. Within the animal kingdom, olfaction is defined as the chemosensory modality dedicated to detecting low concentrations of chemical substances, either airborne or dissolved in an aquatic medium, particularly from a distance. It is different than gustation which is classically defined as chemoreception through direct contact with the source. Olfaction has many general trends that are similar across animals. The sense of smell provides important ecological and locational information for beneficial objects, such as food, water, shelter, and mates. Additionally, it allows for the detection and avoidance of poison, fire, predators, and irritants. There are also similar behaviors across the animal kingdom that are linked through olfaction, such as behaviors that allow for the refreshing of sensory inputs in a time-locked intermittent rhythmic manner for odor recognition and discrimination. This is why snakes flick their tongue, moths fan their wings, lobsters flick their antennae, and snails intermittently retract tentacles (Ache and Young, 2005). The same rhythmic patterning can be seen in animals that perceive odorants through respiratory inhalation. For example, mammals sniff and salamanders ventilate their olfactory cavities (Eisthen, 2002). In addition to these behavioral and ecological similarities, olfactory systems throughout most of the animal kingdom share general morphological features. On the macroscopic scale, olfactory systems can be sub-divided into a 1) a sensory epithelium, 2) a projection or nerve pathway, and 3) an olfactory processing center in the central nervous system (CNS).

The olfactory sensory epithelium (OE) is filled with sensory neurons (OSNs) which contain specific odorant receptors. In vertebrates, it is often located in a semi-enclosed pit (e.g nostril), while some arthropods have antennae. The sensory neurons are morphologically similar across all

metazoans; all are bipolar neurons with filamentous (usually ciliary) dendritic terminals. These cilia project into a fluid-filled medium, regardless of aquatic or terrestrial lifestyle, to allow their olfactory binding receptor proteins to encounter the dissolved odorant molecules. Both mammals and insects have large families of olfactory receptors (ORs). In mammals, they are typical G-protein coupled receptors (GPCRs), while insect's major group of ORs are ligand gated ion channels. Insects also have a group of variant receptors that are related to the ionotropic glutamate receptors and named ionotropic receptors (IRs; Benton et al 2009). In general, individual OSNs express the allele for a single odorant receptor gene so that only one receptor type is expressed per OSN, mutually exclusive of the other OR genes, and regulated by a negative feedback expression in the OSN itself. This unique expression pattern has been coined the one-receptor-one-neuron rule, and is almost exclusively unique to olfaction (Eisthen, 2002; Serizawa et al., 2003; Komiyama and Luo, 2006). However, the rule is not universal across all vertebrates. In some fish, such as goldfish (*Carassius auratus)*, two to three odorant receptor genes can be expressed in a large population of OSNs (Speca et al., 1999). Insects also have unusual ORs. In addition to each common OR, there is an additional universal coreceptor, Orco (previously Or83b), which is broadly expressed across the OSNs in insects. Orco is necessary for the ORs to function. As Orco works in conjunction with the ORs, and does not have an independent function, the one-receptor-one-neuron rule holds true in most insects (Carraher et al., 2015). The ORs of insects have a very similar seven trans-membrane GPCR morphology to vertebrates, with one major exception: the receptor is inverted in the cell membrane. Therefore, with the ability to function independently of their intracellular signaling cascade, the superfamily of chemoreceptors in insects is defined as a novel class of membrane protein (Benton, 2015).

From the OSNs, axons bundle together into a peripheral nerve that projects towards the CNS for processing, usually without synapsing until they reach the olfactory center (Carraher et al., 2015), although there are a few exceptions (see Section 5.2).

OSN projections usually terminate in a specific olfactory center in the brain. In vertebrates, the olfactory nerve projects into an olfactory bulb (OB; Figure 1.1), whereas in insects it projects into an antennal lobe. The insect antennal lobe, which is a spherical part of the deutocerebrum, is very similar to the OB of vertebrates (Hansson and Anton, 2000), in that it receives inputs from the OSN of the mouth and antennal parts.

One of the most intriguing similarities in both the vertebrate (particularly mammals, fish, and amphibians), and some arthropod (including insects and crustaceans) olfactory centers is that of the discrete olfactory units, called glomeruli. A glomerulus is a morphological unit defined broadly as a cluster of nerve fibers, spores, or small blood vessels. In olfactory glomeruli, the tangle is composed of OSN axons, along with other neurites and dendrites from second order neurons (depending on the species), that result in a close clustering of synaptic terminals. In mammals, periglomerular interneurons and mitral and tufted neurons both receive synaptic inputs in the glomerulus. In the antennal lobe of insects, interneurons and output neurons receive synaptic inputs in a similar fashion.

Most glomeruli are uniform in size and have a rounded shape encircled by glial cells (Eisthen, 2002; Ache and Young, 2005). They contain the outputs from OSNs and the inputs from periglomerular interneurons and various output cells (Pinching and Powell, 1971; Eisthen, 2002). All the OSNs of a specific receptor or subset of receptors project their axons to the same glomerulus: a principle known as glomerular convergence (Mori et al., 1999; Eisthen, 2002).

Some studies have suggested that vertebrate glomeruli may have sub-regions or compartments in which different OSNs and output neurons interact with different groups of interneurons (Eisthen, 2002). In mammals, some studies have shown OSNs with the same ORs usually converge on a pair of glomeruli in the OB, typically one on the medial surface and one on the lateral surface (Treolar et al., 2010). Each glomerulus is specific and identifiable and will respond to a certain subset of odorants, so that the same odorant molecule will activate the same clusters of glomeruli across individuals of a species. This specificity causes the activation of a unique pattern of glomeruli, thus creating a spatial pattern known as an odor map (Treloar, et al., 2010). In a single glomerular module, one OSN synapses onto a single glomerulus. In the glomeruli, OSNs synapse with mitral and tufted cells that are the excitatory output neurons (Figure 1.2). Olfactory glomeruli also receive feedback information from the cortex and lateral inhibition via two types of interneurons, granule and periglomerular cells (Mori et al., 1999). Lateral inhibition via the local interneurons enhances tuning specificity and increases the discriminatory ability of odorants to the parts-per-billion range in mice and rats (Mori et al., 1999; Treolar et al., 2010).

There has been debate as to whether glomeruli also impart spatial representation in higher brain centers. Even though OSNs are often generally described as randomly distributed throughout the epithelium, there are four zones in which OR genes are expressed within the OE in mammals and three overlapping but concentric zones in zebrafish (Weth et al., 1996; Eisthen, 2002). Each OR type is expressed exclusively in one of the four zones (Mori et al., 1999; Serizawa et al., 2003). OSNs located in the dorsal nasal cavity converge onto glomeruli in the dorsal OB, and ventrally located OSNs converge in the ventral OB (Treloar et al., 2010). Therefore, each of the four zones of the OE is represented in the OB. This arrangement may suggest some degree of spatial mapping at the odorant level within the cortex. In addition, the axons from the second order neurons in the glomeruli may also have distinct branching patterns and terminal areas when projecting to higher

olfactory centers of the brain (Kauer and Moulton, 1974; Mori et al., 1999; Komiyama and Luo, 2006). However, Eisthen (2002) suggests that because glomeruli do not receive topographically-organized afferent input, they are distinguished from other compartments of the brain, like the barrel whiskers of the somatosensory cortex in mice, which are more spatially tuned.

In insects, the antennal lobe lacks the laminar organization that is found in vertebrates and has its neurons peripheral to the neuropil, as is typical in invertebrate ganglia (Blaustein et al., 1988; Hansson, 1995; Wachowiak et al., 1997). The glomeruli of insects are similar in morphology to those found in vertebrates. The neuropil of the antennal lobe is organized into glomeruli where the projection neurons and local interneurons synapse (Ache and Young, 2005). Most of the glomeruli tend to be uniform in size, although the macroglomeruli complex, found in some species of sexually dimorphic insects, is used exclusively for reception of sex pheromone-sensitive ORs and can be enlarged with input from pheromone receptors (Hansson and Anton, 2000). Most species have 40 to 160 individually identifiable glomeruli, although some have as few as 32 (mosquitos) while others have more than 1,000 (locusts). In several insect species, glomeruli are arranged in one or two layers around a central fibrous core. Like the vertebrate olfactory system, subsets of glomeruli all receive input from the same olfactory receptors activated by the same family of odorant molecules. However, unlike vertebral glomeruli that only receive input from the OE, insects can also receive projections from OSNs located on the antennae, maxillary palps, and labial pit organs (Eisthen, 2002).

Both vertebrates and arthropods use the output neurons surrounding the glomeruli to project their now organized input to higher areas of the brain for olfactory learning, identification, and memory. Many scientists have noticed the striking morphological similarities of the OSNs, glomeruli, interneurons, and olfactory brain centers in both vertebrates and insects, and crustaceans,

and have suggested that such similarities represent an optimal solution to detecting and discriminating odors (Figure 1.2; Hildebrand and Shepherd; 1997; Eisthen, 2002; Ache and Young, 2005; Kaupp, 2010). But did this solution evolve early and remain consistent in vertebrates, insects, and crustaceans, or did glomerular olfactory morphology evolve convergently to solve similar problems in two primarily terrestrial animal groups?

These similarities, and many others, led to questions regarding the evolution and physiology of olfaction in other animals. Are there differences in the evolution and development of olfactory systems between major animal groups? Could there be any similarities between all animals? And if so, could these similarities provide insight into the homology or convergent evolution of olfaction?

1.2 Other Potential Means of Organization

Some have taken on the challenge of trying to answer these evolutionary questions by looking at other comparisons between olfactory systems: at the histological level through comparison of structures like filamentous (F-) actin (Rossler et al., 2002), at the physiological level through comparison of oscillations (Kay, 2014), and at the molecular level through comparison of receptors (Eisthen, 2002),

1.2.1 Histological Comparisons

In a comparative study, Rossler et al. (2002) noted that glomeruli across various species of vertebrates and insects were characterized by the presence of F-actin that this could demonstrate the general organization of the glomeruli neuropil. They therefore concluded that phalloidin, which is a marker for F-actin, consistently labels glomeruli in a broad range of species, and is possible evidence of glomeruli in insects, crustaceans, and vertebrates being homologous structures.

1.2.2 Physiological Comparisons

While the glomerular organization may provide spatial coding information, the quality of the stimulus is encoded by the temporal and combinatorial activation of different glomeruli (Mori et al., 1999). Oscillatory field potentials (also known as network oscillations or OB gamma oscillations in vertebrates) are a purely olfactory function that spread in propagating waves of hyperpolarization and depolarization at the first synaptic relay in the olfactory center (Ache and Young, 2005). Oscillations, which are initiated on the transition from inhalation to exhalation, change over the time span of minutes, matching the time it takes to resample the environment, such as in the behavior of sniffing. These oscillations are thought to improve discrimination by separating out neural space to optimize odor memory storage. For example, when two axons of different mitral and tufted cells converge onto the same target neuron in the olfactory cortex, that neuron can detect a combination (amplification or cancelation) of activity from two different glomerular modules. This synchronization increases the probability of activating that particular neuron due to temporal summation. This selective combination of odorant receptors results in recognition of unique odorants. In addition, the strength of the dendrodendritic synaptic connections is thought to be responsible for odor memory.

Network oscillations are also present in some species of arthropods. For example, in locusts, the lateral neurons in the mushroom bodies respond to graded potentials of odors causing oscillations that provide a synchronization of signals to the projection and protocerebral neurons (Hansson and Anton 2000). However, even though evidence suggests that oscillations are an important part of modulating the synchronization of odorant reception, there have been numerous accounts of odor evoked synchrony not being oscillatory or odor specific in insects and crustaceans (Christensen and Hildebrand, 2002).

Oscillatory field potentials have been most studied and described in the molluscs, particularly in the terrestrial slug *Limax Marginatus*. Sensory cells that project to the tentacle ganglion produce oscillating local field potentials that can be modified by odor stimulation (Ito et al., 2000; Kirino et al., 2005; Cummins and Wyeth, 2014). Depending upon the odor memory representation, different patterns of excitation waves travel across the procerebrum creating regularly oscillating local field potentials. While the role of these specific procerebral neurons in olfaction is not exactly clear, they are thought to be a part of odor discrimination and memory in molluscs (Kirino et al., 2005; Cummins and Wyeth, 2014).

1.2.3 Molecular Comparisons

While vertebrates primarily use GPCRs and insects primarily use ionotropic ORs, there is a third group for comparisons, the molluscs. There have been two olfactory receptor GPCRs described in squid to date, the $G\alpha_{olf}$ and $G\alpha_{q,}$ that mediate either the adenylate cyclase and/or phospholipase C pathway respectively (Mobley et al., 2007). It was observed that type II neurons contained $G\alpha_{q}$ while types III-V showed colocalization of $G\alpha_{q}$ with $G\alpha_{olf}$. These receptor locations suggest that type II OSNs primarily utilize the phospholipase C pathway, while types III-V use both olfactory transduction mechanisms.

However, it is important to note that not all molluscs exclusively use GPCRs. A study done on *Aplysia californica* showed that *A. californica* express IR genes in the olfactory organs, called rhinophores, and the oral tentacles (Croset et al., 2010). A novel family of chemoreceptor genes was also discovered in *A. californica* in 2009 and the proteins were identified as rhodopsin-like GPCRs with a phospholipase C signaling pathway (Cummins et al., 2009). These GPCRs do not have any closely related orthologs, and therefore were suggested to be lineage-specific in the chemoreceptor family of bilaterians. Therefore, it seems that molecularly, molluscs have both IR and GPCRs.

1.3 Olfaction in Another Group

Glomeruli have been identified in another phylum closely related to arthropods, the velvet worms (Schurmann, 1995; Eisthen, 2002; Strausfeld et al., 2006). While nematodes such as *Caenorhabditis elegans* lack the ganglia that would contain glomerular-like sensory structures, studies show the evolutionary similarities between ionotropic ORs can be found as far back in evolutionary history as the protostomes (Croset et al., 2010). Therefore, to further investigate these similarities in the olfactory systems, a sister group would have to have an equivalent degree of cephalization and complex brain structures for comparisons.

Cephalopods, as a highly divergent and complex family of mollusc are a perfect phylum for comparisons. They have a complex CNS and olfactory system, sharing many of the neurotransmitters that are also found in vertebrates and arthropods. As direct developers, they skip a larval stage and develop their peripheral sensory systems, including a complete olfactory system, early in their embryonic phase.

1.4 Chemosensory System of Cephalopods

Although they are known for their excellent vision, many cephalopods are partly nocturnal or live at depths where little light is present. Therefore, it is thought that chemoreception may also be important, although this sense is less well studied. The most understood are the contact chemoreception abilities of *Octopus* suckers (Graziadei, 1962; Wells 1963). *Octopus* have the most chemoreceptors in their suckers, while cuttlefish and squid have fewer (Graziadei, 1962; Budelmann, 1996). This physiological difference may be due to behavioral differences, as octopus are known to hunt in rocky crevices using their arms (Hanlon and Messenger, 1998). Using tactile discrimination, it has been observed that octopus can differentiate between seaweed soaked in different solutions, including salt water, hydrochloric acid, sucrose, or quinine (Wells, 1963).

Distance chemoreception abilities of cephalopods were first noticed when *Octopus* responded to "fish juice" being introduced into a tank (Wells, 1963; Messenger, 1967). Since then, several studies have attempted to determine the sensitivity of cephalopod distance chemoreception. Blind octopuses can move toward a stimulatory chemical, following concentration gradients from 10^{-3} to 10^{-6} M (Chase and Wells, 1986). The chemoreceptors in the olfactory pits are sensitive down to 10^{-5} M (Budelmann, 1995). Another study suggested that squid are generally attracted to amino acids and aversive to tetraethylammonium, tetrodotoxin, and squid ink (Mobley et al., 2008).

Olfaction has been suggested to play a role in social communication (Gilly and Lucero, 1992; Boal and Golden, 1999). It has been demonstrated in adult squid, through behavioral studies observing either chemotaxis towards a stimulatory chemical source or via ventilation rates (Mobley et al., 2008; Walderon et al., 2011). In addition, cuttlefish embryos still in the egg capsule can respond to an aversive odorant, demonstrating that the chemosensory system is functional even before hatching. This early development is evidence of the importance of olfaction in the early life stages of these animals (Romagny et al., 2012).

1.4.1 Olfactory Organs and Other Peripheral Sensory Organs

The ciliated cells of the olfactory organs in cephalopods project their axons via an olfactory nerve to the olfactory lobe in the optic tract region (Shigeno and Yamamoto, 2002). *Sepia officinalis,* the common cuttlefish, have two primary chemoreceptive locations: the olfactory organs, for processing odorants (Woodhams and Messenger, 1974; Wildenbourg and Fioroni, 1989), and contact chemosensory cells scattered over the epidermis, particularly in the arms (Graziadei, 1964; Sundermann-Meister, 1978; Boletzky, 1989; Fioroni, 1990; Mackie, 2008; Baratte and Bonnaud, 2009).

The function of the olfactory organ was not discovered until well after the structure was named (Emery, 1975). Up until the 1980s, scientists thought the position of the olfactory organ, the structure of the receptors, and their projection via the olfactory nerve to the brain, suggested a function for detecting sexual pheromones. Then, three studies demonstrated that water-soluble odors (e.g. betaine, glycine, proline, alanine, lactic acid, and serine) could be sensed from a distance by the olfactory organs (Boyle, 1983; Boyle, 1986; Chase and Wells, 1986).

The other suspected location of chemoreception is the suckers of cephalopods. Within the coleoid (squid, cuttlefish, and octopus) arms, sensory cells have a long apical neurite that extends from the cell body, terminating in cilia (Wells et al., 1965; Buresi et al., 2014). These sensory cells have also been described in the rest of the skin of cephalopods, although the exact modality of these cells is still unknown. It is thought that at least some of these cell types mediate contact chemoreception or gustation (Buresi et al., 2014).

The nautiluses, an ancient clade of cephalopods, differ from the coleoids in several major ways. For example, nautiluses have an external shell and digital tentacles without suckers (Barber and Wright, 1969). In addition, the two different types of nautilus digital tentacles have different functions; the four pairs of slender lateral tentacles are used for distance chemoreception, whereas the medial digital tentacles may be contact chemoreceptors (Ruth et al., 2002). They also do not have olfactory organs, but instead have a fleshy, tentacle-like sensory protrusion termed the rhinophore, (Barber and Wright, 1969). The rhinophore has been suggested to be the olfactory sensory organ after studies showed that the sensory cells share similar properties to those found in the olfactory pit of octopus and cuttlefish. Additionally, behavioral experiments showed that nautilus depend on their rhinophores to detect and follow an odorant plume (Basil et al., 2000). As such, the nautilus rhinophore shares many physiological and functional similarities with gastropod tentacles (See

Cummins and Wyeth, 2014 for a comprehensive review of olfaction in gastropods). Because of these differences I will just discuss the olfactory properties of coleoid cephalopods, with occasional comparisons to the differences of *Nautilus*.

1.4.2 Sensory Cell Morphology and Olfactory Receptors

In cephalopods, there are peripheral nerve cells located within the olfactory organ underneath the epidermis and lamina propria, a layer of connective tissue, smooth muscle, axons, and blood vessels (Mobley et al., 2007). There have been five types of described sensory neurons that all seem to have a chemosensory function with the stereotypical elongated shape of an OSN and numerous ciliary tufts that can be observed throughout molluscs (Woodhams and Messenger, 1974; Emery, 1975; 1976; Sundermann-Meister, 1978; Bonar, 1978; Wildenburg and Fioroni, 1989; Budelmann, 1996; Dickinson and Croll, 2003; Kempf and Page, 2005; Mobley et al., 2008; Mackie, 2008; Wyeth and Croll, 2011; Buresi et al., 2014; Polese et al., 2016, see Figure 3.12). Both epithelial cells and sensory neurons have cilia, although the surface of the olfactory organ also has microvilli (Emery, 1975). While the same flask-shaped ciliated cells are present in the nautilus rhinophore and post-ocular tentacles (Barber and Wright, 1969; Ruth et al., 2002), the receptor cells of coleoid cephalopods are more variable and complex than *Nautilus* (Barber and Wright, 1969; Polese et al., 2016). An estimated 34% of the cells in the olfactory organ were OSNs (Mobley et al., 2008). OSNs with cilia (types III-V) make up approximately 20% of the cells within the squid olfactory organ, all with approximately equal representation.

Several odorants have been identified that excite each neuron type in the olfactory organ of *Lolliguncula brevis* (Mobley et al., 2008). They determined that each OSN type had a different sensitivity to the odors tested. For example, type V was the only OSN type to not be activated by alanine, while OSN type III was most sensitive to the odorants tested. While type IV did not

respond to odors, calcium imaging showed that type IV responds to filtered squid ink. Yet while each profile of expression was unique among the different types of OSNs, no reaction was exclusive to a particular type. This exclusivity suggests that different OSN types may express similar odorant receptors.

1.4.3 The Olfactory Lobe

To discuss the morphology of the olfactory lobe, I will briefly describe how cephalopods are oriented. Like other molluscs, cephalopods have an anterior (foot) and posterior (mantle) end in addition to a dorsal (with the cuttlebone) and ventral (with the siphon) side. However, this anatomical morphology can become confusing when considering the functional swimming orientation of adults. Most cuttlefish swim horizontally, with their ventral end down, in an anterior direction (arms first, which is opposite of most squid which swim mantle first). For consistency and clarity, all the cuttlefish diagrams are depicted with the posterior side up when viewing the whole animal, and dorsal side up when viewing sections of the brain. Cephalopod brains are also bilaterally symmetric, so when discussing the olfactory pathway, only one half of the brain is referred to at a time.

Perhaps due to having a large, complex brain, cephalopods have one centralized location for all olfactory inputs: the olfactory lobes. The olfactory lobe is the main terminus of the olfactory nerve, which originates in the olfactory organ (Figure 1.3). The olfactory nerve, which connects the olfactory organ (on the ventral side) to the olfactory lobe (on the dorsal side), projects around the optic lobe to the olfactory lobe, entering posteriorly near the junction between olfactory lobe and the dorsal-lateral lobe, making it difficult to visualize without sectioning. From there, the olfactory nerve disperses into multiple fibrous branches, most terminating in olfactory lobe.

The cephalopod olfactory lobe is described by Messenger in his explanation of the nervous system of *Loligo* (Messenger, 1979). He describes the olfactory lobes as lateral extensions of the posterior basal lobes, shaped like a long tapering tube, and composed of "at least three 'lobules'," which he termed olfactory lobules one, two, and three. The lobe is thickest medially and tapers on the anterior and posterior ends (Figure 1.3 A). Olfactory lobule one is the most dorsal (Figure 1.3 B) and receives input from the olfactory nerve, while olfactory lobules two and three receive inputs from the surrounding lobes. Some fibers from the olfactory nerve may also innervate olfactory lobule two, making this a complex system when describing connections between the olfactory lobes and the other surrounding lobes. Lobule one integrates with the dorsal-basal lobe, while lobules two and three integrate with the optic and peduncle lobes. The olfactory lobe has interactions and connections with the optic, basal, posterior magnocellular, latero-ventral, palliovisceral, dorsal-lateral, dorsal-basal, sub-pedunculate, and lateral-basal lobes. Messenger (1979) describes the neuropil of the olfactory lobe as a "simple, loosely woven meshwork of fibers" that have no consistent orientation (Messenger, 1979, pg. 301). He also describes the three cell types he observes based upon size: the smallest (< 8um), large cells (15-20 μm) and the "very large" cells (>25 μm). The very large cells were found in the lateral wall of olfactory lobule one and not found in any other lobes of the brain. For clarification and ease of understanding, I have included diagrammatic representations of the cuttlefish embryo (stage 30, immediately prior to hatching) and a medial transverse section of the brain (Figure 1.3).

These are some of the most complete descriptions to date, all using Golgi's method silver stain. Yet Messenger (1979, pg. 298) admits, "cells in the olfactory lobe are rarely impregnated after staining by the Golgi method, so little is known of their form…. the axons are not well defined." This admission demonstrates the need for updated methods in these animals.

The sensory systems develop, differentiate, and function very early in organogenesis. In *S. officinalis,* embryos can react to tactile, chemical, and visual stimuli *in ovo* (Darmaillacq et al., 2008; Baratte and Bonnaud, 2009; Romagny et al., 2012). As early as stage 14, in cells in the squid *Sepioteuthis lessoniana* cluster to form the beginnings of the optic, cerebral, visceral, and pedal ganglia (Shigeno et al., 2001a; Shigeno et al., 2001b). Stages 14-20 are considered the placode stages, in which the ectoderm organs develop, and by stage 21 the lobes are ready to begin differentiation (Shigeno et al., 2001b). Embryos can react to the odor of a predator as young as stage 23, although the exact chemoreceptors involved are not yet understood (Romagny et al., 2012). The beginnings of the olfactory system also appear in stage 23 when the olfactory anlagen are observable as a cellular swelling between the supra-esophageal mass and the optic lobe anlagen. By stage 25 the olfactory lobe anlagen is obvious, with an olfactory nerve running from the olfactory organ to the lobe (Shigeno et al., 2001a; Yamamoto et al., 2003). Serotoninergic neurons also differentiate in the olfactory lobe by stage 24 in the pygmy squid *Idiosepius notoides* (Wollesen et al., 2010b). Therefore, I cannot assume the entire system is fully developed by stage 27-30. We do know much of the fundamental structure and organization of the olfactory system is in place, and that the embryos are behaviorally responsive at an early stage of development. This study is the first step in understanding the development of the olfactory system; by starting at late stages and demonstrating the techniques here as a proof of concept, they can later can be applied to earlier stages, hatchlings, and adults.

1.5 Challenges

Despite all previous evidence as to why cephalopods would be an enlightening and valuable study specimen, there have been relatively few neurobiological and physiological studies of these animals. Even with early description of the olfactory organ in 1844, the peripheral sensory neurons were not described until 1974 and the first olfactory receptors were not identified until 2007 (Woodhams and Messenger, 1974; Mobley et al., 2007). Why such a delay in progress in this field?

One reason is that cephalopod specimens are often harder to obtain than classical models like mice or *Drosophila melanogaster*. This scarcity is partly due to cephalopod ecology, with many species being limited to a narrow ecosystem with few easily accessible coastal species (Boyle and Rodhouse, 2008). Seasonality is also an important consideration, particularly for embryonic studies, since many species spawn only once a year during a few short weeks (Laptikhovsky et al., 2003). Due to climate change and other natural phenomena, the spawning aggregations around the world have been variable at best; some cephalopod populations are booming, while others have been observed to miss an entire spawning season altogether. Many cephalopod labs currently run opportunistically, studying whatever species they can get access to at that time. Cephalopod aquaculture and husbandry are developing fields, but with major complications in larval rearing, it is still very challenging to raise cephalopods from egg capsules (Koueta and Boucaud-Camou, 1999).

In 2010, live cephalopods were included in the European Union directive 63 (European Parliament and Council of the European Union, 2010), which protect any cephalopods used in research from "pain, suffering, distress, or lasting harm equivalent to or higher than that caused by the introduction of a needle in accordance with good veterinary practice." This directive introduced cephalopod researchers to the same guidance and restrictions as vertebrate researchers. "Live cephalopods" are now defined as any cephalopod that has hatched from the egg, and this greatly limits the amount of adult physiology able to be performed unless procedures are followed to demonstrate that Article 4, which outlines the principles of "Replacement, Reduction, and Refinement," have been met. While those laboratories outside of the EU are not restricted to the same guidelines, any collaborations with a laboratory in the EU must adhere to these best practices, and in general, most researchers agree with the principles laid out by the directive to do no more harm than necessary. Due to the objectives, I chose to look at the late embryonic stages of *S.*

officinalis (stage 25-hatching), as it meets the requirements of the directive, but also allowed us to work with a functional olfactory system and describe the development.

While I am particularly interested in the cephalopod olfactory system due to its evolutionary differences from the rest of the animal kingdom, this variance also introduces a challenge in selecting commercial antibodies that have the necessary specificity to a molluscan molecular homologue. When working in a molluscan model, there is a limit to the availability of antibodies on the market that are reactive, partially because the market is often concerned with supplying vertebrate researchers. That is not to say that a vertebrate antibody cannot be used in a molluscan model, but special care must be given to ensure specificity. Sequence alignments (if available) must be done before purchasing to ensure the best possible selection is made. Yet even with a close sequence match, a vertebrate antibody will not always work in a molluscan system, despite evidence that a molluscan homologue of that target protein is present. For this reason, immunohistochemistry in molluscan models is challenging, particularly if a laboratory has limited funding available for antibody purchasing or synthesis.

The histological and molecular experiments have also proven exceedingly difficult. Histology in this species and stage of development has especially proven to be challenging due to the thick epidermis of cephalopods, and even thicker cranium. Late stage embryos of *S. officinalis* are too large for many wholemount studies and yet too small for perfusions into the heart. As such, I have spent many years trying to overcome the issue of proper fixation and penetration technique to visualize the brain. What I report here were the final material and methods that succeeded in observing sections of brain tissue with immunohistochemistry and *in situ* hybridization.

Despite these challenges, *S. officinalis* remains a common species for studies in cephalopod physiology. They are more convenient and abundant than the *Nautilus,* which were submitted for

consideration for the Convention on International Trade in Endangered Species of Wild Fauna and Flora, effective January 2, 2017. Cuttlefish embryological stages and development have been well described as they are an abundant species in the Eastern Atlantic and therefore easy to collect and study in large quantities.

1.6 Objectives

In summary, cephalopods have an unusual combination of features that are reminiscent of other more complex animals. Their olfactory sensory systems have similar complexity to those of both vertebrates, insects, and crustaceans. They also share the same bipolar OSN morphology and follow similar trends in their olfactory receptors. Their early and direct development makes cephalopods a great study specimen for describing the development of the nervous system. To gain further insights into the olfactory system of cephalopods, I have focused my research on two different chapters:

Chapter 3: Histamine in the Olfactory System of *Sepia officinalis*

Hypothesis: Histamine has been suggested as a neurotransmitter in the chemosensory systems of gastropods; therefore, I hypothesize that histamine is a neurotransmitter in a subset of olfactory sensory neurons in *Sepia officinalis*.

Chapter 4: The Organization and Development of the Olfactory Lobe

Hypothesis: *Sepia officinalis* have glomeruli to organize their olfactory inputs into the olfactory lobe, homologous to the glomeruli previously described in vertebrates, insects, crustaceans, and gastropods.

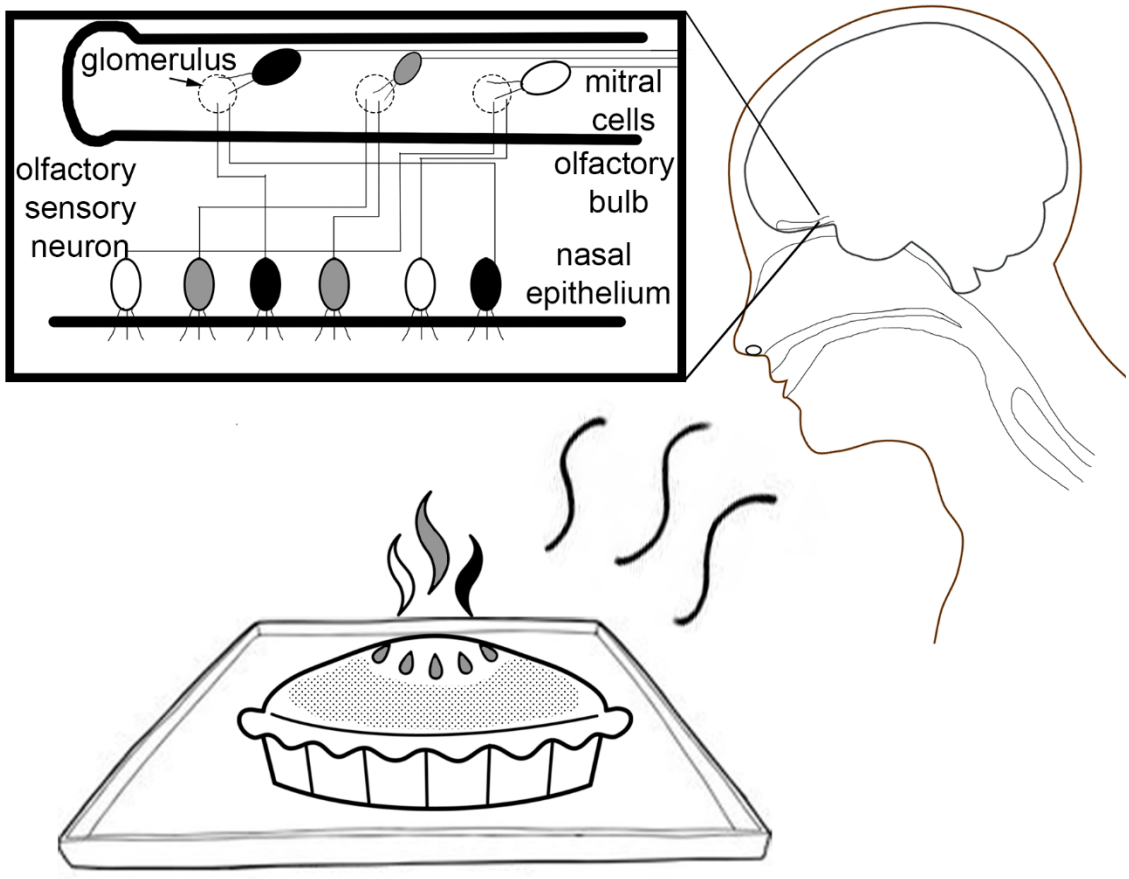
glomerulus
mitral
cells
olfactory
bulb
olfactory
sensory
neuron
nasal
epithelium

Figure 1.1 A diagrammatic explanation of human glomerular functionality. Odorant molecules dispersed in the air bind to specific receptors in the olfactory epithelium. Olfactory sensory neurons with the same receptor type (one receptor type per neuron) project their axons to the same glomerulus, so that all the "cinnamon detecting" OSNs project to one "cinnamon" glomerulus et cetera. The interneurons of the olfactory bulb like the mitral cell, are present in the glomerulus, and transfer now organized odorant information for higher order processing in the rest of the brain.

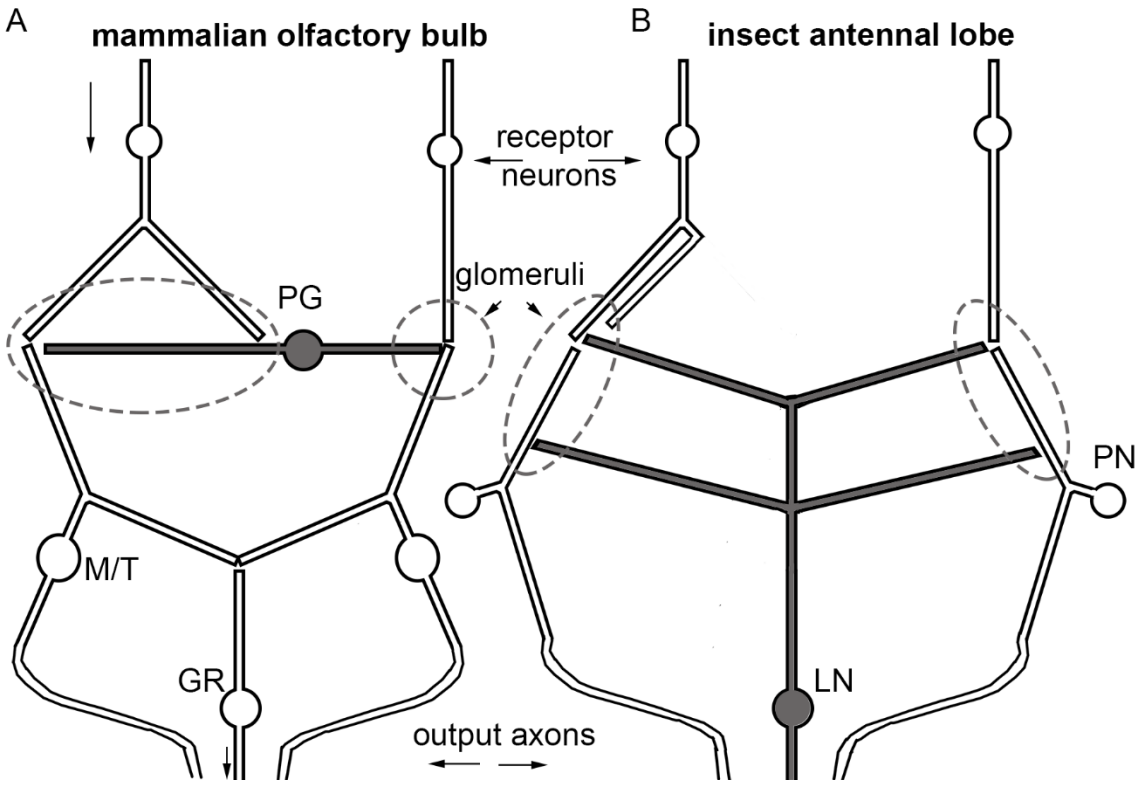
A
mammalian olfactory bulb
B
insect antennal lobe
receptor
neurons
glomeruli
PG
PN
M/T
GR
LN
output axons

Figure 1.2 Schematic of the first olfactory relay in mammals and insects. Based on the diagram in Ache and Young, 2005. (A) The mammalian OB showing receptor cells contacting mitral/ tufted (M/T) and periglomerular (PG) cells in glomeruli organized synapse (dashed circles). Parallel output pathways in the lateral olfactory tract (LOT) are transected by two levels of lateral inhibitory connections, one formed by the PG cells and the other by granular (GR) cells. (B) The insect antennal lobe drawn in the same format as (A) showing essentially the same overall organization of the projection neurons (PNs) and various types of local interneurons (LNs).

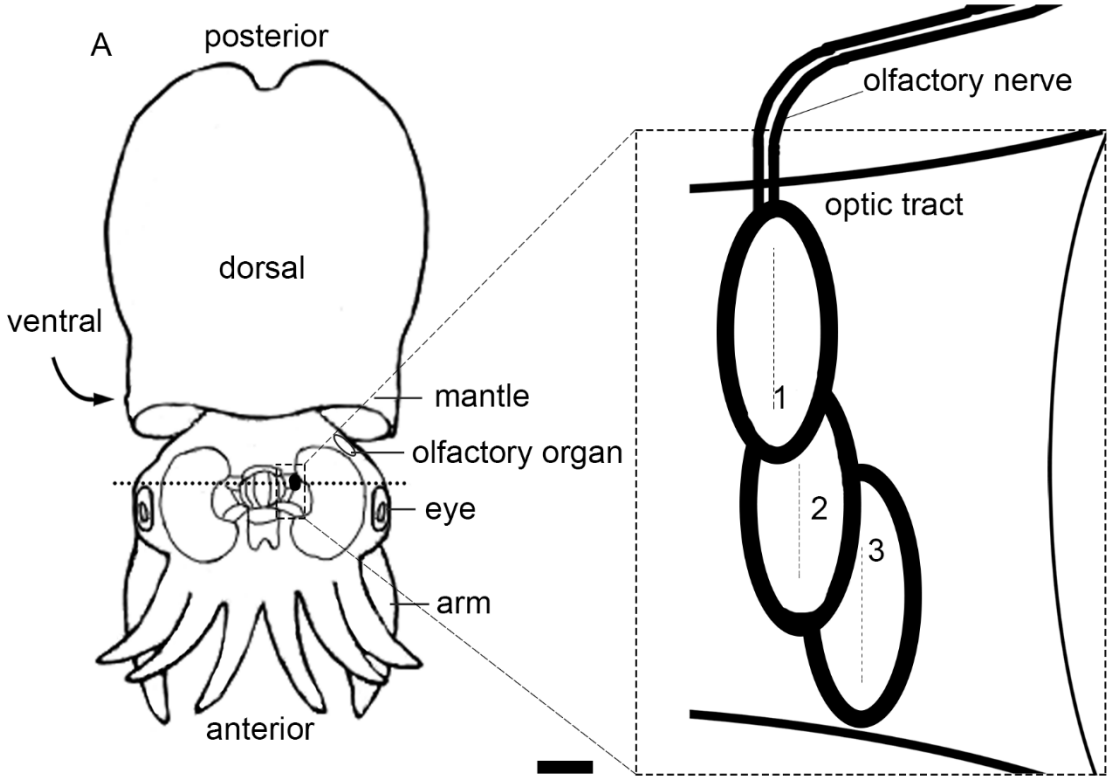
A
posterior
dorsal
ventral
mantle
olfactory organ
eye
arm
anterior
olfactory nerve
optic tract
1
2
3

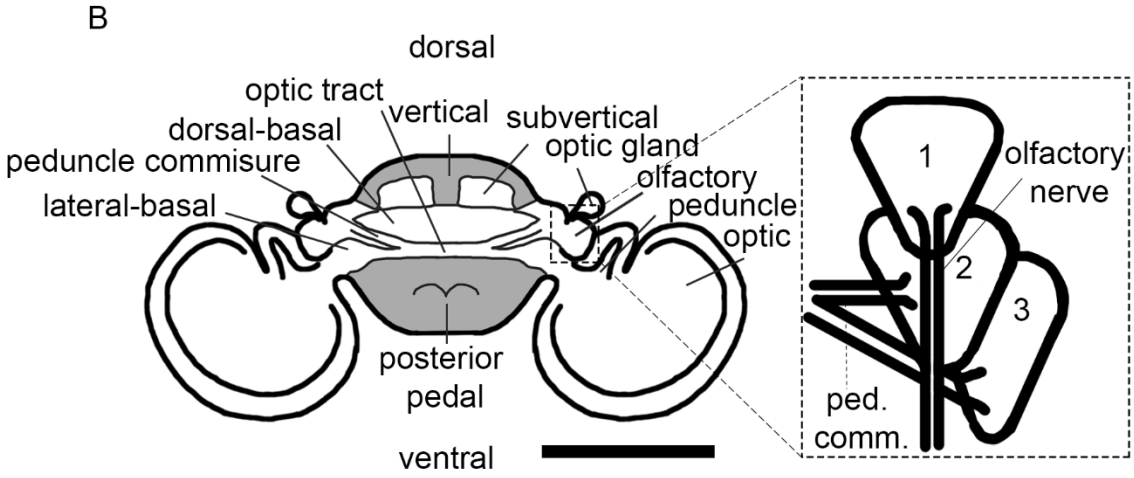
B
dorsal
optic tract
vertical
subvertical
dorsal-basal
peduncle commisure
optic gland
olfactory
lateral-basal
peduncle
optic
posterior
pedal
ventral
1
olfactory
nerve
2
3
ped.
comm.

Figure 1.3 Diagrammatic Representations of the Cuttlefish Embryo and CNS. (A) Facing the dorsal side of the embryo, the posterior end is at the tip of the mantle and the anterior end is at the tip of the arms. Water flows into the mantle right above the olfactory organ (located on the reverse ventral side) and is ejected out the siphon on the ventral side of the animal (not shown). The view box shows a magnified schematic of the olfactory lobe, composed of three lobules numbered one, two, and three from the posterior end to the anterior end. The lobules are rounded on the dorsal side, but on the ventral surface they have a medial ridge (represented by the dotted lines). (B) In a transverse view of the most medial section of the brain, the most peripheral and largest lobes of the brain are the optic lobes. From peripheral to medial: optic lobe, peduncle lobe, lateral-basal lobe, olfactory lobe, optic gland, peduncle commissure, optic tract. From dorsal to ventral: vertical lobe, sub-vertical lobes, dorsal-basal lobe, posterior pedal lobe. The view box demonstrates a schematic of the olfactory lobules positions and shapes in high magnification in the olfactory tract. The ventral ridge makes the lobules appear triangular. The olfactory nerve primarily innervates lobule one, while the peduncle commissure and optic tract primarily innervate lobule two and three. Scale bars represent 1 mm.

Chapter 2: Materials and Methods

2.1 Subjects and Reagents

All animal procedures were in compliance with the guidelines of the European Union (directive 86/609) and the French law (decree 87/848) regulating animal experimentation, as well as the Dalhousie University Committee on Laboratory Animals protocol. All efforts were made to minimize animal suffering and to reduce the number of animals used. Experiments were performed on *Sepia officinalis* embryos gathered from fertilized egg batches that were collected from the coast near Concarneau, France, in May 2014, 2015 and 2016, and June 2017. Eggs were kept at approximately 20° C (Celsius) in aerated seawater and several were opened daily to obtain a collection of all necessary developmental stages (Lemaire, 1970). In these conditions, embryos generally develop over 30 days (approximately 1 day/stage) and are allowed to continue developing until the last stage prior to hatching, stage 30, as hatching begins at stage 31. Embryos develop inside a chorion enclosed in numerous darkly pigmented membranes that make up the egg capsule. After stage determination by a dissecting microscope, each specimen was collected by removing the egg capsule and chorion layers in seawater. Embryos were then anesthetized in 7% magnesium chloride in distilled water for 20 to 40 mins, until they became unresponsive to stimuli, before being immersed in either of two fixatives depending upon the experiment. For those embryos reserved for *in situ* hybridization (*ISH*) experiments, embryos were first opened in RNase-free conditions before fixation.

In the summer of 2016, we also received additional *S. officinalis* hatchlings that were being reared in the Aquatron facility at Dalhousie that were approximately 1 week old (after hatching). These hatchlings were procured for reuse from another study in compliance with the guidelines on procurement of animals used in science published by the Canadian Council on Animal Care. After anesthetization, we separated the head from the mantle before fixation.

2.2 Fixation

All fixations occurred at 4° C with gentle agitation on a shaker. Multiple fixation procedures were used dependent upon the antibody (Table 2.2). Paraformaldehyde (PFA) fixative was prepared using 16% PFA (PFA; RT-15710, Electron Microscopy Sciences, Hatfield, PA, USA) and diluted with phosphate buffered saline (PBS) to form the 4% solution. EDAC (1-ethyl-3(3-dimethyl-aminopropyl)-carbodiimide; Sigma Aldrich Mississauga, ON, Canada) fixative was prepared using 2% EDAC and 0.4% N-hydroxysuccinimide in PBS (Panula et al., 1988). After fixation, the duration of which was dependent on the fixative used and size of embryo (between 12 to 72 hrs; Table 2.1), all embryos were washed in fresh PBS for 12 hrs before storage.

Table 2.1 Protocols for Fixatives Including Target Antigens and Solutions.

Fixative	Target	Contents	Fixation Time	Additional Steps
PFA	General fixative	4% PFA 96% PBS	12-72 hrs depending on embryo size	Rinse in PBS
EDAC	Histamine	2% EDAC 0.4% N-hydroxysuccinimide 97.6% PBS	24-36 hrs	Additional 48 hrs in 4% PFA

One of the largest challenges of this project was determining the optimal fixation time. In 2014, I largely based my fixation procedure on previous studies, which recommended 4% PFA for 2, 4, 6, or 24 hrs (Wollesen et al., 2008; Di Cosmo et al., 2000; D'este et al., 2008). Therefore, in our first year of collections (2014), I primarily focused on 12 hrs (overnight) fixation times, and the results were drastically under-fixed to the point of deterioration of the CNS. Some preparations had the peripheral tissue fixed well enough to see staining in the olfactory organ, which prompted

another collection season in 2015. That collection was focused primarily on developing an EDAC technique. While the periphery was well-fixed, the CNS was still degraded. I hypothesized that this degradation may be due to the weak fixative properties of EDAC; I determined that a longer PFA post-fixation time after the initial EDAC fixation would be sufficient. In 2016, this was attempted a third time, with 12 hrs in EDAC followed by 24 hrs in PFA 4%. Our latest attempt at getting histamine staining in the olfactory lobe was in June 2017. Embryos were fixed for 24 or 36 hrs in EDAC followed by 48 hrs in 4% PFA with the mantle and head severed and the arms removed after 12 hrs for better internal penetration. Some embryos were perfused with EDAC via injection in the sinus between the eye and optic lobe to increase penetration of fixative into the CNS. The remaining embryos collected for other immunohistochemistry experiments were incubated in 4% PFA for 72 hrs with the mantle and head severed and arms removed after 12 hrs.

After fixation, all embryos reserved for immunohistochemical experiments were stored in PBS (phosphate buffered saline, 50mM Na_2HPO_4, 140mM NaCl, pH 7.2) with 0.005% sodium azide at 4° C. Those embryos reserved for *ISH* were stored in RNase-free conditions in 50/50 glycerol/PBS at -20° C.

2.3 Tissue Preparation

S. officinalis embryos were either processed as whole embryos (whole-mount) or as cryosections. In preparation for cryosectioning, embryos were placed in a phosphate saccharose buffer (0.12 M phosphate buffer [0.24 M; 1.70 g $NaH_2PO_4*H_2O$, 10.15 g $Na_2HPO_4*2H_2O$, 300 mL dH_2O], 15% saccharose, pH 7.2) for 48 hrs, after which the solution was changed with fresh buffer after 24 hrs. Next, embryos were incubated in gelatin/saccharose phosphate buffer (0.12 M phosphate buffer, 12% saccharose, and 7.5% gelatin) for an hour, or embedded in Fisher HealthCare Tissue-Plus® O.C.T (optimal cutting temperature) compound (Scigen Scientific

Cardena) or Tissue-Tek® O.C.T. compound (Sakura Finetek USA Inc.) and then rapidly frozen at −80° C. Blocks were cut into 30-60 μm sections along the transverse (also known as the horizontal or axial) plane using a cryostat (CM1510; Leica Microsystems GmbH, Wetzlar, Germany) and placed on either FisherBrand™ SuperFrost™ Ultra Plus Adhesion or FisherBrand™ SupraFrost™ Ultra (Fisher Scientific) slides. Slides were treated with a gelatin-coating solution consisting of 0.5% gelatin and 0.05% chromium potassium sulfate dodecahydrate ($CrK(SO_4)_2*12H_2O$) (R&DSystems Protocol).

2.4 Immunohistochemistry

Staining protocols described by Croll (2006) were used with modifications. Whole preparations were washed and bathed in PBS-Tx blocking/dilutant solution composed of PBS with 2% dimethyl sulfoxide (DMSO), 1% Triton X-100, 0.1% bovine serum albumin (BSA), and 0.1% normal goat serum (all from Sigma Aldrich, Mississauga, ON, Canada) for 24 hrs before incubations at 4° C.

Whole-mount incubations occurred in 1.5 or 2.0 mL micro centrifuge vials containing one individual in each vial. After blocking, specimens were placed in primary antibody diluted 1:200 or 1:500 in PBS-Tx for 10 days at 4° C (See Table 2.2 of antibodies used). Preparations were rinsed with PBS and agitated at room temperature for 10 mins before rinsing again 4 times for 10 mins each. They were then incubated in 1:200 to 1:500 dilutions of secondary antibodies (conjugated to Alexa Fluor 488 nm or 555 nm) in PBS-Tx for an additional 10 days unagitated at 4° C. (Table 2.3). No difference was found between samples that were agitated or not during this time. Specimen were rinsed with PBS using the same procedure as the primary antibody wash. The clearing agent CUBIC (**c**lear, **u**nobstructed **b**rain/body **i**maging **c**ocktails and computational analysis; 4% wt/vol PFA, pH 7.4, 25 wt% Quadrol [Ethylenedinitrilo)tetra-2-propanol], 25 wt% urea, 15 wt% Triton X-100,

dH2O; Susaki et al., 2015) was used to improve visualization in whole-mount specimen. Specimens were prepared with either a single-, double-, or triple- label with one or two primary and secondary antibodies from different hosts so that they were viewable in different fluorescent channels and/or a structural stain such as phalloidin or DAPI. DAPI (4',6-diamidino-2-phenylindole), is a fluorescent marker which binds to A-T rich regions of cellular DNA, resulting in a nuclear label (Wollesen et al., 2009). Phalloidin, composed of phallotoxins from the mushroom *Amanita phalloides,* stains various isoforms of filamentous (F)-actin filaments and traditionally provides a general view of the muscular system of invertebrates (Dancker et al., 1975). It also reliably stains neuropil of cephalopods and molluscs due to their continuous growth and development.

Sections were processed on slides isolated by a hydrophobic pen (Liquid Blocker Pap Pen for Immunostaining, Sigma-Aldrich Mississauga, ON, Canada) to avoid solution dispersal and evaporation. Slides were incubated in the same conditions as in whole-mount, except that they were placed in a humid chamber to avoid dehydration.

2.4.1 Antibodies

See Table 2.2 for primary antibodies and supplier information, and Table 2.3 for secondary antibodies.

Table 2.2 Primary Antibodies Used; including host, clone, estimated concentration, supplier, catalog, and lot number.

Primary Antibody	Host	Clone	Concentration	Supplier	Catalog #	Lot #
Anti-acetylated α-tubulin	Mouse	Monoclonal	1 mg/mL diluted 1:200 ~0.005 mg/mL	Sigma, Oakville, ON, Canada	T6793	034M7828
Anti-histamine	Rabbit	Polyclonal	Lyophilized whole serum (100 µL) diluted 1:200	Immunostar, Hudson, WI, USA	22939	1532001
Anti-serotonin	Rabbit	Polyclonal	Lyophilized whole serum (100 µL) diluted 1:200	Immunostar, Hudson, WI, USA	20080	1431001
Anti-FMRFamide	Rabbit	Polyclonal	Lyophilized whole serum (100 µL) diluted 1:200	Immunostar, Hudson, WI, USA	20091	1331002
Anti-APGWamide	Guinea pig	Polyclonal	Previously aliquoted pure diluted 1:200	Smit et al., 1992 Croll and Van Minnen, 1992	N/A	N/A

Table 2.3 Secondary Antibodies and Histochemical Labels; including host, clone, conjugated molecule, estimated concentration, supplier, catalog and lot number.

Secondary	Host	Conjugated	Concentration	Supplier	Catalog #	Batch/Lot #
Anti-mouse	goat	Alexa Fluor 488	1 mg/mL diluted 1:200 ~0.005 mg/mL	Invitrogen, Burlington, ON, Canada	A28175	QJ222814
Anti-rabbit	goat	Alexa Fluor 555	2 mg/mL diluted 1:200 ~0.01 mg/mL	Invitrogen, Burlington, ON, Canada	A21428	1670185
Anti-rabbit	donkey	Alexa Fluor 488	2 mg/mL diluted 1:200 ~0.01 mg/mL	Invitrogen, Burlington, ON, Canada	A21206	1754421
Anti-mouse	donkey	Alexa Fluor 555	2 mg/mL diluted 1:200 ~0.01 mg/mL	Invitrogen, Burlington, ON, Canada	A31572	1636859
Anti-rabbit	goat	Biotin	1.5 mg/mL diluted 1:200 ~0.0075 mg/mL	Vector Laboratories, Burlingame, CA, USA	BA-1000	126K4804
Anti-guinea Pig	goat	Alexa Fluor 555	2 mg/mL diluted 1:200 ~0.01 mg/mL	ThermoFisher Scientific Waltham, MA, USA	A21435	1235796

2.4.2 Biotin

In addition to the fluorescent immunohistochemistry, some preparations were stained with DAB (3,3'-diaminobenzidine) to increase amplification of staining. In these cases, the secondary was anti-rabbit conjugated to biotin (Sigma). After incubation, the embryos were transferred to an Avadin-Biotin-HRP Complex kit for 1 hr (ThermoFisher Scientific, Waltham, MA, USA; reagent A [Avidin DH], reagent B [biotinylated horseradish peroxidase H] in PBS that was left to mix for a

half-hour before application). I also used VECTASTAIN Elite ABC HRP Reagent, R.T.U. (Peroxidase, Ready-to-Use; Catalog # PK-7100; Vector Laboratories, Burlingame, CA, USA). Finally, the DAB staining (Catalog # SK-4100; Vector kit: DAB in peroxidase buffer, and peroxide) was applied for 5-7 minutes until the optimal contrast and background had been reached.

2.4.3 DiI and Other Structural Stains

DiI, ((2Z)-2-[(E)-3-(3,3-dimethyl-1-octadecylindol-1-ium-2-yl) prop-2-enylidene]-3,3-dimethyl-1-octadecylindole; perchlorate), a fluorescent lipophilic dye that follows continuous membranes, was used to trace the nerve from the olfactory organ to the olfactory lobe. Cuttlefish heads that were fixed in 4% PFA overnight were mounted in 10% agarose in PBS in a culture dish well with 0.05% sodium azide. This agarose gel provided a stable base in which the head could be oriented so that the olfactory epithelium was exposed (see Figure 2.1). A small crystal of DiI was placed directly on the olfactory pit for 24 hrs. Embryo heads were then carefully removed from the agarose and the external DiI was rinsed with PBS before being stored in PBS with 0.05% azide for several months to allow the diffusion of DiI through the olfactory nerve to the brain.

Table 2.4 Other Structural Stains and Conjugates. Including name, conjugated molecule, estimated concentration, supplier, catalog, and lot number.

Name	Conjugated	Concentration	Supplier	Catalog #	Lot #
Phalloidin	Alexa Fluor 488	200 units/mL (6.6 µM) diluted 1:200	Invitrogen, Burlington, ON, Canada	A12379	1656101
DAPI	Naturally absorbs 358 nm (UV)	5 mg/mL	Molecular Probes, Eugene, OR, USA	D1306	1138415
DAB	Nickle-Silver	84 µL in 164 µL buffer solution	Vector Laboratories, Burlingame, CA, USA	SK-4100	N/A
DiI	Alexa Fluor 555	Pure crystal	Molecular Probes, Eugene, OR, USA	D-282	4591-24

2.4.4 Controls

Alexa Fluor labelled secondary antibodies yielded consistent staining over a range of washes and incubation times. Omission controls were conducted as tissues were tested for background autofluorescence in the absence of antibodies under a fluorescent microscope. Fixed tissue showed no autofluorescence (Supplementary Figure A2.2). In addition, secondary antibodies were tested without the use of primary antibodies to demonstrate the omission of staining patterns (Supplementary Figure A2.3).

Most antibodies used were commercially obtained so their specificity and affinity to their respective antigens has been systematically demonstrated over several different conditions and species. Information on the specificity of the antibodies used was provided by the supplier. The

cross-reactivity of anti-serotonin (5-HT) was tested by Immunostar Inc. and does not cross-react with 5-hydroxytryptophan, 5-hydroxyindole-3-acetic acid, or dopamine. Additionally, the antibody has been used extensively in peer-reviewed studies in several diverse phyla including Chordata (Yee et al., 2001), Arthropoda (Novak et al., 1995), Xenacoelomorpha (Raikova et al., 1998), and Mollusca (Elekes et al., 1990; Kreiling et al., 2005). While preabsorption control experiments have been previously conducted with anti-5-HT incubated with 5-HT conjugated to bovine serum albumin, in *Idiosepius notoides*, western blots have not been conducted in *S. officinalis* and therefore cross-reactivity of the antibody cannot be known for certain.

Anti-FMRFamide (Phe-Met-Arg-Phe) has been widely accepted as labelling the family of FMRFamide-related peptides (FaRPs) that all share an -RFamide sequence at their C-terminus. Labeling with this antibody has been published in multiple different phyla including Gastrotricha (Hochberg and Atherton, 2011), Mollusca (Röszer et al., 2004), Arthropoda (Christie et al., 2004), Xenacoelomorpha (Reuter et al., 1998), and Chordata (Honkanen and Ekström, 1990). Preabsorption controls have been conducted in previous literature with FMRFamide peptide, although cross reactivity cannot be excluded as the FMRamide antibody most likely reacts to multiple peptides within the FMRFamide-related peptide family (Di Cosmo and Di Cristo, 1998; Aroua et al., 2011).

Acetylated alpha (α)-tubulin (AcTub) results from the post translational modification of an α-tubulin (See Howes et al., 2013 for a review on AcTub). Traditionally, there has been one AcTub antibody (clone 6-11B-1). This clone, isolated from sea urchin, been shown to reliably stain AcTub in a variety of species, including *Maritigrella crozieri* (Rawlinson, 2010), *Wirenia argentea* (Todt et al., 2008), *Capitella teleta* (Biggers et al., 2013), *Axiothella rubrocincta* (Brinkmann and Wanninger, 2010), *Ilyanassa obsolete* (Gharbiah, Nakamoto, and Nagy, 2013) and cephalopods *Idiosepius notoides* (Wollesen,

Degnan, and Wanninger 2010) and *Sepia officinalis* (Baratte and Bonnaud, 2009; Buresi et al., 2014). While this antibody has been extensively used in a wide variety of species, and consistently labels tubulin structures including cilia, to my knowledge no cross-reactivity studies have been conducted in cephalopods.

The antibody against Ala-Pro-Gly-Trp-NH_2 (APGWamide) was synthesized for a study in *Lymnaea stagnalis* and was paired with an *ISH* experiment to confirm specificity of the antibody (Croll and Van Minnen, 1992). Since then, the antibody has been positively identified as labeling APGWamide neurons and neuropil in *Aplysia spp.* and *Placopecten magellanicus* (Fan et al., 1997; Smith et al., 1997). No cross-reactivity studies have been conducted with this antibody in *Sepia officinalis.*

The HA antibody used in this project has also been extensively published, and reactivity has been demonstrated in *Drosophila* (Stenesen et al., 2015), *Biomphalaria alexandrina, Biomphalaria glabrata* (Habib et al., 2015), and *Mus musculus* (McCann et al., 2014), to name a few recent examples. All staining was blocked by preabsorption of the histamine conjugate antiserum. Cross reactivity was tested in rat hypothalamus by the company, and showed no cross reactivity with L-histidine or L-histidine containing luteinizing hormone-releasing hormone peptide (Immunostar Inc).

Because histamine has never been described in a cephalopod, I also conducted a pre-absorption control for the anti-HA antibody. I incubated the antibody with antigens before applying it to the tissue to prevent the antibodies from binding to endogenous histamine to prove specificity of the antibodies against the tissue tested.

2.4.4.1 Synthesizing a Histamine-Conjugate

Due to the unavailability of a commercial source of the immunogen that the HA antibody was raised against, I synthesized my own conjugate by combining 20 mg/mL histamine dihydrochloride (H7250, Sigma Aldrich Mississauga, ON, Canada), 33 mg/mL BSA, and 4.6

mg/mL EDAC in 0.1 M phosphate buffer, pH 7.4. After incubating for 18 hrs, 1.0 M hydroxylamine hydrochloride (159417, Sigma Aldrich, Mississauga, ON, Canada) was added and the solution was stirred for an additional 5 hrs. The conjugate was dialyzed with Slide-A-Lyzer Dialysis Cassette 0.1-0.5 mL molecular weight cut-off 10,000 (ThermoFisher Scientific, Waltham, MA, USA) for two 2 hr increments, replacing the dialysis buffer each time, before a final dialysis in fresh buffer overnight.

Next, the concentration of the dialyzed solution was determined using a Micro BCA™ Protein Assay Kit (23235, ThermoFisher Scientific, Waltham, MA, USA). The phosphate buffer (2 μL) was used as a control and 2 μL of the dialyzed HA-BSA conjugate were mixed according to instructions of the manufacturers along with several concentrations of BSA (10%, 20%, 30%, and 60% 1mg/mL) to form a standard curve (Figure 2.2). After allowing 40 mins. for a color formation reaction on a shaker at room temperature, absorbance was read with a Beckman Coulter AD340 Plate Reader Analyzer (Beckman Coulter Canada, LP. Mississauga, Ontario) and AD LD Analysis Software (Beckman Coulter Canada, LP, Mississauga, Ontario) using single test, BCA kit settings. Absorbance was measured under 562 nm wavelength and a standard curve was plotted by subtracting the phosphate buffer control from the BSA standards and the conjugate. Using these data points, I calculated a standard line with a slope of $y = 0.0522$ and $R2 = 0.8398$ (Figure 2.2). The sample reading was divided by the slope of the standard line to get the concentration. Finally, the sample concentration (25.1916 μg/2 μL) was divided by 2 μL to get a final concentration of 12.6 μg/μL.

2.4.4.2 Pre-absorption Controls

Pre-absorption was tested by incubating 50 μL of HA-conjugate stock solution/mL of 1:200 HA antibody in a similar experiment to that conducted by Hegedűs et al., 2004, and the remaining immunohistochemistry protocol was followed as normal (Supplementary Figure A2.4).

2.5 Confocal Microscopy

All slides were first viewed on a conventional Leica DM 4000 B fluorescent microscope before being photographed on a Zeiss LSM 510 laser scanning confocal microscope (Carl Zeiss, Thornwood, NY, USA) using 543 nm helium-neon laser or 488 nm argon laser to view Alexa Fluor conjugates. Emissions were collected using band-pass filters (BP565-615, Carl Zeiss AG): 480-520 nm and 500-615 nm through a 10x 0.45 NA objective (Plan-Apochromat SF25, Carl Zeiss AG), 25x 0.80 NA objective (LCI Plan-Neofluar, Carl Zeiss AG), or a 40x 0.95 NA objective (Plan-Apochromat M27, Carl Zeiss AG). Preps double-labelled with DAPI were visualized under UV light using a Zeiss LSM 710 laser scanning confocal microscope (Carl Zeiss, Thronwood, NY, USA). Confocal image z-stacks of sections ranged from 30-60 μm depth (depending on thickness of cryosection). Whole-mount confocal images were more variable; however, care was taken to ensure that z-stacks also included several scans above and below the regions of interest to ensure that the entire area of interest was captured. The distance between sections was set using optimal interval settings, resulting in a range between 0.8- 0.9 μm. Z-stacks were converted into maximum intensity or standard deviation projections using Fiji (ImageJ v3.2.1 for Mac OS X, National Institute of Health, Bethesda, MD, USA, Schindelin et al., 2012) and Zeiss ZEN2009 software. Final figures were constructed using Adobe Photoshop CC 2015 (Adobe Systems, Inc., San Jose, CA, USA) and Fiji with adjustments for size, contrast, and brightness to ensure figure consistency without compromising scientific validity. Schematic diagrams were drawn using Adobe Photoshop CC 2015.

2.6 Data Analysis

Numerical values, including neuron diameter, were measured with Fiji with scale information captured by Zeiss ZEN2009 software. Values are expressed as mean ± standard deviation (n = number of measurements). Scale bars in figures were also measured via Zeiss ZEN2009 and Fiji software, and are representative of 100 μm lengths, unless otherwise specified.

2.7 Molecular Work

While one cephalopod genome has been completely sequenced (*O. bimaculoides,* Albertin et al., 2015), the *S. officinalis* genome is still in progress. Thanks to previous work from the BOREA laboratory in Paris, France, I had access to the mRNA probe sequences and primers for FMRFamide and synaptotagmin. Using the National Center for Biotechnology Information (NCBI) database, I searched for the histidine decarboxylase (HDC) gene sequence using a Basic Local Alignment Search Tool (BLAST) to find the gene in two closely related genera, *Octopus* and *Loligo*. I then found small segments of base pair sequences that were conserved across the two genera using multiple sequence alignment software Clustal Omega (EMBL-EBI, Cambridgeshire, UK). The hypothesis was that if they were highly conserved across these two genera, then the sequence is most likely important for protein expression and therefore it should also be conserved in *S. officinalis*.

From these mRNA sequences, I selected several potential primer pairs, each containing a forward primer near the beginning of the sequence and a reverse primer near the end. Primer sequences were selected with special care to design a primer that would ensure an appropriate probe length, n (by limiting the number of specific nucleotides in the sequence that were uncertain), and prevent the primer from folding on itself. The primers were then synthesized by Eurofins Genomics (Ebersberg, Germany). The primers reported in Table 2.5 are the primer pairs that ultimately succeeded in replicating the gene of interest and were used in the remainder of the study.

2.7.1 Polymerase Chain Reaction

I performed polymerase chain reaction (PCR) with previously extracted cDNA from *S. officinalis*. RNA was extracted from a separate collection of unfixed *S. officinalis* embryos from stages 29 to 30 using Tri Reagent (MRC, Cincinnati, OH, USA). cDNA was then obtained via reverse transcription with Omniscript reverse-transcriptase (QIAgen, Valencia, CA, USA) and frozen in aliquots at -20° C for future experiments. PCR was performed using a pair of forward and reverse primers (see Table 2.5). PCR conditions were: primary denaturing step; 95° C for 5 min cycles for 30 secs., 60° C for 1 min, and 72° C for 1 min for 35 cycles; and a final extension at 72° C for 15 mins. In addition to amplification, this step also confirmed that our sequence was part of the natural transcriptome of *S. officinalis,* since it must be available from the extracted cDNA template to be amplified. After PCR, I performed gel electrophoresis to determine the product length was comparable to our predicted length (see Section 3.2.1.1 and Figure 3.1). The PCR products were cloned into TOPO4 vector (Invitrogen, Carlsbad, CA) and sequenced by Eurofins-Cochin (Cochin Sequencing Platform, Paris, France; Figure 2.3). The TOPO4 vector has M13 forward and reverse polymerase sites, that were used in combination with forward and reveres primers to obtain the sense and antisense probes. RNA probes were obtained with digoxigenin (DIG) RNA labeling mix kit from Roche (Mannheim, Germany).

2.7.2 Probe Synthesis

I synthesized probes from our HDC, FMRFa, and synaptotagmin sequences for *ISH*. The probe synthesized in the forward direction (from the T3 site in the vector using a T3 polymerase) is the sense probe which acted as a negative control (Supplementary Figure A2.1) because it cannot bind to the endogenous mRNA in *ISH*. The antisense sequence, synthesized in the reverse direction (from T7 using a T7 polymerase), is a complement of the mRNA and therefore binds to

endogenous mRNA, resulting in a localized reaction that labels the presence of mRNA in the tissue of a *ISH* experiment.

Table 2.5 Primer Designs for *ISH* Probe Synthesis. Including gene name, Accession number from NCBI, forward and reverse sequences, fragment length, and reference if previously published.

Gene Name	GenBank Accession Number	Forward (5′-3′) Reverse (5′-3′)	Fragment length (in base pairs)	Reference (if previously published)
FMRFamide-related peptides	Y11246	Forward: GCCCTGTCAGGAGATGCTTTC Reverse: GAACCTCTTGTCGGCTTCTG	668	Loi and Tublitz, 1997 Aroua et al., 2011
Synaptotagmin	JX983553	Forward: GACCATAGTGTGTCTCGATAT Reverse: TAGTCCATAGAATATTGAAGT	665	Nomaksteinsky et al., 2013
Histidine decarboxylase	MF358902	Forward: CCATTGATTACATGCA Reverse: CACATGGTCCCAGCTTCTTTCAAGGG	352	Current study

2.7.3 In situ Hybridization in whole-mount

ISH was performed in RNase free conditions on whole embryos with at least 3 replicates. After rinsing the stored embryos in PBS at room temperature, the embryos were washed in PTW (1% Tween 20 [Sigma Aldrich, Mississauga, ON, Canada] in PBS). Tissues were gradually dehydrated in a 25%, 50%, and 75% methanol/PTW solution for 5 mins each, before resting in 100% methanol for an hour. The reverse was then done to gradually rehydrate the tissue (25%, 50%, and 75% PTW/methanol) before returning the embryos to 100% PTW for 10 mins. In addition to the dehydration/rehydration procedure, proteinase K (Invitrogen) was added to the PTW at 0.50 mg/mL for 45 mins at 37° C to disrupt the protein matrix in the outermost epithelium. Embryos were then refixed for 1 hr in 4% PFA.

Next, the embryos were transferred gradually from PTW to a hybridization solution (50% deionized formamide, SSC (sodium chloride/sodium citrate; 20x, 0.3 M sodium citrate, 3 M NaCl), H_2O treated with DEPC (diethyl pyrocarbonate; Sigma), and 1% Tween 20). A pre-hybridization mixture was created by adding heparine (0.075 mg/mL) and tRNA (0.015 mg/mL) to the hybridization solution for blocking. The embryos were then incubated in this mixture for 6 hrs at 55° C. Hybridization with probes (60 ng/mL) was then performed for a minimum of 16 hrs to several days at 41° C. Embryos were then gradually transferred to SSC solution at 55° C, and then transferred to MABT (maleic acid buffer containing Tween 20) buffer (100 mM maleic acid, 150 mM NaCl, 175 mM NaOH, 0.1% Tween 20). Embryos were then further blocked in blocking buffer solution (4% blocking powder (Roche), 15% fetal bovine serum [Sigma], in MABT) for 1 hr at room temperature. They were then incubated overnight in the antibody mix (blocking buffer solution with anti-Digoxigenin- alkaline phosphatase; DIG-AP antibody; Roche) at 4° C.

After several quick washes in MABT to remove unbound antibody, a 10 mM EDTA (Sigma Aldrich, Mississauga, ON, Canada) solution removed extra calcium and magnesium chloride from the embryos. The embryos were then repeatedly rinsed in MABT for the remainder of the day.

Finally, embryos were placed in AP (alkaline phosphatase) buffer (0.1 M TRIS pH 9.5, 0.1 M NaCl, 0.05 M $MgCl_2$, and 0.1% Tween 20). The revelation step was done with the addition of levamisol (0.5 mM), 5-bromo-4-chloro-30-indolyphosphate p-toluidine salt (BCIP; Roche) and nitroblue tetrazolium chloride (0.34 mM) until desired contrast was reached, approximately 24-72 hours incubation time. The reaction was stopped by washing in PTW solution. Embryos were then fixed again in 3.7% PFA in PBS for 24 hrs. Embryos incubated with sense probe did not show any coloration after revelation.

2.7.4 *In situ* Hybridization on Sections

ISH was also conducted on cryosections prepared in RNase-free conditions. While most of the procedure is consistent with whole-mount preparations, any permeability treatments such as the methanol dehydration steps and proteinase K were unnecessary and therefore omitted. After initially rinsing the slides in room temperature PBS, sections were rinsed in SSC (5x). Slides were then incubated in a humid chamber at 65° C for 2 hrs in the pre-hybridization buffer (50% deionized formamide, SSC (5x), 40 μg/mL salmon sperm DNA, Denhard's (5x), and Dextran sulfate 10%). The hybridization buffer included an addition of 300 ng/mL of probe to the prehybridization buffer and was left overnight in the humid chamber. After rinses in SSC 2x and SSC 0.1x at 65° C, slides were transitioned to MABT and then 1 hr in MABT with blocking buffer 4% and fetal bovine serum 15% at room temperature. Sections were then incubated in antibody anti-DIG-AP 1/500 (in blocking buffer 1%, fetal bovine serum 5%, and MABT 94%) at 4° C for 2 hrs. Slides were rinsed in MABT and then left at room temperature in MABT overnight. Finally, AP buffer (Tris-HCl pH 9.5

100 mM, NaCl 100 mM, $MgCl_2$ 50 mM, Tween 20 0.1%)-levamisol 1 mM was added to the sections for 20 minutes before revelation with the addition of 150 μg/mL BCIP and 300 μg/mL nitroblue tetrazolium chloride until desired contrast was reached. Slides were then rinsed and mounted with Mowiol (EMD Milipore, Billerica, MA, USA) mounting medium (6 g glycerol, 2.4 g MOWIOL (Hoechst); 6 mL dH_2O, 12 mL 0.2 M Tris, pH 8.5) for viewing.

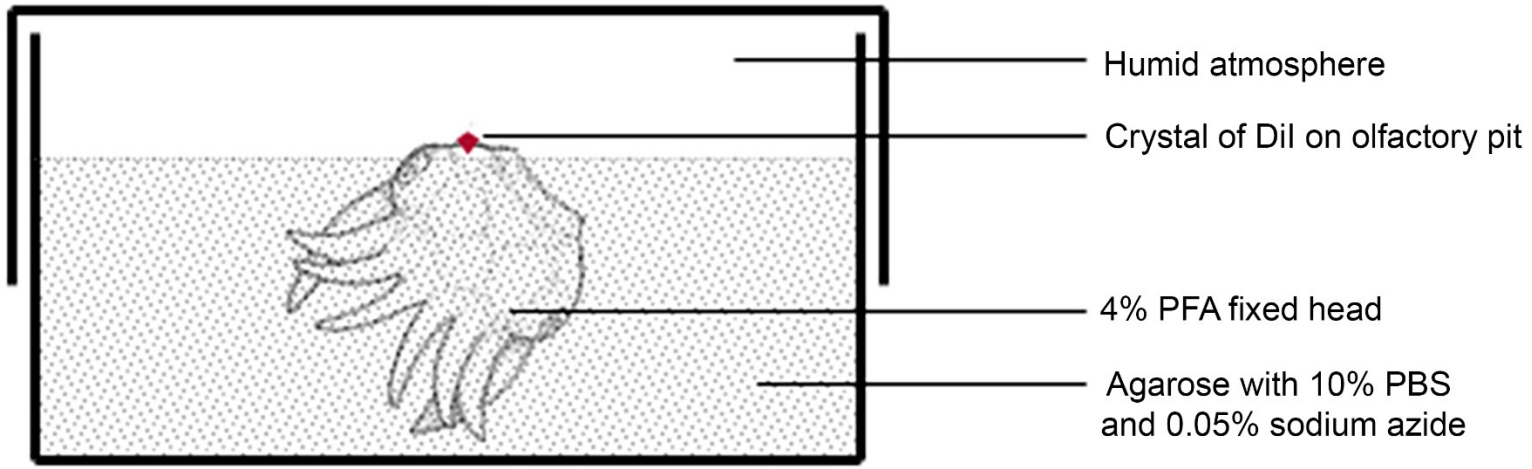

Figure 2.1 Diagram Illustration of DiI Protocol Experiment Design. Cuttlefish embryos fixed in 4% PFA overnight were mounted in 10% agarose medium in a culture well so that the olfactory epithelium was exposed but the rest of the head was completely immobilized. A crystal of DiI was placed on the olfactory pit for 24 hrs. External DiI was then rinsed with PBS and the embryos were stored in PBS to allow appropriate time for migration of the dye to the olfactory lobe.

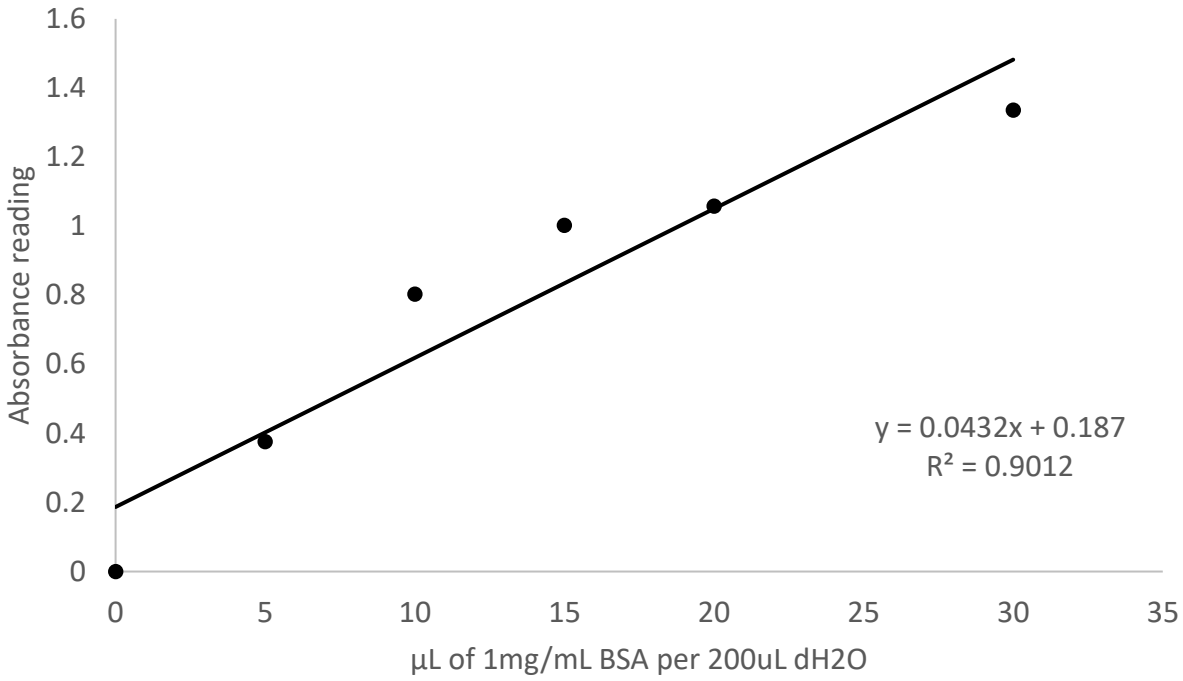

Figure 2.2 Linear Plot to Determine Histamine-BSA Conjugate Concentration. Absorbance for each concentration of BSA protein was plotted with a standard linear plot to determine slope and extrapolate the concentration of the HA-BSA conjugate.

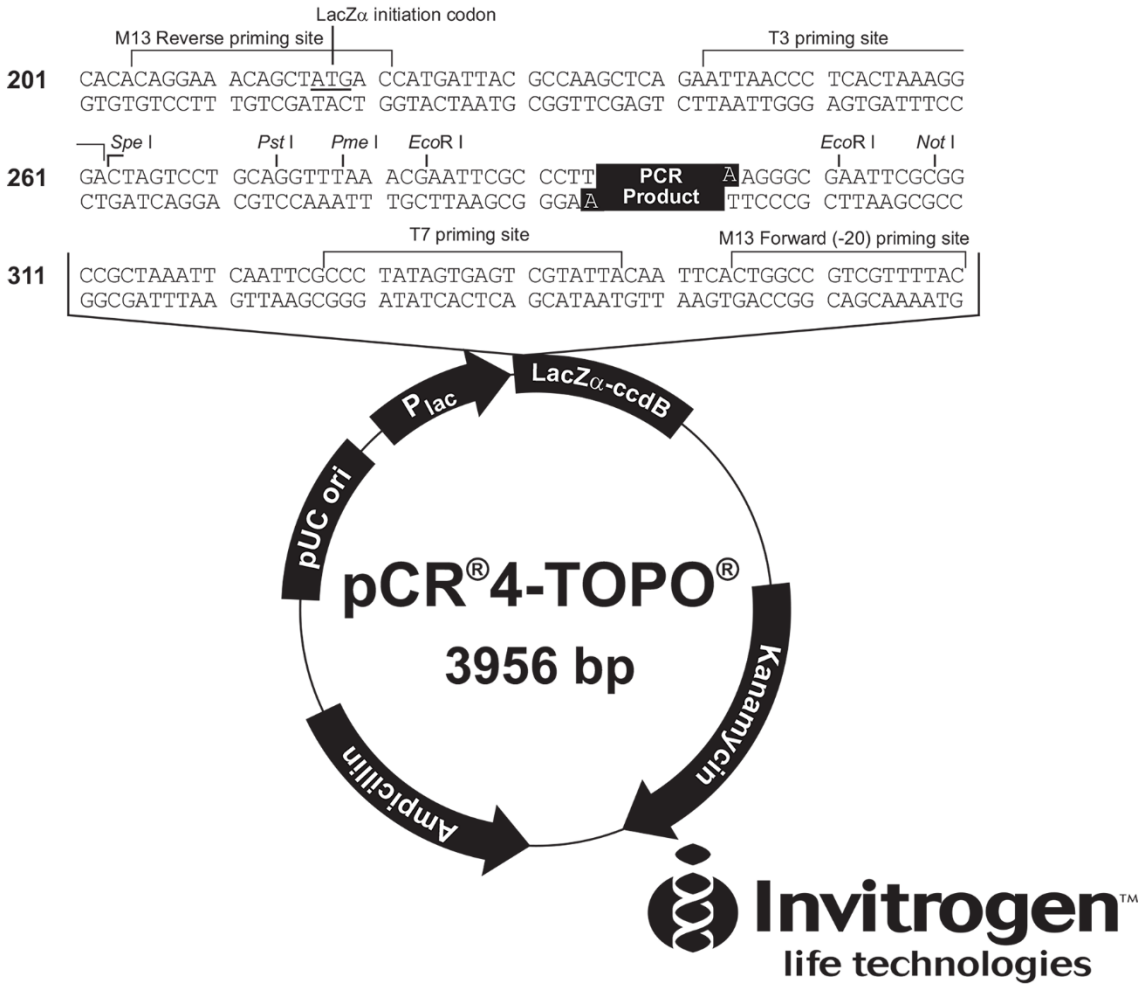

Figure 2.3 Topo4 Vector Map by Invitrogen Life Technologies. Used to create T3 or T7 probes including locations and sequence for reverse primer site, T3 priming site, insertion location of PCR product, T7 priming site, and forward priming site.

Chapter 3: Histamine in the Olfactory System of *Sepia officinalis*

3.1 Histamine

Histamine (HA) is used for intercellular communication throughout the animal kingdom and is found in multiple systems including digestion, immune-defense, bronchoconstriction, vasodilation, and respiration (Haas et al., 2008). HA is perhaps most associated with the immune system, as it is critical to inflammatory responses and auto-immunity. It is also important for gastric acid secretion in the stomach. HA is in the vertebrate brain, found in the hypothalamus, pineal, and olfactory bulb (OB; Halasz and Shepherd, 1983). HA acts as a neurotransmitter in second order neurons in peripheral sensory systems, such as the somatosensory, nociception, cutaneous itch, and chemosensory systems. It is present in the glomerular layer of the rat OB (Haas et al., 2008). There, it is thought to be a presynaptic inhibitor of the primary olfactory sensory neurons (OSNs) (Wachowiak et al., 2002).

HA is also involved in insect and crustacean sensory systems. Although most often cited as the neurotransmitter of photoreceptors in arthropods (Stuart, 1999), HA also inhibits OSNs by activating the ligand-gated chloride channels present in OSNs, thereby suppressing both spontaneous and odor-evoked spikes and mediating inhibition (McClintock and Ache, 1989; Wachowiak et al., 2002). Synthesis of HA has been observed in the central nervous system (CNS) of lobsters where the axons of the OSNs terminate (McClintock and Ache, 1989; Orona et al., 1990).

In molluscs, several studies have identified HA-ergic neurons in the CNS of *Aplysia californica, Lymnaea stagnalis, Helix pomatia, Biomphalaria spp.,* and *Limax valentianus* (Soinila et al., 1990; Elste et al., 1990; Hegedűs et al., 2004; Habib et al., 2015; Matsuo et al., 2016). As in vertebrates, insects, and crustaceans, molluscs have HA in the olfactory processing center, the procerebrum, where it modulates oscillating local field potentials which are thought to assist in the modulation and

storage of olfactory memory (Gelperin et al., 2000; Matsuo et al., 2009; Kay, 2014; Matsuo et al., 2016). There is also evidence of HA-ergic fibers in receptor cells of the statocysts (Soinila et al, 1990; Ohsuga et al. 2000; Braubach and Croll, 2004), in the chemosensory neurons of the superior tentacles of *L. valentianus* (Matsuo et al., 20016), upper tentacles of *H. pomatia* (Hegedűs et al., 2004), and tentacles in *L. stagnalis* and *Biomphalaria spp.* (Wyeth et al., 2011; Habib et al., 2015).

In previous reviews of neurotransmitters in the cephalopod brain, some have suggested HA may be present in the cephalopod CNS (Tansey, 1979; Messenger, 1996). Since then, there have been few studies of HA in cephalopods, but to my knowledge it has never been described in the olfactory system.

Therefore, based on previous studies in molluscs, vertebrates, insects, and crustaceans, I hypothesized that HA is present in the olfactory system of *S. officinalis* and have sought to describe the location and role of HA in this system. To do so, I developed and synthesized an ISH probe for histidine decarboxylase (HDC), the enzyme which catabolizes the decarboxylation of histidine into HA.

3.2 Results

3.2.1 Histidine Decarboxylase mRNA *ISH* Probe

3.2.1.1 Sequencing Histidine Decarboxylase

As stated in Chapter 2, I designed two primers by aligning other HDC sequences in *Octopus* and *Loligo* genome fragments (not shown). Based on these alignments, the *S. officinalis* sequence had an expected length of 550 base pairs. The PCR of the *S. officinalis* cDNA with the two primers was analyzed via gel electrophoresis to determine if the PCR product had a comparable sequence length (Figure 3.1).

3.2.1.2 Phylogenetic Analysis

The PCR product was sequenced to confirm that it was HDC. The nucleotide sequence was aligned with *Octopus bimaculoides* histidine-decarboxylase-like predicted mRNA sequence (Figure 3.2).

3.2.1.3 HDC Probe Synthesis

Based on this alignment, we ordered a plasmid containing a smaller region of the sequence (352 base pairs) and synthesized two new primers for the two new ends of our shorter sequence. Our results from five PCRs on the plasmid are shown in Figure 3.3. As a control experiment, the PCR amplicon of the forward and reverse primer was run in column one of the gel, and demonstrates a HDC sequence length of 352 base pairs. The other four columns are combinations of the M13 DNA sequencing primers and our custom primers which were then isolated and purified to be used as our sense and antisense probes. The final sequence was published to the GenBank under accession number MF358902.

The amino acid sequence of the *S. officinalis* was predicted using a +3-forward frameshift reader with the *Octopus* HDC peptide sequence as a guideline (Figure 3.4) which I used to create the phylogenetic trees and alignments shown in the Chapter 5 Discussion.

3.2.2 Olfactory Organ

ISH of the HDC antisense probe (Figure 3.5) stained the olfactory organ in whole-mount (Figure 3.5 A-C). At higher magnification and in sections, this appeared as darkly stained spherical cell bodies within a more lightly stained olfactory epithelium (OE). Most of the cell bodies were found in the ventral end of the olfactory organ (Figure 3.5 B). In sections, the majority of the staining was seen below the outer layer of OE (Figure 3.5 D-F), with cell bodies approximately 10 μm in diameter (n= 12). The most intense staining was restricted to the olfactory organ, although there was sparse staining surrounding the OE (Figure 3.5).

3.2.3 Olfactory Nerve

ISH also showed the olfactory nerve (Figure 3.5 A), visible from its starting location on the anterior end of the olfactory organ.

3.2.4 Olfactory Lobe

HDC antisense probe ISH showed cell bodies in the olfactory lobe (mean width [left-right] = 98.6 μm ± 14.5 μm, n= 4; mean length [dorsal-ventral] = 111.8 μm ± 17.6 μm, n= 5). The olfactory lobe tapered at the posterior and anterior ends, creating a smaller area in the anterior and posterior sections, as seen in Figure 3.6. At its maximum width, the lobe contained 14 identifiable cell bodies (mean diameter 7.1 μm ± 2.3 μm, n=5) with HDC mRNA. HDC-positive cell bodies were also visible in the optic, dorsal-basal, peduncle, and dorsal-lateral lobes (Figure 3.6).

3.3. Histamine Immunohistochemistry

To further elucidate the cell-body structures that were observed in the olfactory organ and lobe using HDC *ISH*, I also used HA antibody in immunohistochemistry.

3.3.1 Olfactory Organ

Whole-mount immunohistochemical staining at stage 28 revealed the olfactory organ due to the isolated immunoreactivity of that region. The olfactory organ was approximately 96 μm thick (from apex of outer curve to the nerve), and 492 μm in base diameter. The most apparent features observed were small, high intensity elements, 3.6 μm^2 ± 2.1 μm^2 (n=63) in area found throughout all layers of the olfactory organ in a dispersed pattern (Figure 3.7 A). This staining was consistent in all olfactory organs and was not in the head or mantle epithelium. The histamine-like immunoreactivity (HA-LIR) at higher magnification Figure 3.7 B) demonstrated that these elements were consistently at the apical ends of faintly stained cell bodies, either directly proximal to a cell body or along a thin neurite extending to the organ's surface OE (Figure 3.7 C, D). These cell bodies had dim staining

around the membrane and in the cytoplasm, but not in the large nucleus. Their diameters averaged 14.0 μm ± 2.2 μm (n=11).

To demonstrate that anti-HA staining was not a result of autofluorescence, immunohistochemistry was also performed with a secondary antibody conjugated to biotin (not shown). Again, anti-HA labeled round neuronal shaped cells appeared in several transverse sections (40 μm thick) taken through the olfactory organ.

3.3.2 Olfactory Nerve

The olfactory nerve, which originates in the underlying neuropil of the olfactory organ (Figure 3.7 A), contained brightly stained HA-LIR fibers bundled into a thick projection approximately 17.5 μm ± 2.7 μm in diameter (n=10). The projection trajectory of the olfactory nerve is described in more detail in Chapter 4.

3.3.3 Olfactory Lobe

The triangular shape of the olfactory lobe was easily observed with immunohistochemistry of anti-HA (Figure 3.8). Numerous cell bodies (n= ~30) with mean diameters of 9.7 μm ± 1.8 μm (n=13) were distributed around the lobe. While there was no neuropil apparent in the olfactory lobe of Figure 3.8, there was dim neuropil staining in the peduncle (the narrow band of neuropil directly lateral to the olfactory lobe), as well as the neuropil and cell bodies on the dorsal edge of the dorsal-basal lobe. The area was calculated by multiplying the width at the widest point by the perpendicular length, and then dividing by two (the equation for the area of a triangle), to give us an approximate average area of 202.0 μm^2 ± 64.9 μm^2 (n=16) in medial sections of developmental stage 27 embryos. The main branch of the olfactory nerve was also seen entering the ventral end of the olfactory lobe (diameter= 42.7 μm ± 9.2 [n = 3]).

3.4 Discussion

For the first time, HA-LIR and HDC expression has been described in the olfactory system of *S. officinalis*. To my knowledge, this is also the first visualization of HA and HDC in the CNS of a cephalopod.

BLASTp (basic local alignment search tool, protein) algorithms retrieved 80 sequences that were available as of May 2017 from the National Center for Biotechnology Information (NCBI) database, confirming that both nucleotide and amino acid sequences were recognizable as HDC in other invertebrates, including other molluscs and arthropods (Figure 3.9) and in well described model organisms (Figure 3.10). In addition, a multi-sequence alignment of the five molluscan HDC amino acid sequences available on NCBI showed a high level of conservation with the *S. officinalis* sequence (Figure 3.11).

HA-LIR and HDC expression both appear in the neurons of the olfactory lobe and organ. Although I was not able to double-label anti-HA and HDC *ISH,* cells were consistent in approximate number, size, and relative location between the two procedures. These consistencies suggest that both *ISH* and immunohistochemistry are labeling the same neurons. Due to the presence of HA and HDC in both the organ and lobe, it is not possible to comment on efference or afference.

Cell bodies and their apical projections were visible with HA-LIR in the olfactory organ. Their morphology greatly resembled a type V neuron (Figure 3.12; Emery, 1975). These cells are suggested to be differentiated sensory cells with "ciliated plates" at the end of apical neurites. Emery also describes a dense granule at the distal end of the ciliated cavity which is thought to act as a plug with cilia extending through it. The high intensity elements described here with HA-LIR may be the ciliated plates or plugs that Emery describes.

Considering that the HA-LIR neurons had a relatively low concentration in the olfactory organ compared to the abundance of DAPI nuclear stain (not shown), HA cannot be the only neurotransmitter of OSNs in cephalopods. This conclusion is consistent with previous estimates that approximately 20% of the cells in the olfactory organ are OSNs, and 3-5% of cells are type V (Mobley et al., 2007). However, it is difficult to determine if all type V OSNs are HA-LIR, so the estimate may be lower.

The presence of HDC in the olfactory organ could be an indication of HA synthesis. HDC would not be present in the olfactory organ if HA was synthesized elsewhere and used as an efferent neurotransmitter on the OSNs unless HDC mNRA could experience anterograde transportation down the axon. The increase in HDC *ISH* staining intensity suggests an increased concentration of this enzyme during stages 28 to 30.

Both the HA antibody and HDC mRNA probe also clearly labeled the olfactory nerve. While there have been no indications of HDC mRNA transport previously (Eriksson et al., 1998), axons sometimes contain mRNA (Piper and Holt 2004). This has been particularly observed in OSN axons (Vassar et al., 1994; Mombaerts et al., 1996; Treolar et al., 2010). Therefore, it is possible that HDC may be transported in the axon. I suggest future studies examine HDC as a candidate for an mRNA that undergoes axonal transport and HA as a protein that undergoes synaptic synthesis.

There was also an abundance of HDC-mRNA in the cell bodies of the olfactory lobe, which suggests another location of HA synthesis. HA may also be a neurotransmitter of the second-order neurons. HDC-positive cell bodies were also in the optic lobe, dorsal-basal lobe, and peduncle lobe, although not as dense as in the olfactory lobe. Because of this sparsity in the rest of the CNS, and the lack of visible HA-labeled projections from the olfactory lobe to other parts of the brain, HA in the olfactory lobe may not project to other areas of the brain, but instead be contained in the

olfactory system. This isolation would suggest that the only connection between the HA in the olfactory lobe and the HA in the olfactory organ is the nerve. However, this hypothesis cannot be verified without confirmation from anti-HA immunohistochemistry in the CNS.

This experiment is the first instance of HA being suggested as an OSN neurotransmitter, as none of the previously described vertebrate, insect, nor crustacean species have produced HA in their OSNs. Rather, in vertebrates, insects, and crustaceans HA is produced in glomerular interneurons and is used as an efferent inhibitor on the OSNs. Due to the consistent staining of anti-HA in the OSNs (although faint) and presence of HDC in the olfactory organ, efferent inhibition cannot be the only functionality of HA in cuttlefish, although it cannot be discounted completely. There may be an efferent modality in addition to the afferent modality where HA-LIR neurons in the olfactory lobe project their axons via the nerve to the organ, which would explain the HA-LIR and HDC expression in the lobe.

In this chapter, I presented evidence that HA is synthesized and utilized as a putative neurotransmitter in the olfactory system of *S. officinalis*. Its presence in the olfactory organ type V sensory neurons and in the olfactory lobe second-order neurons suggests that it is involved with OSN messaging, but more analysis must be done to determine the exact functionality and directionality.

This conclusion implies that HA may be a common neurotransmitter of sensory neurons throughout the molluscs. HA has been well described in the sensory neurons of statocysts (Soinila et al., 1990; Elste et al., 1990; Ohsuga et al., 2000), and has also been described as an abundant neurotransmitter in other peripheral regions of gastropods such as the tentacles, lips, and anterior foot (Hegedűs et al., 2004; Wyeth and Croll, 2011; Habib et al., 2015). If HA is found to be a shared characteristic of the OSNs in all molluscs, this would distinguish them from vertebrates, insects, and

crustaceans, which use HA to inhibit the OSNs (McClintock and Ache, 1989; Orona et al., 1990; Wachowiak et al., 2002) and glutamate as the primary OSN messenger (Croset et al., 2010). It will therefore be interesting to note the principal neurotransmitter of OSNs in future gastropod and cephalopod studies, as more species are described and amalgamated into our ever-expanding understanding of olfactory evolution.

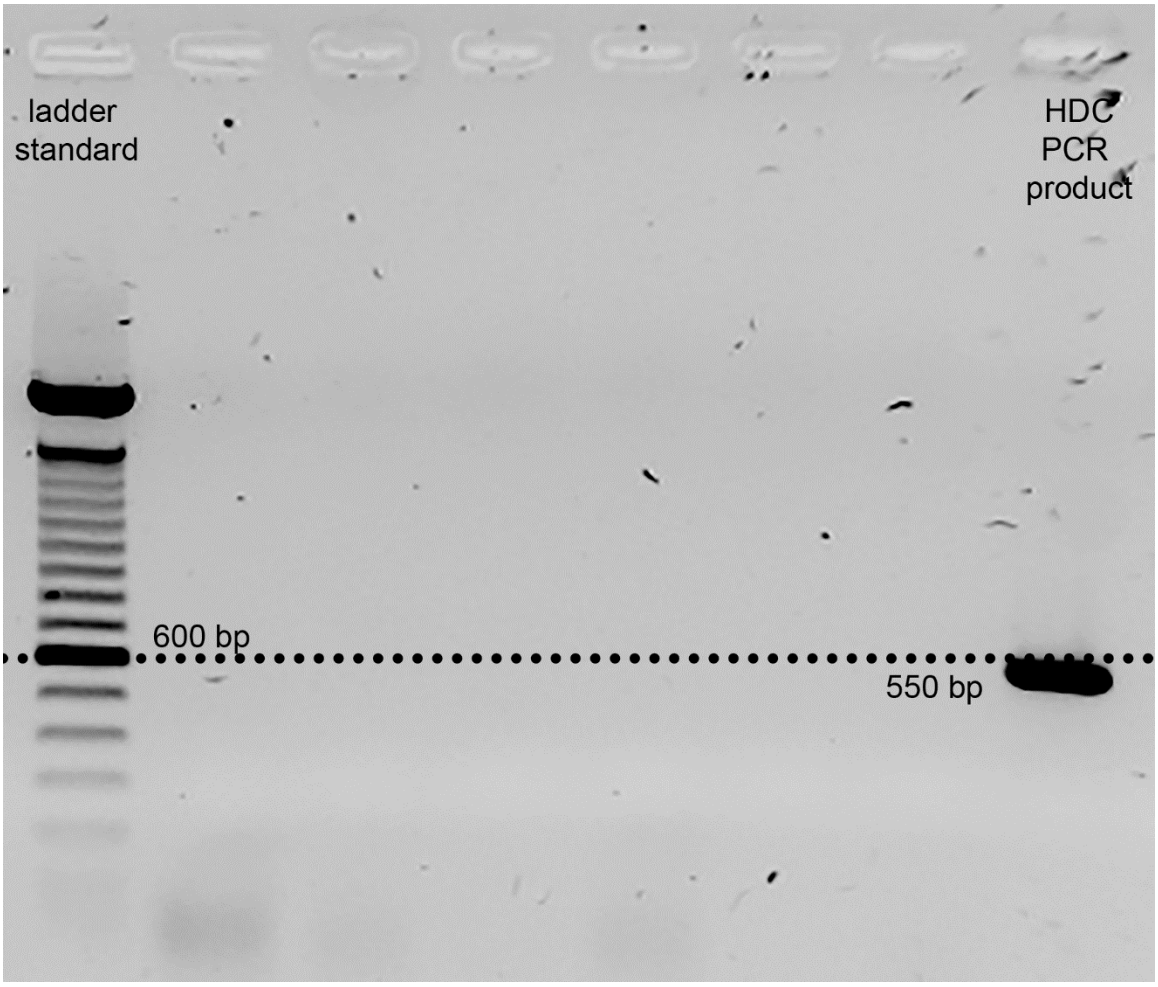

Figure 3.1 Gel electrophoresis of histidine decarboxylase (HDC). The PCR product was estimated to be approximately 550 base pairs based on its migration distance compared to the standard ladder where the thick middle band represents 600 base pairs (dotted line).

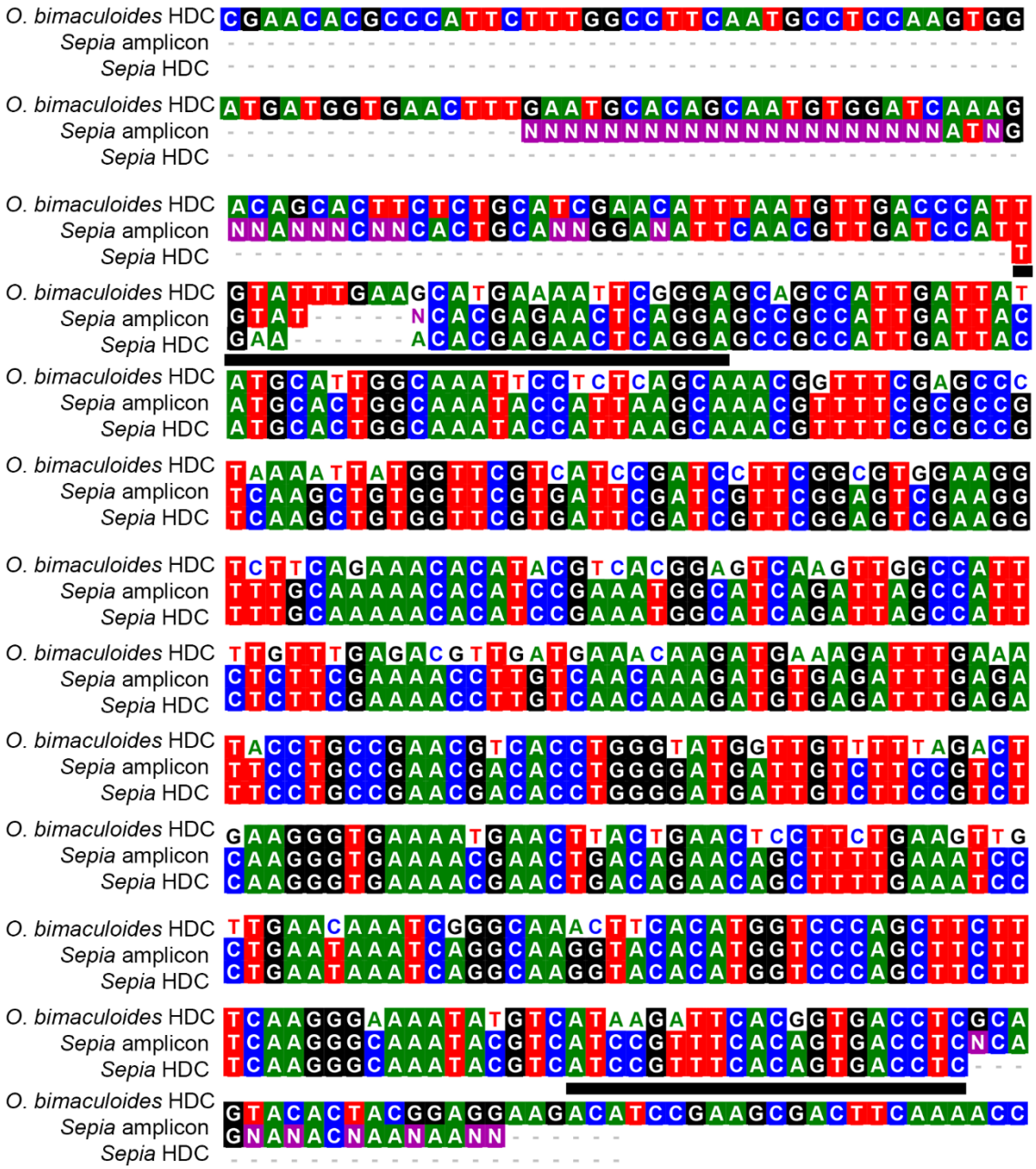
O. bimaculoides HDC
Sepia amplicon
Sepia HDC

Figure 3.2 Alignment of *S. officinalis* and *O. bimaculoides nucleotide sequences*. Final published sequence of *S. officinalis* HDC (MF358902) aligned with the *O. bimaculoides* predicted HDC mRNA sequence (NCBI Reference Sequence: XM_014913957.1) and the original *S. officinalis* 550 base pair PCR amplicon. Brackets represent the forward and reverse primer pair used to design the HDC probe.

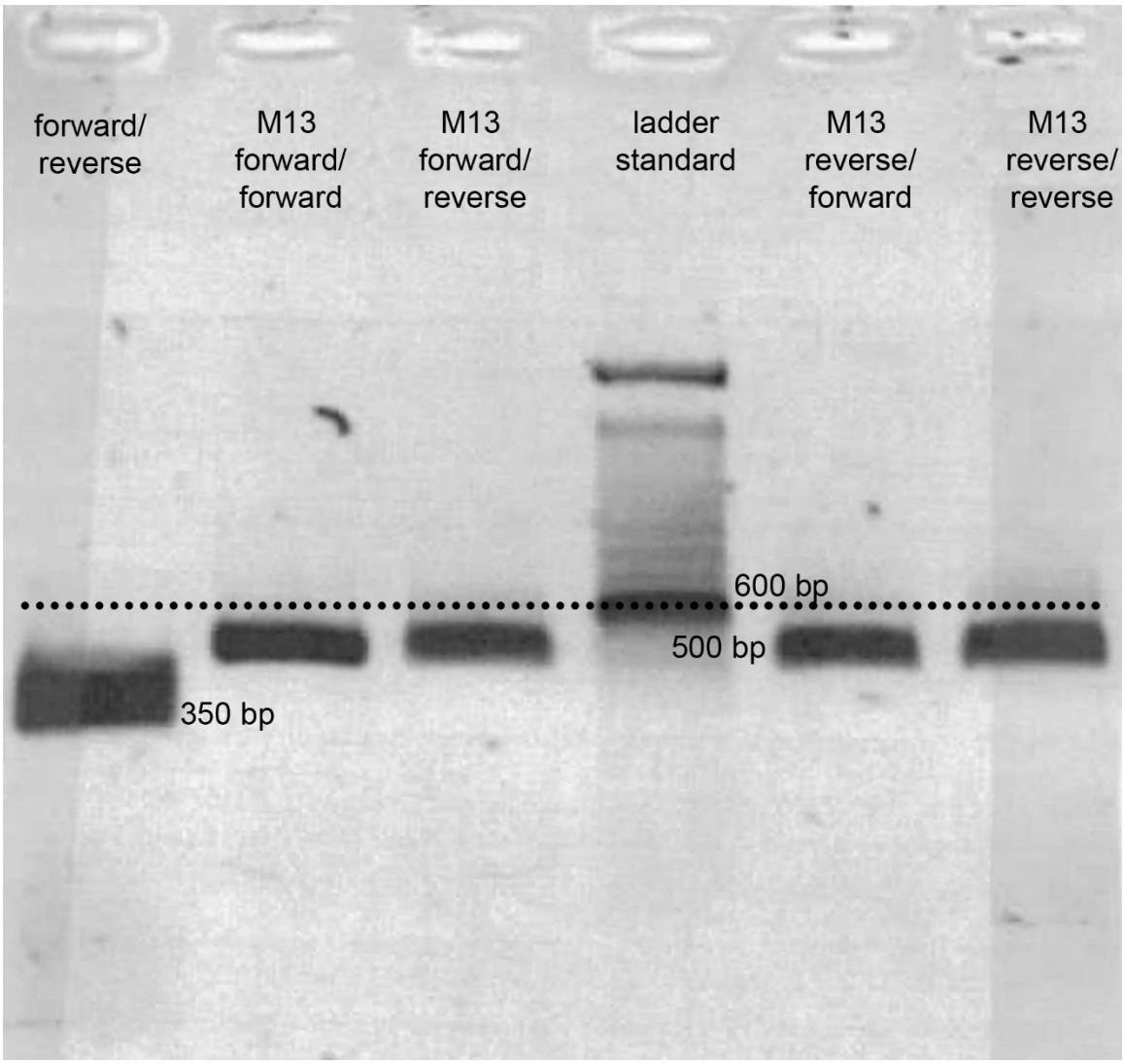

Figure 3.3 Isolated and purified segments for probe synthesis. Column one: gene forward and reverse primers demonstrate HDC sequence (352 base pairs). Comparison to the thick ladder band (600 base pairs). Columns two through four: the other possible combinations of M13 polymerase sites and sequence primers.

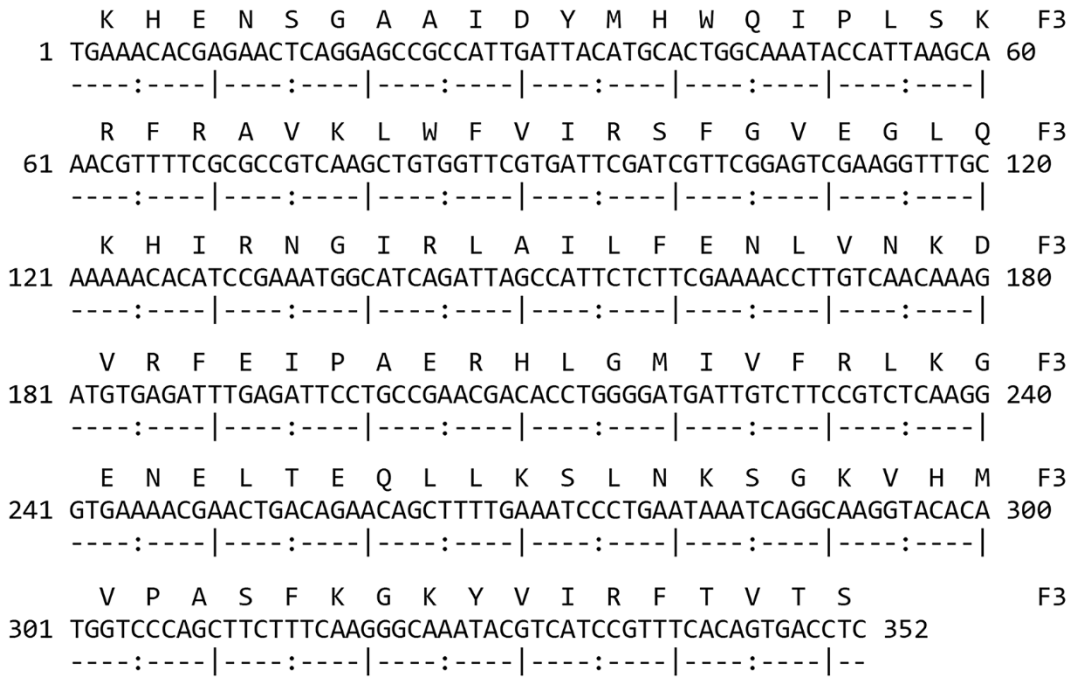

Figure 3.4 Nucleotide to amino acid translator and frameshift reader. Frameshift was +3 to match peptide sequence with *O. bimaculoides* histidine decarboxylase-like amino acid sequence (NCBI Reference Sequence: XP_014769443.1).

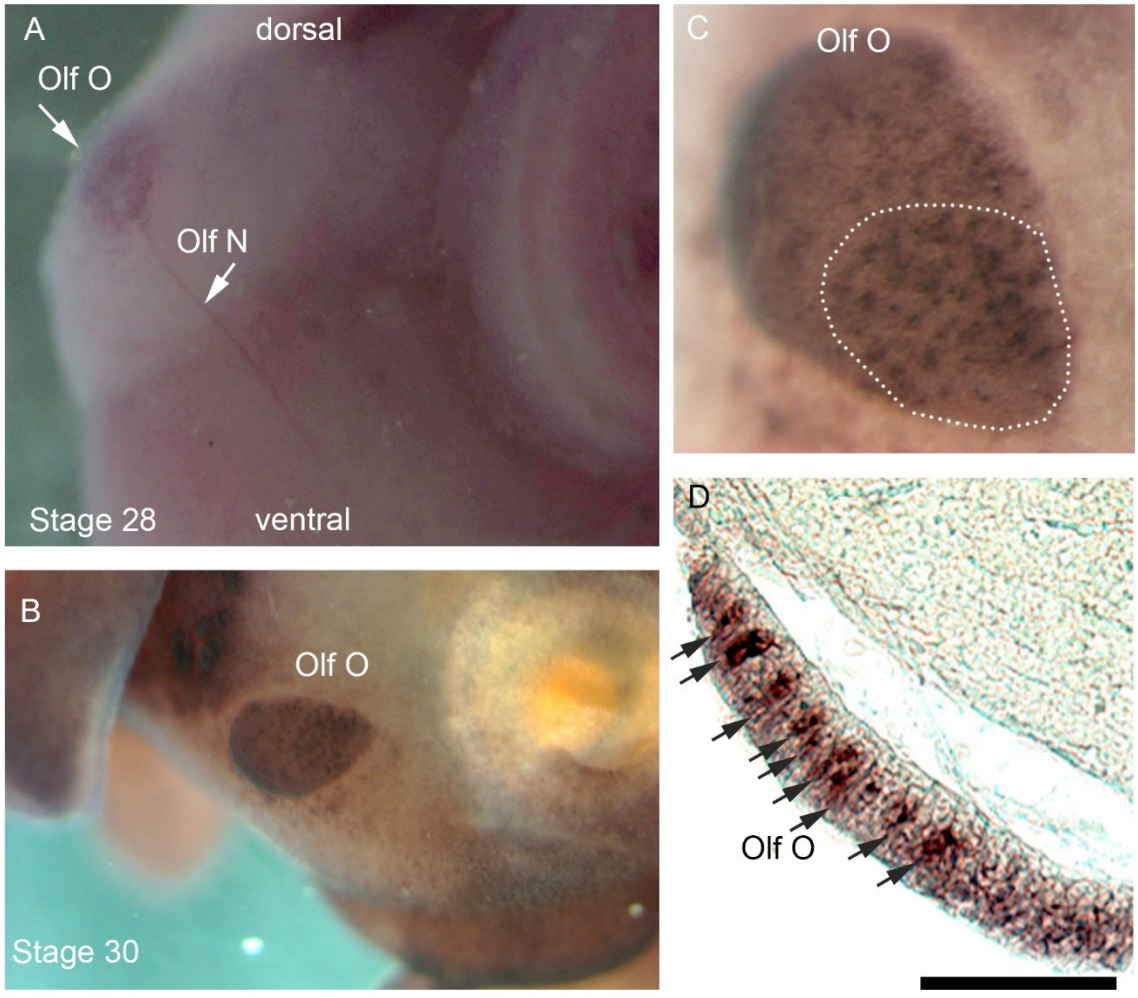
A
dorsal
Olf O
Olf N
Stage 28
ventral
B
Olf O
Stage 30
C
Olf O
D
Olf O

Figure 3.5 Histidine decarboxylase mRNA *ISH* probe in the olfactory organ. (A) Whole-mount staining of the olfactory organ at stage 28 with the olfactory nerve visualized with the HDC probe. (B) HDC probe in the olfactory organ at stage 30. (C) Higher magnification of the olfactory organ in whole-mount. Dotted line indicates cluster of cell bodies at the ventral end of the organ. (D) HDC *ISH* in sections of the olfactory organ with cell bodies in the OE (arrows). Scale bars = 100 μm.

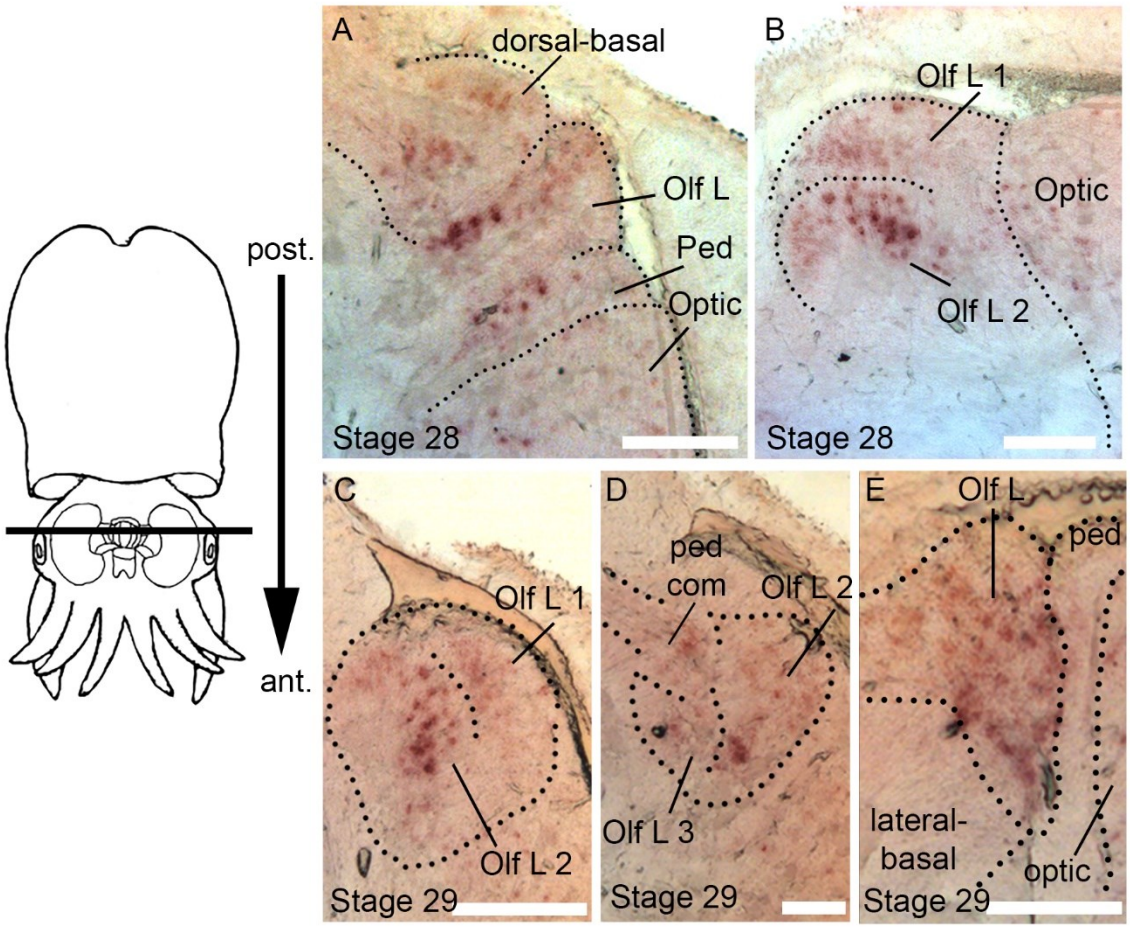

Figure 3.6 Histidine decarboxylase *ISH* mRNA probe in the olfactory lobe. Diagrammatic representations of the orientation of the embryo and the direction of sectioning. From posterior (A) to anterior (D): transverse sections are 40 µm thick. Scale bars are approximately 100 µm.

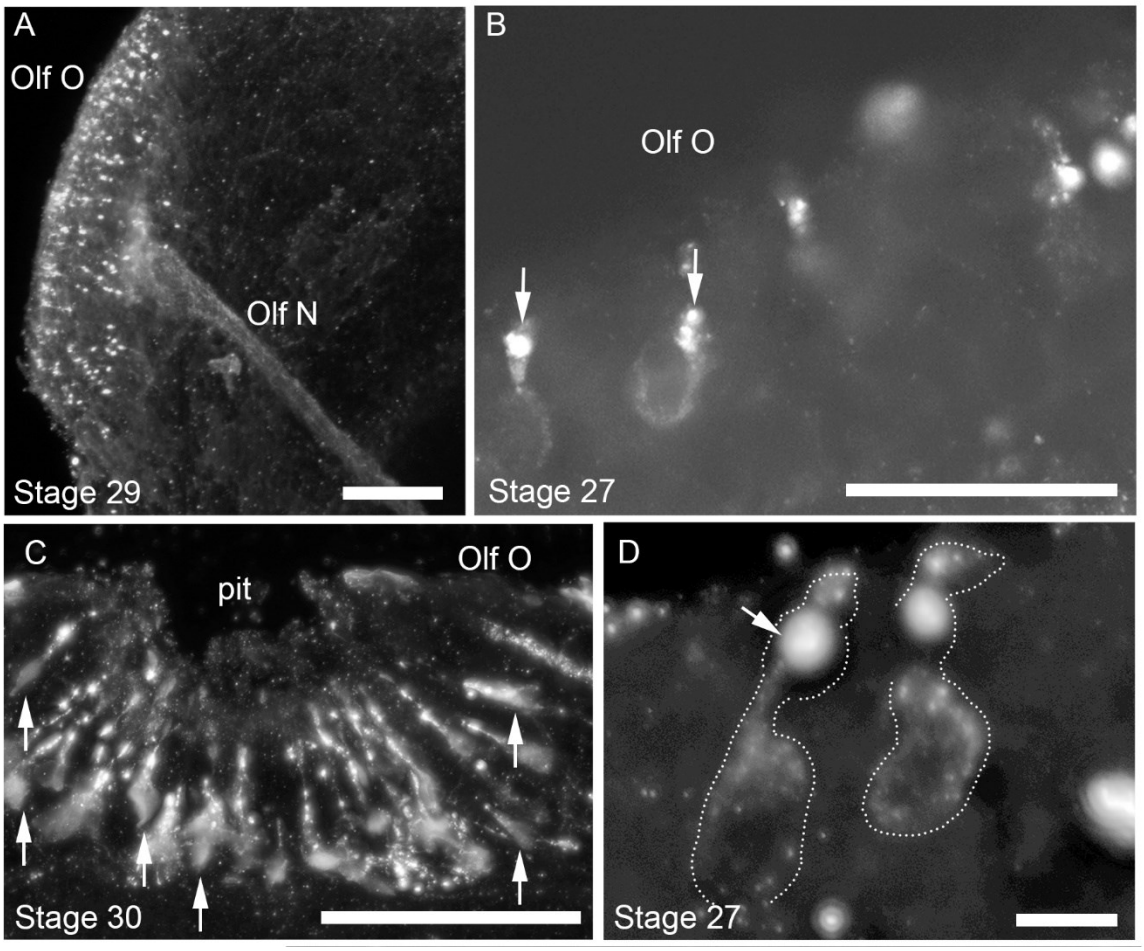
A
Olf O
Olf N
Stage 29
B
Olf O
Stage 27
C
pit
Olf O
Stage 30
D
Stage 27

Figure 3.7 Histamine-immunoreactivity in the olfactory organ. (A) Whole-mount olfactory organ (Olf O) in stage 29 embryo labeled with anti-HA, with bright elements (arrowheads) in the olfactory organ and a distinct olfactory nerve (Olf N). (B) High magnification (40x) of HA staining in stage 27 section the olfactory organs with bright elements along apical projections (arrows). (C) HA-LIR in elements along apical projections and in dimly labeled cell bodies in a section of olfactory organ. (D) A high magnification image of HA-LIR cell bodes extending apical projections (arrow) to the surface of olfactory organ, with a bright element near the tip in stage 27 section. Scale bars A and C: 100 μm; B and D: 50 μm.

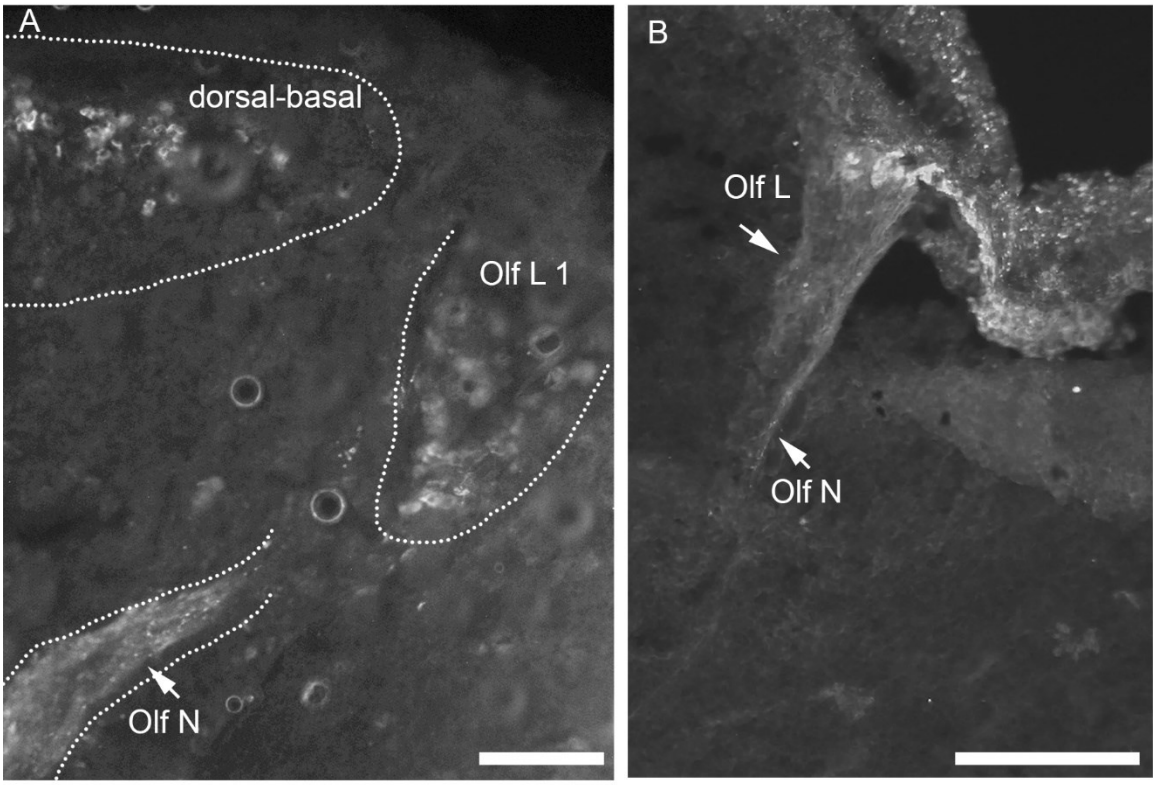
A
dorsal-basal
Olf L 1
Olf N
B
Olf L
Olf N

Figure 3.8 Histamine immunoreactivity in the olfactory lobe. Representation of the general results from EDAC fixation and anti-HA staining in the CNS. (A) A posterior section of a stage 28 embryo showing possible cell bodies in the olfactory lobe (lobule one) with almost no visible neuropil. The olfactory nerve (the olfactory tract once it enters the brain) projects toward ventral end. (B) A more anterior section in the olfactory lobe region of the optic tract. A possible olfactory tract (Olf. N) may be visible entering the ventral end of lobule one, but the staining is insufficient for proper interpretation. Scale bar represents 100 μm.

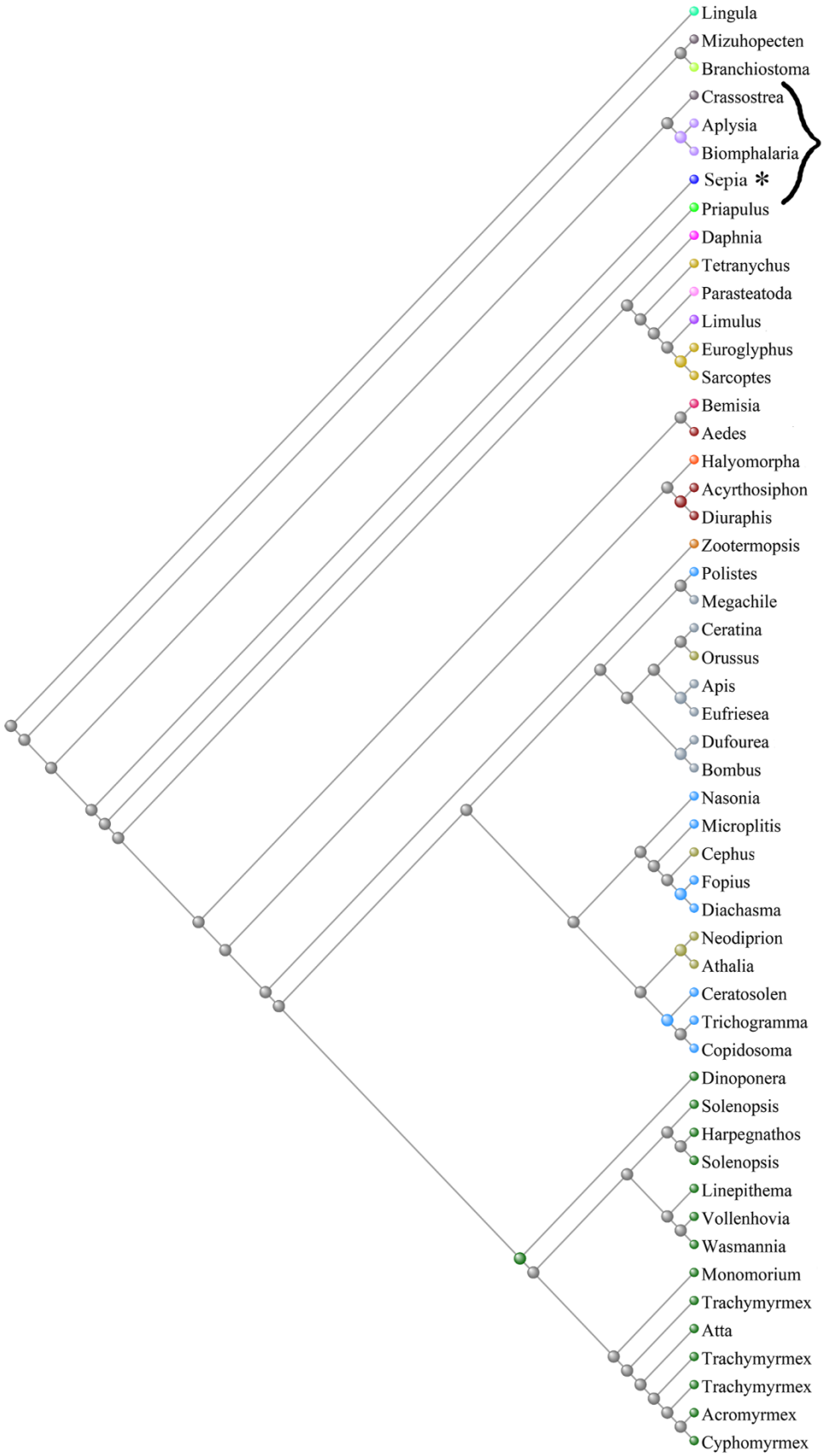
Lingula
Mizuhopecten
Branchiostoma
Crassostrea
Aplysia
Biomphalaria
Sepia *
Priapulus
Daphnia
Tetranychus
Parasteatoda
Limulus
Euroglyphus
Sarcoptes
Bemisia
Aedes
Halyomorpha
Acyrthosiphon
Diuraphis
Zootermopsis
Polistes
Megachile
Ceratina
Orussus
Apis
Eufriesea
Dufourea
Bombus
Nasonia
Microplitis
Cephus
Fopius
Diachasma
Neodiprion
Athalia
Ceratosolen
Trichogramma
Copidosoma
Dinoponera
Solenopsis
Harpegnathos
Solenopsis
Linepithema
Vollenhovia
Wasmannia
Monomorium
Trachymyrmex
Atta
Trachymyrmex
Trachymyrmex
Acromyrmex
Cyphomyrmex

Figure 3.9 A phylogenetic tree of HDC peptide using BLASTn algorithm. Pairwise alignments of sequences were used to query the non-redundant sequences database with the neighbor-joining method. The distance was measured using the Grishin (protein) method. *S. officinalis HDC* sequence denoted with a *; bracket denotes molluscs.

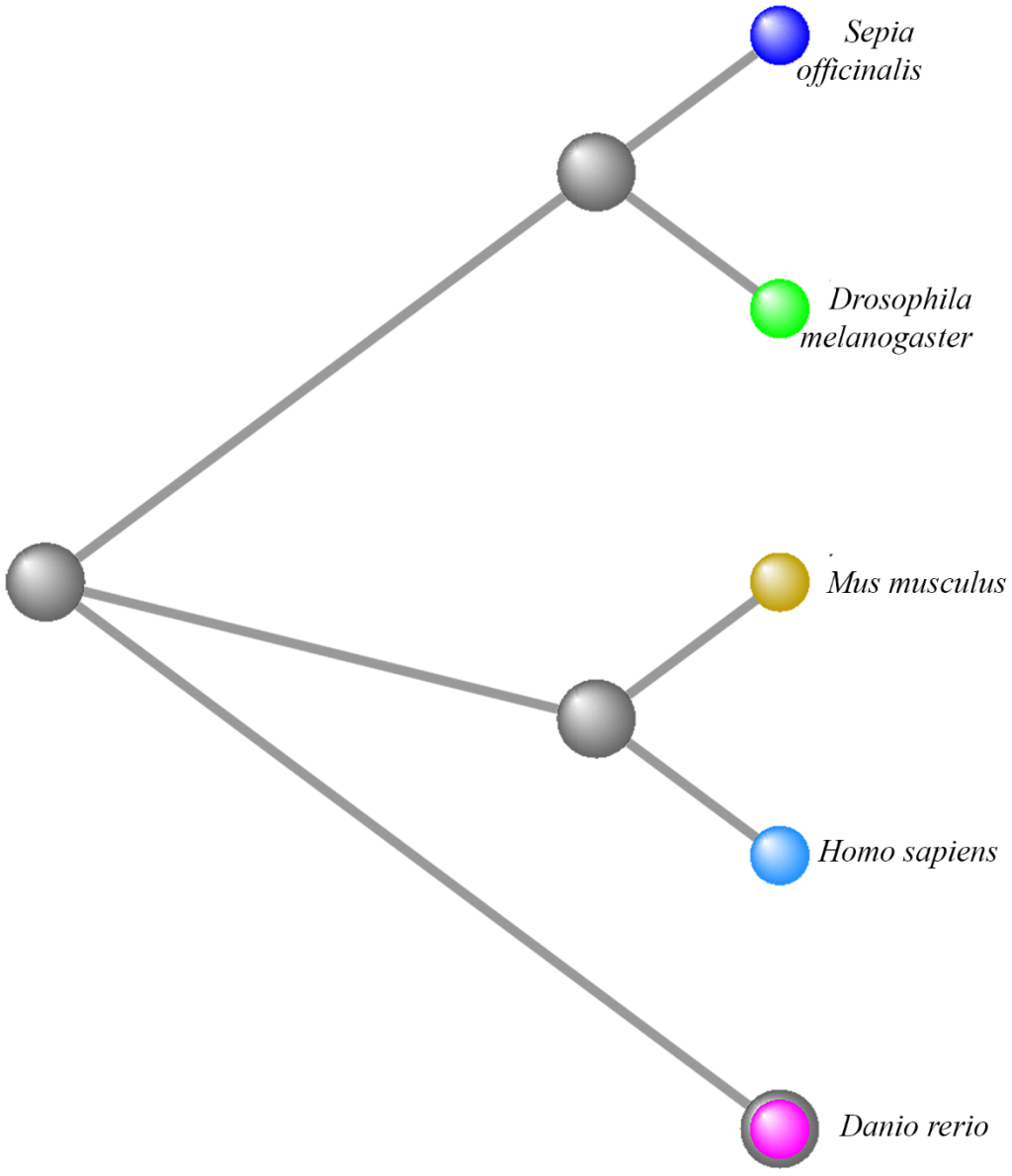
Sepia officinalis
Drosophila melanogaster
Mus musculus
Homo sapiens
Danio rerio

Figure 3.10 A phylogenetic tree of HDC sequences using a BLASTn algorithm. Pairwise alignments were used to query the model species (landmark) database with the neighbor-joining method. The distance was measured using the Grishin (protein) method.

Figure 3.11 Alignments constructed by BioEdit (v7.2.6.1, Tom Hall, 1997-2017) of HDC in five different mollusc species. Forward and reverse primers denoted with brackets.

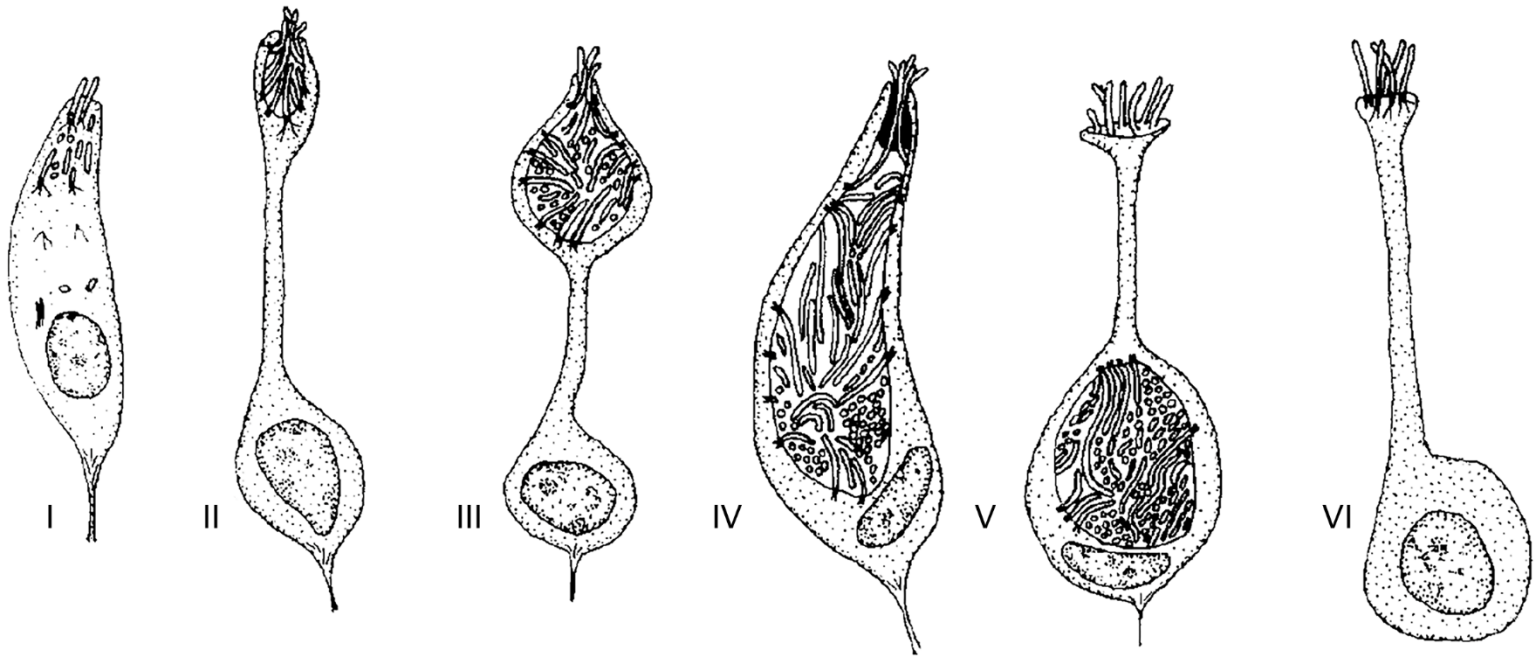

Figure 3.12 Cephalopod olfactory receptors cells 1-5. Adapted from Emery, 1975 and published with permissions. Diagrammatic representations of the types of receptors found in this study. Type V is most consistent with what I observed as HA-LIR cell bodies.

Chapter 4: The Organization and Development of the Olfactory Lobe

4.1 Introduction

In the previous chapter, I described histamine (HA) as a putative neurotransmitter in a class of olfactory sensory neurons (OSN) in the olfactory organ of the cuttlefish. These OSN axons enter the olfactory lobe through the main branch of the olfactory nerve. There are also HA-LIR neurons and histidine decarboxylase (HDC)-positive neurons in the olfactory lobe. However, the HA pathway would only comprise 3-5% of the OSNs if HA is limited to the type V neurons of the olfactory organ (See Chapter 3: Histamine in the Olfactory System of *Sepia officinali*s; Mobley et al., 2007). Therefore, to further augment the previous descriptions of the organization of the olfactory system, I used other neurotransmitters and structural stains.

In addition to improving historical descriptions of the olfactory lobe (See Section 1.4.3) using more modern techniques, my secondary purpose was to look for glomerular-like structures. Here, I define olfactory glomeruli as being of relatively similar size and shape to vertebrate, insect, and crustacean glomeruli, and containing interneurons and synaptic terminals of OSNs. Thus far, there have been no descriptions of glomerular-like structures in cephalopods. The *Nautilus* olfactory lobe has previously been described as layered, with multiple laminated zones of bands of fibers (Young, 1965). Additionally, the *Octopus* olfactory lobe was much smaller than the nautilus lobe and had no apparent large-scale organization (Young, 1971). However, these descriptions were included as subsections of large bodies of work describing the entire nervous systems, and have not been the focus of isolated study. These studies also were conducted before glomerular structures were defined as a unit, and before the realization that they may be morphologically similar across phyla. Therefore, in describing the organization of the olfactory lobe in unprecedented detail, I also look for glomerular-like structures in *S. officinalis*.

In preceding literature, all descriptions of axons from the olfactory organ project to or around the olfactory lobe. It has been thought to be the termination location of synapses of OSNs (Boycott, 1961). I therefore hypothesized that if there were olfactory glomeruli, they would be present in the olfactory lobe, the location of the OSNs synapses.

4.1.1 Development

Embryos from three distinct timepoints in development, early (stage 25), late (stage 27-29), and after hatching (approximately 1 week old), were used to describe the development of the olfactory system and the neuropil of the olfactory lobe (Figure 4.1). For a general understanding of CNS development in Cephalopods, see Shigeno et al., 2001a; Shigeno et al., 2001b; and Yamamoto et al., 2003.

Two structural stains, phalloidin and DiI ((2Z)-2-[(E)-3-(3,3-dimethyl-1-octadecylindol-1-ium-2-yl) prop-2-enylidene]-3,3-dimethyl-1-octadecylindole; perchlorate), were used in conjunction with several neurotransmitters and peptides that have been previously described as abundant in the olfactory lobe: FMRFamide (FMRFa), serotonin (5-HT), and APGWamide (APGWa), in addition to the newly described HA.

4.1.2 Phalloidin

Phalloidin has often been used in molluscan musculature research (Haszprunar and Wanninger 2000) and labels neurofilaments in cephalopod CNS (Wollesen et al., 2009). Phalloidin has also been described as a consistent marker used to visualize glomeruli in a wide variety of species (Rossler et al., 2002). Vertebrate OSNs are replaced by basal cells throughout the lifetime of an organism, so there is a constant turnover of glomerular synapses (Rossler et al., 2012). Likewise, due to the multiple changes to the nervous system during embryonic and adult development, insect glomeruli experience a high degree of plasticity. Rossler et al., (2012) used phalloidin to label the

filamentous (F)-actin in glomeruli through a wide diversity of species, including vertebrates: frog (*Xenopus laevis*), axolotl *(Ambystoma mexicanum),* goldfish *(Carassius auratus)*, and invertebrates: moth (*Manduca sexta,* and *Antherea Polyphemus),* honeybee (*Apis mellifera*), ant (*Harpegnathos saltatory*) and cricket (*Gryllus bimaculatus).* In all species, glomeruli have a much higher phalloidin concentration and intensity than the surrounding tissue. This concentration is most likely because actin-based cytoskeleton plays an important role in synaptic plasticity of glomeruli, particularly in terminals of OSN axons in insects and dendritic terminals of vertebrate olfactory bulb neurons (Ennis et al., 1998). Due to this inter-phylum consistency, and the ability to use phalloidin to describe cephalopod CNS, I used the F-actin stain to identify the neuropil of the olfactory lobe and to look for glomerular-like structures in cuttlefish.

4.1.3 DiI

DiI, a fluorescent lipophilic dye that follows continuous membranes, has been used in a variety of physiological studies, to identify the *Xenopus* extrabulbar olfactory pathway (Pinelli et al., 2004), the moth olfactory lobe (Oland and Tolbert, 1998), and gastropod peripheral sensory cells (Wyeth and Croll, 2011). In this study, I used it to trace the olfactory nerve from the olfactory organ, mapping its projection to the olfactory lobe.

4.1.4 Synaptotagmin

Synaptotagmin is a secretory protein abundant in synaptic vesicles in neurons and endocrine cells (Marquèze et al., 2000). There have been 11 synaptotagmin genes found in vertebrates, four in *Drosophila,* and four in *C. elegans*. Synaptotagmin has also been identified in molluscs *L. stagnalis (*Gardzinski et al., 2007), *B. glabrate (*Lockyer et al., 2007), and *S. officinalis* (Buresi et al., 2016). It is highly evolutionarily conserved and a key component of the exocytosis-endocytosis machinery. Synaptotagmin is a useful marker for understanding neuronal connections and visualizing nervous

systems because it is universally present in almost all synapses. I used a synaptotagmin mRNA probe which was previously designed and synthesized for *S. officinalis* (Buresi et al., 2016). It was identified in the eye, olfactory organ, and palliovisceral ganglia. I used the synaptotagmin mRNA probe to visualize the neuropil, delineate separate lobes, and identify key structures in the cuttlefish CNS.

4.1.5 Acetylated α-tubulin

The acetylation of α-tubulin is a post translational modification that is thought to increase microtubule stability. Cells can carefully control their acetylation levels depending on the sub-cellular structure. Due to this modification, acetylated α-tubulin (AcTub) is often found in the axons and ciliated cells of adults and developing larvae (Shigeno and Yamamoto, 2002; Baratte and Bonnaud, 2009; Wollesen et al., 2009; Rawlinson, 2010; Buresi et al., 2014).

4.1.6 FMRFamide

FMRFamide-related peptides (FaRPs) are a large family of neuropeptides originally identified in molluscs, but also found in the rest of the animal kingdom. One general function that spans almost the entire animal kingdom is their modulation of peripheral sensory inputs, including inhibition of feeding and regulation of food intake and behavior (Bechtold and Luckman, 2007; Peymen et al., 2014). FMRFa modulates OSN responses in vertebrates (Eisthen, 2002) and can be found in terminal nerve fibers (that originate in the olfactory placode) and olfactory nerves of bony fish and amphibians (Northcutt and Muske, 1994; Wirsig-Wiechmann and Oka, 2002). FMRFa is also present in the developing embryonic olfactory placode and the olfactory nerve (Roskams et al., 1994).

In arthropods, neuropeptides including FMRFa are found in local neurons, although their function in the olfactory system is less understood (Hansson and Anton, 2000; Yasuda-Kamatani et al., 2006). FMRFa is important for feeding in various gastropod species (Kyriakides and McCrohan,

1989; Alania et al., 2004; Bechtold and Luckman, 2007; Peymen et al., 2014; Zatylny-Gaudin and Favrel, 2014; Cummins and Wyeth, 2014). The apical sensory organ, a presumptive chemosensory organ in larvae, also contains FMRFa-positive cells (Dickinson et al., 2000). FMRFa-positive bipolar cells have also been described in the tentacle tips of *Limax marginatus* (Suzuki et al., 1997) and sensory cells in the osphradium in *Lymnaea stagnalis* (Nezlin and Voronezhskaya, 1997).

In cephalopods, FaRPs are also known to be neuromodulators of the CNS. They have been described to impact chromatophore slow excitation in cuttlefish and octopus, and regulation of the circulatory system in cuttlefish (Fiedler, 1992; Loi et al., 1996; Messenger 1996; Mackie et al., 2008). FMRFa is present in the olfactory organs, nerve, and lobe (*I. notoides*, Wollesen et al., 2010a; *S. officinalis,* Le Gall et al., 1988; Aroua et al., 2011; and *Octopus vulgaris* Di Cosmo and Di Cristo, 1998).

4.1.7 Serotonin

In vertebrates, 5-HTergic fibers were visualized entering the olfactory bulb (OB) and can be found in all layers, but not in the olfactory nerve (Halasz and Shepherd, 1983). In moths and cockroaches, 5-HT is localized in centrifugal neurons that project into the antennal lobes (Hansson and Anton, 2000). These 5-HTergic neurons are suggested to serve a modulatory function on olfaction.

In gastropods, 5-HT is found more consistently in the apical sensory organ than FMRFa (Dickinson et al., 2000). 5-HT has also been described in the chemosensory rhinophore neurites of *A. californica* (Wertz et al., 2007; Cummins and Wyeth, 2014). 5-HT reactivity is isolated to cellular neurites and not found in the somata, so 5-HT production is most likely extrinsic to the rhinophore (Cummins and Wyeth, 2014).

However, 5-HT is not specific to just the sensory systems. 5-HT is associated with the innervation of chromatophores (Messenger, 2001; Mackie, 2008) and has also been previously

described in the olfactory system (Messenger, 1996; Wollesen et al., 2010a; Polese et al., 2015). It first appears in the developing olfactory lobes of the pygmy squid *Idiosepius notoides* around stage 24 (Wollesen et al., 2010b) and therefore is present in the olfactory system from the early stages of its development.

4.1.8 APGWamide

In a study on *Octopus* reproduction, several neuropeptides, including FMRFa, neuropeptide Y, gonadotropin-releasing hormone (GnRH), and APGWa were discovered in the OSNs and fibers of the *Octopus vulgaris* olfactory lobe (Polese et al., 2015). Based on this observation, Polese et al. proposed that olfaction may have a possible modulatory role over reproduction based on chemical cues. Although no odorant molecules have been linked to the sexual activity of octopus, there have been studies in which waterborne pheromonal attractants were purified from *S. officinalis* (Zatylny et al., 2000; Boal et al., 2010; Enault et al., 2012) and *Aplysia* (Cummins et al. 2009). The abundance of the reproductive peptides in the olfactory system suggests APGWa would be a good marker to help describe the organization of the olfactory lobe.

APGWa functions as a neurotransmitter in the gastropod CNS, as well as in the CNS and peripheral axons of bivalves (Smith et al., 1997). In some molluscs, such as *Helix aspersa* (now classified as *Cornu aspersa*), FMRFa and APGWa have been shown to act synergistically, often co-expressed in the same neurons, with dual projections involved in penile expression (Li and Chase, 1995; Zatylny-Gaudin and Favrel, 2014). However, other species, like *L. stagnalis,* have different neurons expressing either FaRPs or APGWa that have distinct and different actions on the penis retractor muscles (van Golen et al., 1995; Li et al., 1992). In cephalopods, APGWa has been described in the inferior frontal system, where it is thought to be involved in reception and analysis

of chemosensory information from the suckers (Young, 1972), as well as in the posterior olfactory lobule (Polese et al., 2015).

4.2 Results

4.2.1 Acetylated α-tubulin and the Olfactory Organ

The sensory structures of *S. officinalis* have already been described using anti-AcTub (Buresi et al., 2014) and therefore will not be covered in much detail. AcTub immunohistochemistry in whole-mount consistently label the olfactory organ. The olfactory organ is identifiable with immunohistochemistry against AcTub by stage 25 (Figure 4.2 A). AcTub clearly labels ciliated cells in the olfactory epithelium (OE), a basal neuropil, and the olfactory nerve (Figure 4.2). The olfactory organ at this stage is approximately 343 μm in diameter and 75 μm thick. The thickness of the organ was measured as the longest visible distance from the pit (or the apex of the curve in stage 25 before pit formation), to the base of the neuropil where it meets with the olfactory nerve. As the embryo develops, the olfactory organ diameter increases in size, while the thickness decreases. The average diameter of the olfactory organ in stage 29 is 428.8 μm ± 116.4 μm (n = 15) and the average thickness of the olfactory organ is 65.6 μm ± 20.9 μm (n = 24). (Figure 4.2). Approximately one week after hatching, the diameter does not increase in size, and has a smaller average diameter than the stage 29 measurements (376.5 μm ± 32.4 μm [n = 10], a 12% decrease). The thickness of the olfactory organ by approximately one week after hatching increases 89% from stage 29 (average depth is 106.7 μm ± 14.0 μm [n = 10]). In addition, an olfactory pit appears in the center of the OE, and after sectioning the organ is found to be invaginated with a dome of OE on top. Cilia stained with AcTub thickly lined the lumen of the pit.

Surface visualizations in whole-mount shows large cilia clusters in surrounding the OE which is apparent over the entire embryo (Figure 4.2 A). The surface of the organ contains smaller

clusters of cilia than the rest of the epithelium and cell bodies that appear to have internalized cilia (Figure 4.2 B). Deeper into the tissue, the underlying neuropil of the olfactory organ gathers into the olfactory nerve (Figure 4.2 C). In week old hatchlings, the AcTub shows more cell bodies and bundles of cilia that appear sub-surface, which are referred to as internalized cilia, than the earlier stages (Figure 4.2 D), although surface cilia are still observable around the embryo (not shown). The internalized cilia had a mean diameter of 13.5 μm ± 2.0 μm (n = 12). Anti-AcTub labeling was also conducted in a double-label experiment with anti-HA in the olfactory organ. At high magnification, HA-labeled cell bodies (red, arrows) appear to be completely independent of the AcTub labeling, and no co-expression is apparent (Figure 4.2 F). The location of ciliary tufts in relation to the HA-LIR cells are variable, sometimes appearing near the HA-labeled cell bodies or neurites, but not consistently.

4.2.1.1 Synaptotagmin

The synaptotagmin probe (previously designed for *S. officinalis*, Nomaksteinsky et al., 2013) was used for *ISH*. It is abundant in the olfactory organ underneath the outer-most layer of OE and extends toward the underlying neuropil (Figure 4.3 A). The dark staining of synaptotagmin probe can also be clearly visualized in whole-mount, as the rest of the head and mantle epithelium do not have synaptotagmin-positive staining (Figure 4.3 B).

4.2.1.2 FMRFamide-related Peptides

FaRP-like immunoreactivity (-LIR) showed dimly labeled bipolar cell bodies (mean 8.4 μm ± 1.5 μm in diameter, n=11) that project one strongly fluorescent thin neurite to the surface of the OE, and the other neurite to the olfactory neuropil below the epithelium (Figure 4.4 A-C). The neuropil under the olfactory organ is approximately 38.8 μm in width by 84.1 μm in length (Figure 4.4 A).

The olfactory nerve (mean diameter = 10.3 μm ± 1.6 μm [n = 2]) is also visible in anti-FMRFa immunohistochemical sections. It starts in the swelling of thick neuropil immediately under the olfactory organ and follows the curvature of the olfactory organ before traversing posteriorly to the olfactory lobe (Figure 4.4 B).

The olfactory organ of a stage 27 embryo also contained cell bodies that were visible with *ISH* of a *S. officinalis* FaRPs mRNA probe that was previously designed (Aroua et al., 2011). The FaRPs mRNA antisense probe labels the olfactory organ, as the epithelium of the head and mantle is devoid of FaRP-positive staining (Figure 4.5 A). This positive staining in the olfactory organ is absent with the FaRPs mRNA sense probe, which was used as a control (Supplementary Figure A2.2). At higher magnification, ~33 cell bodies (average diameter ~10 μm) can be quantified in the olfactory organ (Figure 4.5 B). No axons nor olfactory nerve are apparent via *ISH*. Figure 4.5 C and D shows the distribution of the FaRPs-*ISH* labeled cell bodies (n=13, diameter = ~10 μm) through two representative sections (40 μM thick) of olfactory organ in an anterior (Figure 4.5 C) and medial section (Figure 4.5 D).

4.2.1.3 Serotonin

There was no labeling in the cell bodies of the olfactory organ, 5-HT-LIR was completely isolated to the neuropil and nerve beneath the OE. This immunoreactivity is visible via immunohistochemistry with both DAB (not shown) and fluorescence (Figure 4.6 A, B). The neuropil never extended to the edges of the OE; it is restricted to an area 251.7 μm ± 45.6 μm in length and 49.3 μm ± 25.3 μm thick (n = 4) at a mean depth of 53.9 μm ± 7.0 μm (n = 5) from the surface of the OE (Figure 4.6 A, B).

4.2.1.4 APGWamide

APGWa does not have any immuno-positive cell bodies or neurites in the olfactory organ, although the outer membrane neuropil of the optic lobe is intensely immuno-positive (Figure 4.7 A). To confirm the lack of APGWa staining, a double-label experiment with anti-FMRFa and anti-APGWa showed FaRP-LIR cell bodies in the olfactory organ but no APGWa-LIR (not shown).

4.2.2 DiI and the Olfactory Nerve

A crystal of DiI, previously placed directly on the olfactory organ for 24 hrs, permeated into the olfactory nerve for several months. By looking at individual sections, I can map the pathway of the olfactory nerve as it projects from the olfactory organ and terminates in the olfactory lobe (Figure 4.8 A, B, grey). As the olfactory organ is positioned more anteriorly than the posterior apex of the optic lobe, the nerve first travels posteriorly up the ventral side of the head to reach the top of the optic lobe before turning almost 180º and descending anteriorly to the olfactory lobe which sits on the optic tract medial to the two optic lobes (Figure 4.8 A, B). Unsurprisingly, the brightest staining is where the crystal was placed on the surface of the OE (Figure 4.8 C). The olfactory nerve projects from the medial basal neuropil and immediately bends to follow the posterior curve of the optic lobe (Figure 4.8 C, D). Sections of the nerve can be followed around the ventral to the medial edge of the optic lobe (Figure 4.8 E), where it changes direction and begins to project dorsally, through the brain, to the olfactory lobe on the dorsal side (Figure 4.8 E, F). Once it reaches the olfactory lobe, the nerve immediately fans into multiple small branching projections that become much fainter than the main nerve and therefore harder to visualize (Figure 4.8 F).

The olfactory nerve is already completely developed by stage 25 and can be traced around the optic lobe to the olfactory lobe in sections stained with anti-AcTub. The olfactory nerve has a smaller diameter than in later stages (14.6 μm ± 4.0 μm, n= 4) in comparison to the 20.4 μm ± 3.0 μm (n= 4) that was described in stage 30.

4.2.3 The Development of the Olfactory Lobe

The olfactory lobe is composed of loosely organized neuropil by stage 25, approximately 107 μm across (left-right) and 160 μm in length (along the dorsal-ventral axis). In late stage embryos (stage 27-29), the neuropil averages approximately 255.4 μm ± 86.5 μm (n = 15) in length (dorsal-ventral axis) and 89.4 μm ± 48.3 μm (n = 15) in width (left-right) across sections. As an extension of the optic tract, the lobe also has a substantial thickness (along the anterior-posterior axis) and is easily recognizable as being a collection of three lobules (posterior, medial, anterior, or also known as lobules one, two, and three, respectively). The lobules are not perfectly in line with each other and are off-set in such a way that in medial sections, both lobule one and two are visible in the same 30 μm thick section, and in more anterior sections lobules two and three are visible together. In transverse sections, the olfactory lobe is widest on its dorsal end and narrows towards the ventral end forming a triangular shape (See Figure 1.3). In addition, the lobe tapers at its anterior and posterior ends, so that the narrowest regions of neuropil are in the far anterior end (lobule three) (159.5 μm x 32.9 μm), and the widest regions are the most median section (256.2 μm x 89.6 μm). The posterior sections are composed of a layer of neurons that leads to a central neuropil core surrounded by neurons in more anterior sections. Lobule three is composed primarily of neuropil with fewer cell bodies than lobules one or two due to it being the most interwoven with the optic tract. Including the neurons surrounding the olfactory lobe neuropil, the total lobe length (dorsal-ventral) averages to approximately 271.3 μm ± 81.9 μm (n = 11) and average mean lobe width (left-

right) is 127.4 μm ± 46.4 μm (n = 11), with the smallest areas being in the anterior-most and posterior-most sections (130.0 μm x 70.5 μm and 136.4 μm x 81.1 μm, respectively).

In the week-old hatchlings, the olfactory lobe has not changed in structure, shape or organization, but has increased greatly in size from stage 29. The neuropil in the anterior and posterior sections average approximately 411.7 μm by 195.2 μm and 435.4 μm by 67.0 μm. The average size of the total lobe length (dorsal-ventral) averages to approximately 528.1 μm ± 67.0 μm (n = 15) and mean lobe width (left-right) is 213.0 μm ± 78.4 μm (n = 15). The optic tract innervates the dorsal end of the lobe and the olfactory nerve innervates the ventral end.

4.2.3.1 Acetylated α-tubulin

AcTub was a particularly inconsistent stain in the CNS, resulting in approximately 50% of experiments successful across all stages (n=40). The most consistent immunohistochemistry results (n=3) were from week-old hatchling that were fixed in 4% PFA for 48 hrs. Tubulin stained the neuropil of the CNS, particularly in the dorsal-lateral lobe, olfactory lobe, dorsal-basal, optic lobe, and peduncle lobe (Figure 4.9 A). It also demonstrated the interconnectivity of the lobes via long projections extending from one neuropil to another; in particular, the peduncle commissure between the olfactory lobe and the peduncle lobe Figure 4.9 B) and the optic commissure, between the dorsal-basal and olfactory lobe (Figure 4.9 D).

4.2.3.2 Synaptotagmin

Synaptotagmin mRNA stains dark regions of cell bodies surrounding lobes of the CNS. (Figure 4.10). The dark outlines delineate the border between the cell body and neuropil layers. In the most posterior section, the peduncle lobe is connected to the dorsal-basal lobe through the peduncle commissure (Figure 4.10 A). In Figure 4.10 B, olfactory lobule one is more pronounced and its connection to the dorsal-lateral lobe is visible. In more anterior sections, the orientation of

the peduncle and dorsal-basal lobes are more apparent (Figure 4.10 C). In the anterior sections, olfactory lobules two and three connect to the dorsal-basal lobe via the optic commissure (Figure 4.10 D).

4.2.3.3 FMRFamide-related Peptides

FaRP-LIR is almost exclusively limited to lobule one, although there are a few FaRP-positive cell bodies visible in lobules two and three. There are consistently FaRP-LIR cell bodies surrounding a central neuropil that connects to the optic commissure (Figure 4.11C). In a posterior section, the first cell bodies of olfactory lobule one are labeled (average cell body diameter 11.3 μm ± 2.7 μm [n=17]; Figure 4.11 A). As the sections progress in an anterior direction, the neuronal surface of olfactory lobule one is visible (cell body average diameter= 10.6 μm ± 2.0 μm [n= 23]; Figure 4.11 B). The central core of neuropil is visible in the most anterior sections of lobule one, and the cell bodies of olfactory lobule two are also visible (Figure 4.11 C).

Intense FaRP-LIR staining was also present in the rest of the brain, including cell bodies and a centralized neuropil in the dorsal-basal lobe (Figure 4.12 A). There are also connections between the dorsal-basal and olfactory lobe through the optic tract and peduncle commissure which connects the dorsal-basal, olfactory lobe, optic gland, and peduncle lobe (Figure 4.12 B).

FMRFa mRNA antisense probe stains a large quantity of neurons in the olfactory lobe (mean diameter approximately 10 μm, n=45, Figure 4.13 A'-F'). The general shape of the olfactory lobule is also apparent, with most of the olfactory neurons located dorsally and as the lobe tapers to a narrow point on the ventral end (Figure 4.13 A-F).

4.2.3.4 Serotonin

5-HT-LIR is present in both neurons and neuropil throughout the CNS of *S. officinalis*. It is found in neurons of the optic and dorsal-basal lobe, and the fibers of the peduncle lobe and olfactory nerve. The olfactory nerve innervates the ventral end of the olfactory lobule one (Figure 4.14 A). The neuropil is apparent in more anterior sections with a few cell bodies around the periphery of lobule two (Figure 4.14 B). The neuropil is connected to the dorsal-basal lobe by the thick peduncle commissure. Upon viewing at a higher magnification of a medial section, neurons project their axons to the cluster of neuropil which does not seem to have any consistency of layout or directionality (Figure 4.14 C). To confirm the staining without fluorescence, DAB was used to visualize 5-HT-LIR in the neuropil of the olfactory lobe (Figure 4.14 D and insert).

4.2.3.5 APGWamide

Despite the lack of APGWa in the olfactory organ, the neuropeptide is abundant in olfactory lobe neurons (mean cell body diameter 10.7 μm ± 2.3 μm [n=43]) and core neuropil and occupies a high percentage of the volume in the lobe. The most posterior section shows only APGWa-LIR neurons around the exterior surface of the olfactory lobule one (Figure 4.15 A). More anterior sections demonstrate how cell bodies wrap around the peripheral and ventral edges of lobule one with a centralized neuropil (Figure 4.15 B). As the section moves deeper into lobule two, the beginning of the optic commissure is visible (Figure 4.15 C). The anterior most section contains the cell bodies of lobule two, the neuropil of lobules three, and the optic tract connecting the lobules to the dorsal-basal lobe.

APGWa is also present in the rest of the CNS, particularly in the neuropil of the optic lobe, peduncle lobe, optic tract, and dorsal-basal lobe (Figure 4.16 A). The densest population of APGWa-LIR neurons is in the olfactory lobe. The staining also projects down to the sub-esophageal mass and the optic lobe (Figure 4.16 B).

The olfactory lobe was double-labeled with anti-FMRFa and anti-APGWa to determine spatial orientation of the different neurotransmitters and to determine if APGWa and FMRFa were colocalized. In the posterior surface of olfactory lobule one, approximately 66% (n~ 50) of the neurons are APGWa-positive, 26% (n~ 25) are FMRFa-positive, and 8% (n~ 6) are co-localized (Figure 4.17 A). Individual neurons were analyzed in each slice of the Z-stack for shape, position, and size, to ensure that there was no overlap artifact. In more anterior sections, more FaRP-LIR-cell bodies were apparent in the medial dorsal region of lobule one, and the interior neuropil was visible with anti-APGWamide staining (Figure 4.17 B). Both FMRFa and APGWa-positive fibers were visible projecting into the anterior end of lobule one (Figure 4.17 C). Although no co-labeling was apparent in the fibers of the nerve, several cell bodies in the dorsal end of the lobule are co-labeled. Distinct co-labeling of anti-FMRFa and anti-AGPWa can be seen at high magnification of the posterior cell body layer of olfactory lobule one (Figure 4.17 D).

4.2.3.6 Phalloidin

Phalloidin was analyzed around the olfactory lobe region (Figure 4.18 A-E). F-actin filaments in the neuropil were brightly labeled in the optic, peduncle, and olfactory lobe, with labeling in the supra-esophageal mass in more anterior sections. The neuropil was semi-organized with a general directionality, although individual fibers often crossed each other at different angles. This observation is less true for the neuropil at the center of lobes, in which individual fibers seem to project at all angles without any organization. At no point were there round clusters of F-actin apparent in the olfactory lobe or anywhere else in the brain.

4.3 Discussion

Taken together, antibodies against neurotransmitters and structural stains used in this thesis provide an in-depth description of the organization and development of the olfactory lobe. To determine what hypothetical function the neurotransmitters and neuropeptides might have in the olfactory lobe, I first analyzed their presence in the olfactory organ. If there was immunoreactivity in the OSNs, that would suggest that it was an OSN neurotransmitter. Therefore, any presence of the same neurotransmitter in the olfactory lobe would be valuable in determining its organization, particularly if the lobe contains glomeruli. If the neurotransmitter or neuropeptide were localized elsewhere, this information would have different implications when analyzing the results from the olfactory lobe. For this reason, the immunohistochemistry and *ISH* results in the olfactory organ are discussed first, before discussing the results from the olfactory lobe.

ISH labels endogenous mRNA; therefore, the synaptotagmin mRNA probe labels the cell bodies that contain the message for the synaptic protein (Figure 4.10) and would not label the synaptic terminuses, unless the mRNA is transported down the axons to the synapses. Anterograde messenger transport has not been previously reported for synaptotagmin, although it has for

syntaxin mRNA, a member of the Q-SNARE protein family that interacts with synaptotagmin (Hu et al., 2003; Piper and Holt, 2003). The staining is consistent with other *ISH* in the olfactory organ, with long bipolar cell bodies that project neurites to the surface epithelium and neuropil (Figure 4.3). Likewise, in the synaptotagmin *ISH* in the CNS, the outer neuronal layers of each lobe are darkly labeled, while the neuropil is paler (Figure 4.10). Therefore, synaptotagmin was useful for delineating and identifying the lobes and interconnections because of this dark outline.

Within the olfactory organ, anti-AcTub frequently stained internalized clusters of cilia, which resemble type IV OSNs since they have large ciliated cavities that occupy almost the entire cell body (Figure 3.12; Emery, 1975). They also seem to lack the long distal process that defines a type V OSN. There are several other morphologies that are apparent with AcTub at high magnification (Figure 4.2 E), including type I and type II.

While AcTub has been used consistently in a variety of species, occasionally studies report difficulty visualizing neuronal structures. For example, anti-AcTub in *Bonellia viridis* did not stain any neuronal structures and displayed a higher background noise ratio than other organisms (Hessling and Westheide, 2002). They suggested this species might be more sensitive towards minor protocol variations than other annelids. Likewise, immunohistochemical staining with anti-AcTub in the pygmy squid *I. notoides* did not yield consistent results and was faint in double-labeled experiments, which is consistent with the results in this study (Wollesen et al., 2009). Previous publications suggested that phalloidin is the superior counter-stain for identifying neuronal structures, since phalloidin has a smaller molecular weight, less procedural steps, and is more reliant in labeling neurites. While external and internal cilia were consistently brightly labeled, particularly in the OE (Figure 4.2), neuronal structures were not. Even in sections, neuropil of the CNS was often faint or non-existent when paired with a second label. However, there were several occasions, particularly in

the week-old hatchlings fixed with 4% PFA for 48 hrs, where anti-AcTub in sections labeled neuropil, and resulted in similar staining to that labeled with phalloidin (Figure 4.9, Figure 4.19). Due to these restrictions and inconsistency, phalloidin may be the more reliable structural stain for cephalopods, at least in those species where consistent anti-tubulin immunohistochemistry has not been demonstrated.

FaRP-positive staining is present in several bipolar OSNs in the olfactory organ, with dendrites that extend to the surface of the OE and axons to the olfactory nerve (Figure 4.4 and Figure 4.5). These neurons are morphologically more diverse than the OSNs previously described as HA-positive in Chapter 3. While there are some FaRP-LIR neurons that appear very similar in size, shape, and position in the olfactory organ to the type V OSN, there are also several FaRP-positive neurons that are more consistent with descriptions of type I neurons (Emery, 1975). These neurons are more elongated in shape, closer to the surface of the OE, and slightly smaller than the type V OSNs (Figure 4.4, insert). This immunostaining, in conjunction with the abundance of cell bodies visible with FMRFa *ISH* in the olfactory organ*,* suggests that FaRPs are another neurotransmitter of the OSNs. Due to the high immunofluorescence of the olfactory nerve, it would also be expected to see FaRPs-LIR in the olfactory lobe.

There is a high presence of FaRP-LIR and ISH-positive neurons in the olfactory lobe (Figure 4.11, Figure 4.13, and Figure 4.17), suggesting that FaRPs are also a second order neuropeptide in addition to being a neuropeptide of the OSNs. This pattern is similar to what was observed with HA and HDC in the previous chapter. However, HA and FMRFa, as two different neurotransmitters, should have different functions.

To confirm the fluorescent immunohistochemical staining of anti-FMRFa and anti-5-HT-LIR in the olfactory lobe and organ, a series of experiments were conducted using DAB which

validated the fluorescent results (Figure 4.14; FMRFa not shown). Because DAB includes an extra conjugation step (Avadin + Biotin + horseradish peroxidase), it has an amplification effect in which the final immunohistochemical staining is often more sensitive than a fluorescent conjugated-secondary antibody. Again, DAB confirms that 5-HT in the olfactory organ was confined to the neuropil of the olfactory organ, with no 5-HT-LIR cell bodies in the periphery. Due to the lack of cell bodies in the olfactory organ (Figure 4.6), 5-HT may be an efferent modulator of the OSNs.

5-HT neuropil in the olfactory lobe (Figure 4.14) contradicts a previous study of 5-HT in adult *I. notoides* which reports only 5-HT-LIR cell bodies with few fibers in the neuropil (Wollesen et al., 2010b). In this study, both cell bodies around the olfactory lobe and brightly stained central neuropil are present in the olfactory lobe. The explanation for this major discrepancy is unknown, except that perhaps there are species-specific differences in the structuring of the olfactory lobe. However, this is unlikely as it would be a drastic change in neurotransmitter physiology between two closely related species. Another possibility could be that a more narrowed study that is focused on a single lobe resulted in additional details that were previously overlooked in a study in which the objective was to categorize the presence of a single neurotransmitter in the entire CNS.

Anti-APGWa did not show any cell bodies in the olfactory organ (Figure 4.7), although cell bodies in the OE have been previously described with APGWa-LIR in previous studies (Polese et al., 2015). The cause of this discrepancy is currently unknown and deserves further investigation. Based upon the results of this study, APGWa is not a neurotransmitter of the OSNs. The clear majority of the APGWa-LIR described in this study is in the olfactory lobe. Regardless, APGWa-LIR is useful in describing the structure and interconnectivity of the lobe (Figure 4.15 and Figure 4.16). The olfactory lobe is heavily integrated with the reproductive system, as apparent by the abundance of the APGWa, a reproductive neuropeptide in molluscs, in the olfactory lobe. In

addition, there are many visible inputs from the olfactory lobe to those lobes described as part of the reproductive system, including the dorsal-basal and peduncle lobes (Figure 4.16).

Phalloidin, in addition to being a marker for musculature, has previously been suggested to be a general marker for glomeruli across multiple diverse species (Rossler et al., 2002). Phalloidin reliably labels glomeruli and distinct F-actin aggregations are a fundamental feature of glomeruli across phyla due to their role in synaptic plasticity within the olfactory centers. Here, I report no patterns of F-actin which resemble glomeruli as previously described (Figure 4.18). Instead, F-actin stains a diffuse neuropil of overlapping fibers that do not seem to have a consistent directionality.

In conclusion, there are no spherical clusters of synapses in the olfactory lobe of *S. officinalis*, even at a week after hatching, nor does the neuropil seem organized in any large-scale fashion. Therefore, cuttlefish may have an alternative means of organizing their olfactory inputs at the early life history stages other than the glomerular structures found in vertebrates, insects, and crustaceans. This conclusion has major implications about the homology and evolution of the olfactory system, as will be discussed in the next chapter.

4.4 Development of the Olfactory System

The olfactory system is already developing by the stage 25, the earliest stage presented here. The olfactory organ, including its underlying neuropil, is already in place, although much smaller in all dimensions than the more developed embryos (Figure 4.2). The olfactory nerve is also visible by stage 25. As the embryos develop, the diameter of the olfactory organ and nerve increase while the thickness of the organ decreases, most likely due to the stretching of the organ over a larger surface area as the embryo grows. Between stages 29 and 30, the opening to the olfactory pit expands at the surface of the epithelium, and the olfactory organ appears more as an invaginated structure than a bump on the cheek hills. The pit diameter expands with the development of the embryo, so that by

a week after hatching, it is large relative to the organ. Numerous cilia appear to line the lumen of the pit, as can be seen with anti-AcTub (Figure 4.2). It is yet unknown if the size of the olfactory pit affects the perception abilities of embryos, as it is difficult to isolate olfactory perception from other chemosenses, and no olfactory ablation studies have been conducted in embryos.

The olfactory lobe neuropil at stage 25 is a very diffuse collection of fibers, visible both with AcTub and phalloidin (Figure 4.19). As the embryo develops, its structure begins to take shape. The overall shape of the olfactory lobe (triangular in transverse sections, elongated through the anterior-posterior axis and differentiated into individual lobules) is in place by stage 27. This lobe shape does not change, even through hatching. The size, however, increases from stage 27 through hatching in all dimensions. The number of fibers and surrounding neurons also increases in density from a sparse neuropil at stage 25 to a dense composition of indistinguishable fibers at hatching.

The olfactory organs increased an average of 25% in diameter from stage 25 to 29, but decrease in depth by 13%. In comparing the stage 29 embryos to the week-old hatchlings, the olfactory organs do not have a significant change in diameter (-12%). However, the depth increased by 89%. This large increase in depth is consistent with the timing of the development of the olfactory pit and the invagination of the olfactory organ.

The olfactory lobe increased in area an average of 33% from stage 25 to 29. There was also considerable growth even after hatching; from stage 29 to one week after hatching, the olfactory lobe expanded 393%. The changes were most apparent along the length of the lobe (dorsal-ventral) although there was also a large expansion in width (left-right axis).

It is difficult to comment on the organization of the neuropil in the late stage embryos and hatchlings because the olfactory lobe appears an almost solid structure of continuous overlapping neuropil as stained with phalloidin and AcTub (Figure 4.19 B).

4.5 Olfactory Organization in Cephalopods

If glomeruli are absent in cephalopods, then these animals must have evolved a different mechanism for organizing olfactory inputs from the periphery into a repeatable and recognizable signal for the brain to process. In the Introduction, I stated that at the macroscopic scale the olfactory system can be sub-divided into three parts, 1) sensory epithelium, 2) projection or nerve pathway, and 3) an olfactory processing center in the CNS. More accurately, however, would be the addition of a fourth subdivision, the integration of the olfactory lobe with the rest of the brain. This can be clearly seen by the immunohistochemistry and structural stain experiments with anti-5-HT, anti-FMRFa, anti-APGWa, anti-AcTub, and phalloidin as fibers extend from the olfactory lobe to the dorsal-basal lobe, peduncle lobe, and optic tract (Figure 4.9, Figure 4.10, Figure 4.12, Figure 4.16 and Figure 4.18).

Based upon the evidence presented here, I propose that the organization of olfactory inputs in cephalopods cannot be understood without first understanding the integration of the olfactory lobe with higher brain center (summarized in Figure 4.20).

The integration of the olfactory lobe with the brain was first described through the Golgi method (Messenger, 1979). The olfactory lobe is thought to be innervated by the optic, peduncle, and basal lobes, and peduncle commissure. It was previously noted that the neuropils of the peduncle and olfactory lobe are so intertwined that there must be interaction (Messenger, 1979). The peduncle commissure is thought to exit through olfactory lobule one, cross the midline, and innervate the contralateral olfactory lobules two and three, which indicates some sort of cross-talk between the two olfactory lobes.

The olfactory lobe also has a few "assumed" output nerves to the sub-esophageal mass (as seen in Figure 4.16), but most project to the dorsal and posterior section of the supra-esophageal

mass. Olfactory lobule one innervates the lateral-basal lobe and regions of the magnocellular, which are thought to be responsible for jetting and escape responses. It also innervates to the palliovisceral which is thought to control inking behavior.

The olfactory lobe also projects to the dorsal-lateral lobe. The dorsal-lateral lobe has two possible functional interactions with the olfactory system; the detection of danger and/or detection of mates.

The sub-pedunculate, as part of the reproductive system, has been recently described in greater detail. It is thought to negatively control activity of the optic gland, which promotes gonadal development, and is assumed to release GnRH (Di Cristo, Chapter 7., Saleuddin, 2017). No trace of the optic gland is visible in the embryonic stages in *Octopus* and it cannot be found in the planktonic larvae. The optic gland appears in young animals and seems to develop from nerve cells close to the olfactory lobe. It is innervated by FaRP-LIR fibers that originate in neurons in the sub-pedunculate and olfactory lobes. The optic lobe has been suggested to have a stimulatory effect on the GnRH in the optic glands (Di Cosmo and Di Cristo, 1998). This is opposite of the inhibitory effect of the sub-pedunculate via FMRFa-ergic innervation. So far, there have been no behavioral studies tying olfaction to courtship and copulation, but the physiological evidence seems consistent across studies.

In a review of the cephalopod neural networks, the olfactory and peduncle lobes were described as part of the main projection pathway (the optic tract) from the optic lobe (Williamson and Chrachri, 2004). The location of the lobes and direct interconnectivity suggest that the olfactory and peduncle, sometimes referred together as the cephalopod cerebellum, could play a role in processing visual information. This interpretation complicates the current perceived functionality of

the olfactory lobe; however, this interconnectivity must be kept in mind in future analysis of the olfactory system.

The dorsal-basal lobe has efferent connections to the olfactory lobe, peduncle, optic glands, and optic lobes, and a few to the medial basal lobes (Boycott, 1961). It was later confirmed that the lateral fibers of the dorsal-basal lobe seem to terminate in the olfactory lobe (Di Cosmo et al., 2004). This interaction is said to be important for olfactory stimulation of reproduction, and feedback would be necessary from the basal lobes to the olfactory lobes for chemoreception (Messenger, 1971). While FaRPs have previously been described in the dorsal-basal lobe (Wollesen et al., 2012), and have been described in this study as well, the functionality is currently unknown. Two possibilities have been suggested. The dorsal-basal lobe may be a site of learning and memory (Zhang et al., 2012), or, because the basal and peduncle lobes receive sensory information, they must regulate output like swimming, respiration, and muscle movement (Budelmann, 1995).

Therefore, it appears the whole olfactory system can be represented as a chain. The olfactory nerve projects primarily to the olfactory lobe, and that lobe in turn projects to the dorsal-basal and sub-pedunculate, which influences the reproductive system via the optic glands (Woodhams and Messenger, 1974). To focus purely on the olfactory organ, nerve, and lobe, and ignore this final integration of the olfactory lobe with the rest of the CNS, would be to disregard potential sites of integration and organization.


A
St. 25
mantle
eye
arms
B
St. 27
cuttlebone
yolk
C
St. 28
D
St. 29
E
Hatchling

Figure 4.1 The developmental stages of *S. officinalis*. (A) Stage 25; identifiable base on the light orange eyes and T-shape formed by the head and mantle. (B) Stage 27; eyes are red/brown, head has begun to round, and the cuttlebone is visible with 2 rings of calcium deposits. (C) Stage 28; first chromatophores are now visible (arrowhead), eyes are dark brown/black color, the head and mantle have taken on their final shape, and the cuttlebone has 3 rings of calcium deposits. (D) Stage 29; chromatophores continue to multiply and are more pronounced (arrowhead), eyes begin to have iridescence, arms elongate, and the cuttlebone has 4 calcium deposit rings. (E) Approximately one week after hatching, skin is no longer transparent, chromatophores are completely developed. Scale bars are equal to 1 mm.

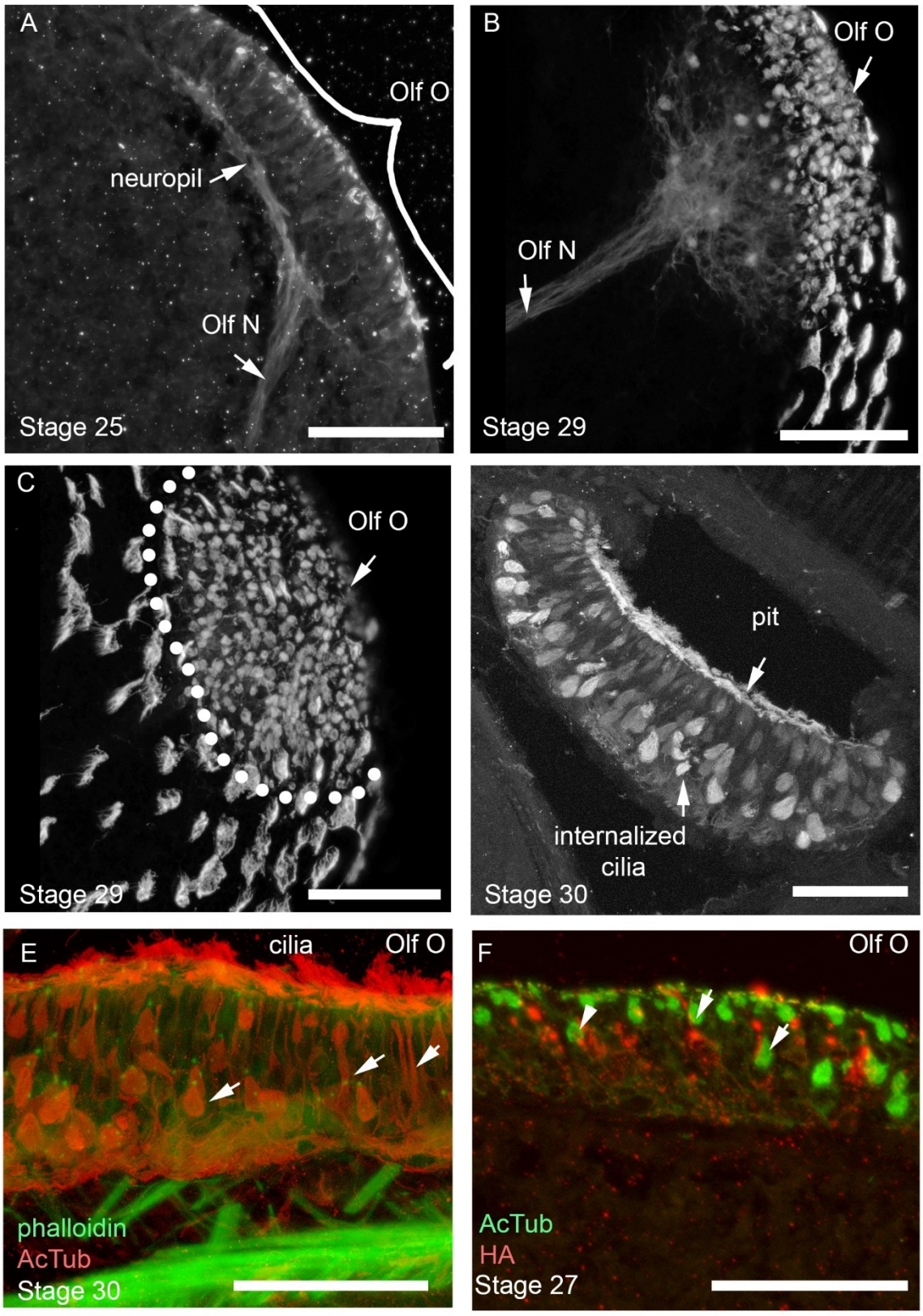
A
Olf O
neuropil
Olf N
Stage 25
B
Olf O
Olf N
Stage 29
C
Olf O
Stage 29
pit
internalized
cilia
Stage 30
E
cilia
Olf O
phalloidin
AcTub
Stage 30
F
Olf O
AcTub
HA
Stage 27

Figure 4.2 Acetylated α-tubulin (AcTub) of the olfactory organ. (A) At stage 25, olfactory organ in section with cilia, neuropil, and olfactory nerve are already developed. (B) A surface view of the OE in a stage 29 embryo. Large cilia surround the olfactory organ and smaller clusters of cilia cover the OE. (C) The structure of the olfactory organ with the olfactory nerve projecting toward the brain and the surface OE cilia. (D) A medial section through a week-old hatchling olfactory organ. Due to its pit and dome shape, the olfactory organ appears like a semi-torus (doughnut shape) when sectioned at an angle. Cilia can be observed lining the inside of the pit (arrows). (E) Double-labeling of AcTub (red) and phalloidin (green) shows minimal co-localization. AcTub shows multiple different cell body morphologies (arrows) in addition to the cilia that lines the lumen of the olfactory pit. (F) Double-labeling of AcTub (green) and anti-HA (red). Again, there is no co-localization between tubulin-LIR and histamine-LIR cell bodies. Olf N, olfactory nerve; Olf O, olfactory organ. Scale bars represent 100 μm.

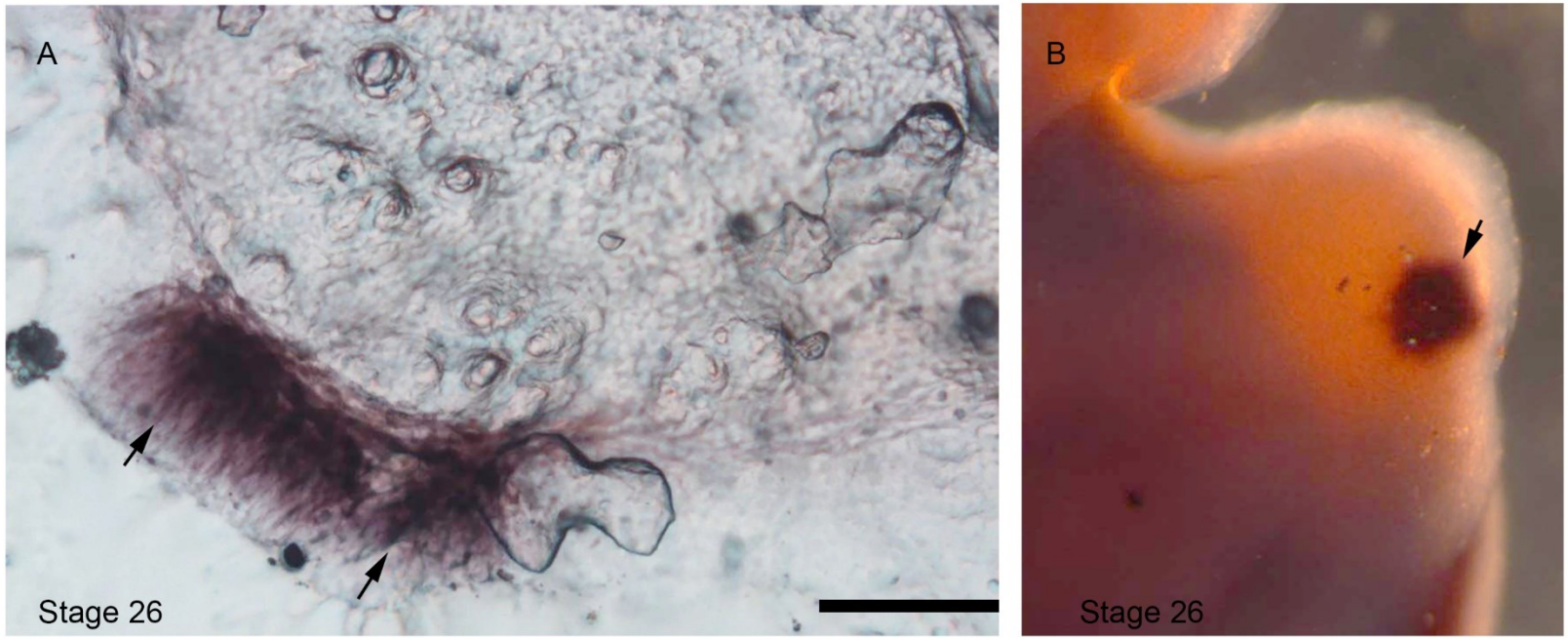
A
Stage 26
B
Stage 26

Figure 4.3 Synaptotagmin mRNA probe for ISH in the olfactory organ. (A) Synaptotagmin probe in a stage 26 embryo in a section of olfactory organ with staining extending from neuropil to sub-epithelium (B) Olfactory lobe labeled with synaptotagmin probe in whole-mount demonstrates the absence of synaptotagmin-containing cell bodies in the head epithelium except for the olfactory organs. Scale bar represents 100 μm.

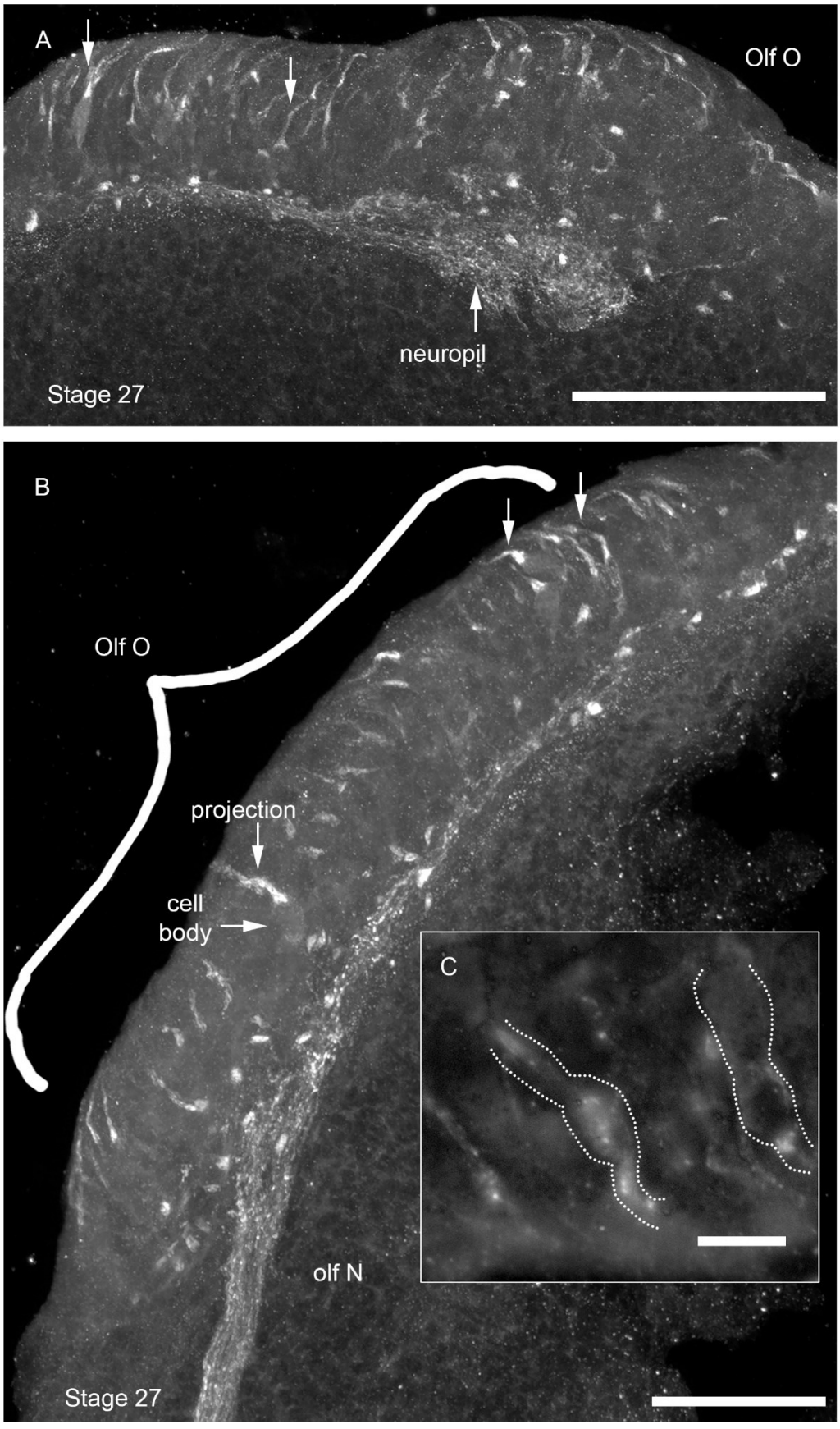
A
Olf O
neuropil
Stage 27
B
Olf O
projection
cell
body
C
olf N
Stage 27

Figure 4.4 Anti-FMRFamide immunohistochemistry in the olfactory organ. (A) Anti-FMRFa in a section of a stage 27 olfactory organ with FaRP-LIR bipolar cell bodies extending neurites to the OE and neurites to the neuropil. (B) A more medial section of the olfactory organ shows the olfactory nerve projecting from the olfactory organ neuropil. (C) A high magnification of FaRP-LIR dimly fluorescent bipolar cell bodies with two brighter projections in the olfactory epithelium. Olf O, olfactory organ. Scale bars: A= 100 μm, B= 50 μm, C= 10 μm.

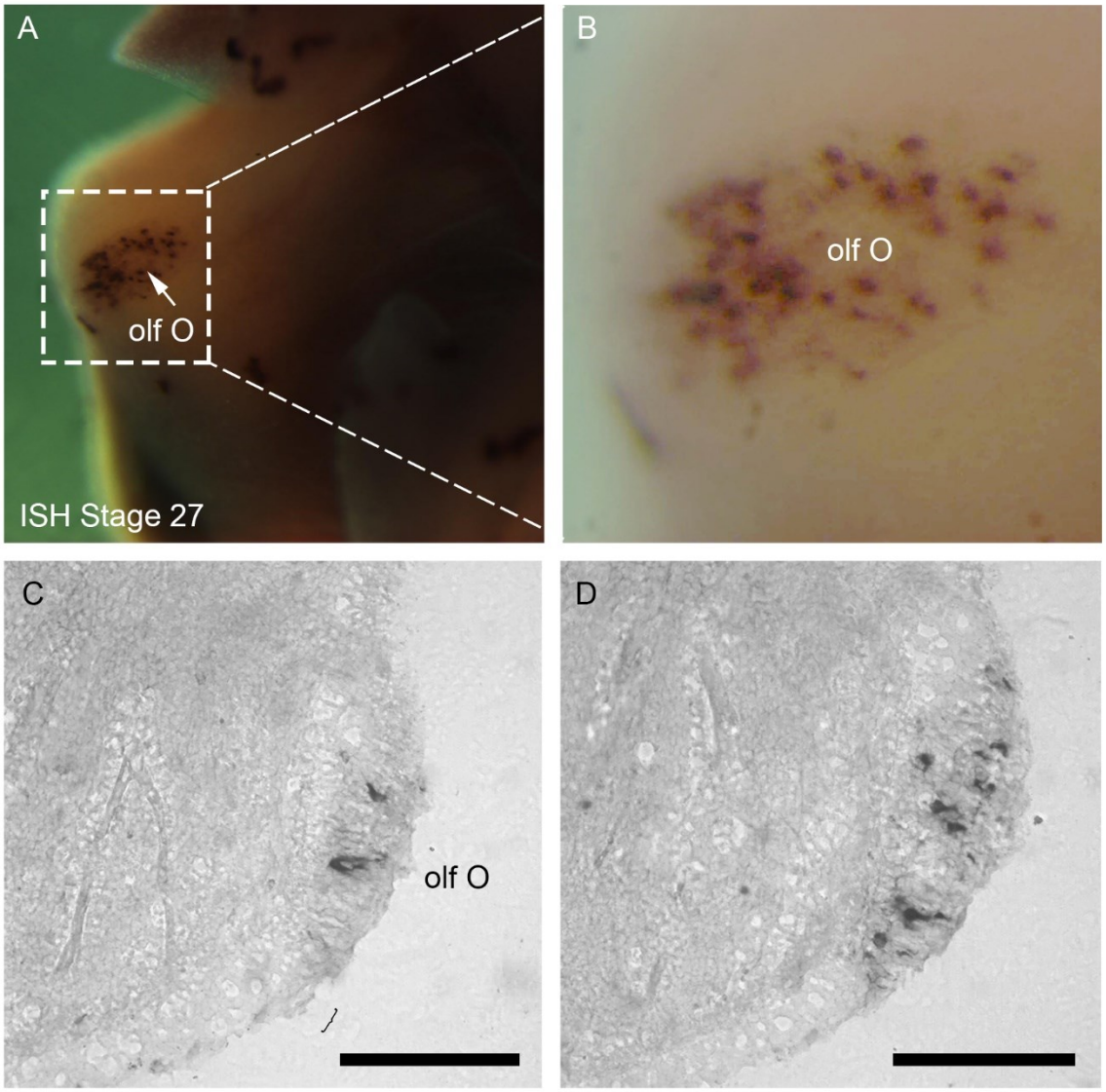
A
olf O
ISH Stage 27
B
olf O
C
olf O
D

Figure 4.5 FMRFamide *ISH* in the olfactory organ. (A) The olfactory organ of a stage 27 embryo in whole-mount has dark labeling of cell bodies exclusive to the olfactory organ region of the head. (B) Higher magnification of the FaRPs-positive cell bodies in (A). (C) A representative anterior section of the olfactory organ containing two FaRP-positive cell bodies. (D) A representative medial section containing 7 FaRP-mRNA containing cell bodies. Olf O, olfactory organ Scale bars represent 100 μm.

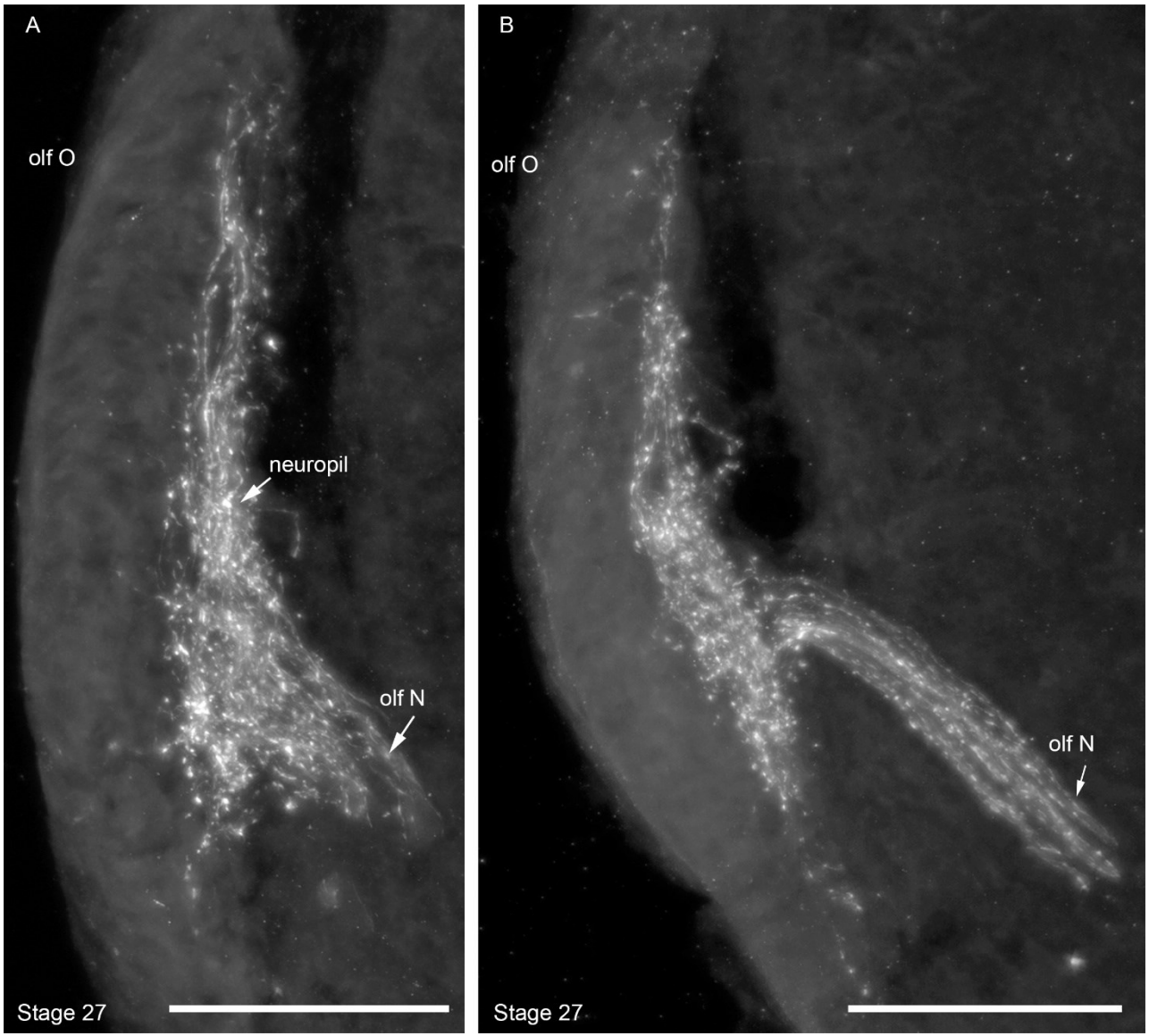
A
olf O
neuropil
olf N
Stage 27
B
olf O
olf N
Stage 27

Figure 4.6 Serotonin immunohistochemistry in the olfactory organ. (A) In a stage 27 embryo, neuropil extends along the basal edge of the olfactory organ and but does not connect to the OE. (B) The olfactory nerve projects from the neuropil in the olfactory organ. Olf N, olfactory nerve; Olf O, olfactory organ. Scale bars represent 100 μm.

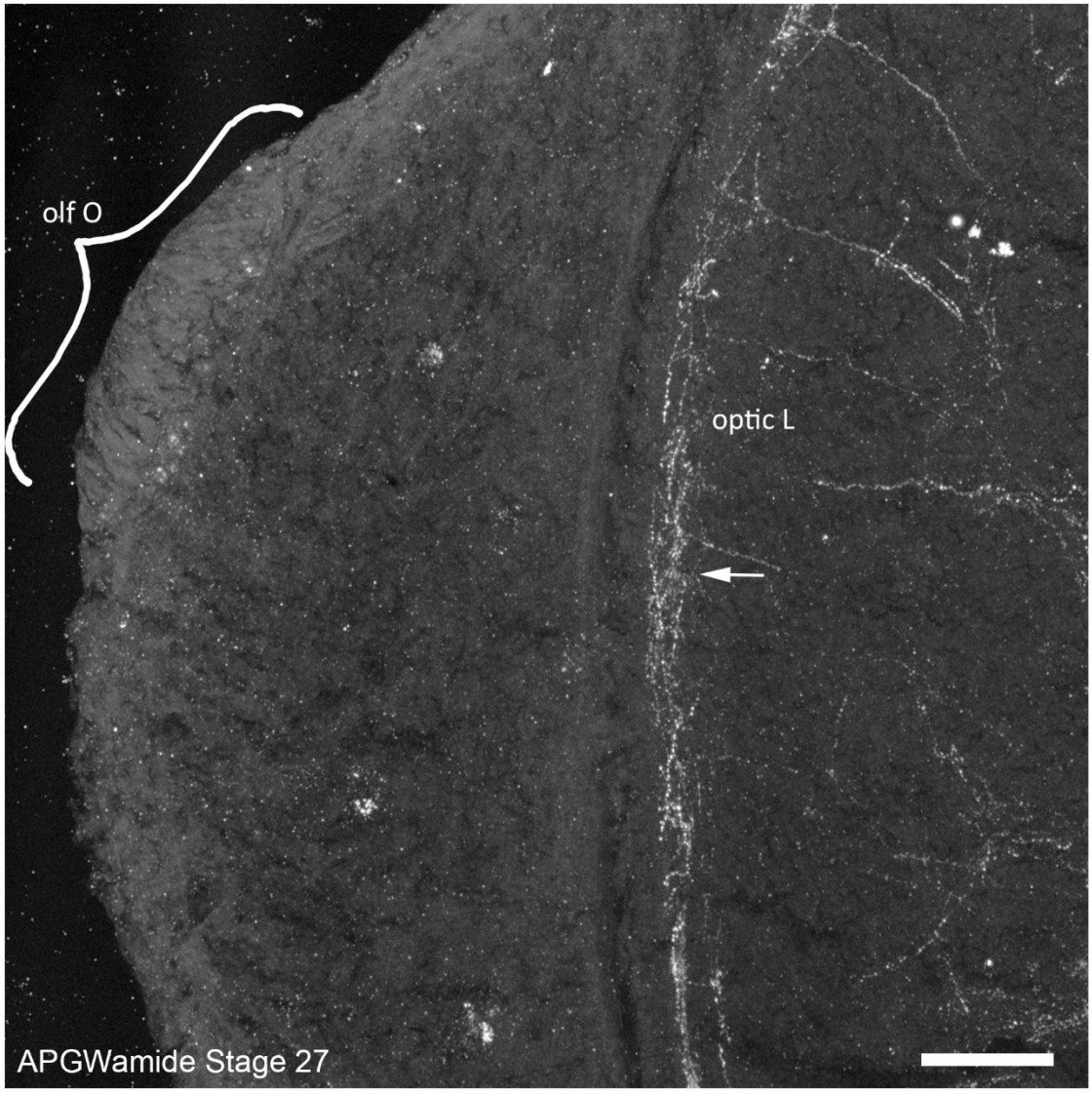

Figure 4.7 APGWamide immunoreactivity in the olfactory organ. (A) The olfactory organ of a stage 27 embryo stained with anti-APGWa has no immunoreactivity, nor observable cell bodies or neuropil. The optic lobe, however, has neuropil that is clearly visible with APGWa-LIR (arrow). Olf O, olfactory organ. Scale bars represent 100 μm.

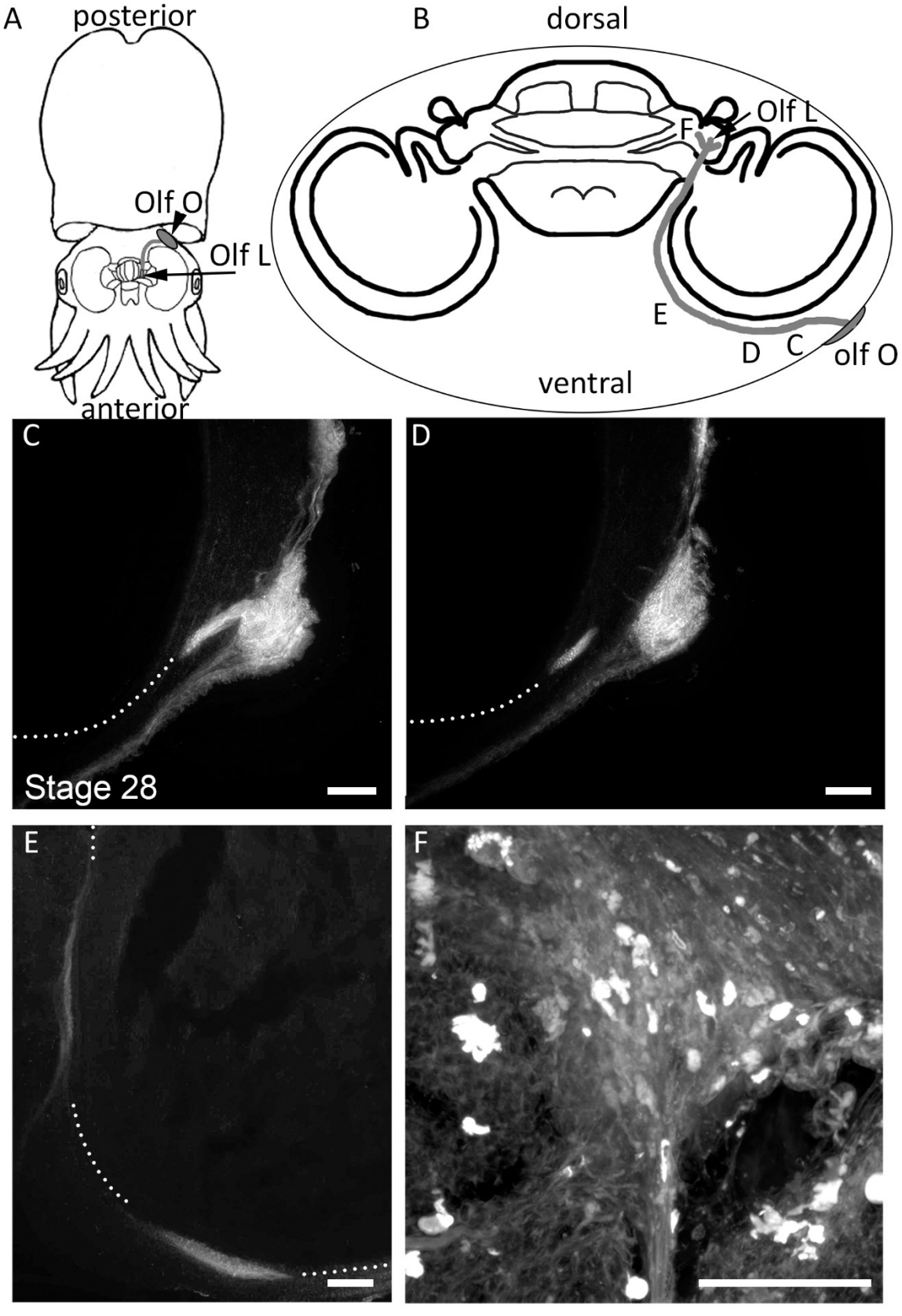
A
posterior
Olf O
Olf L
anterior
B
dorsal
Olf L
F
E
D
C
olf O
ventral
C
Stage 28
D
E
F

Figure 4.8 Olfactory organ and nerve stained with DiI in 40 µm sections. (A) Diagrammatic representation of whole embryo positioned along its anterior-posterior axis demonstrating location of olfactory organ, lobe and nerve (grey). (B) Diagrammatic representation of a transverse section through the brain with dorsal up and ventral down demonstrating respective locations of the olfactory organ on the ventral side and olfactory lobe on dorsal side of brain. (C) Olfactory organ in a stage 28 embryo is brightly labeled and the olfactory nerve can be seen projecting from its base. (D) The next section of olfactory nerve can be seen further away from the olfactory organ as it follows the ventral and posterior curve of the optic lobe. (D) The olfactory nerve begins to curve up (towards the dorsal side) once it reaches the other medial side of the optic lobe. It then projects in an anterior direction through the middle of the brain from the ventral to the dorsal side. (F) The nerve innervates the anterior end of the olfactory lobe where it then branches into smaller nerves. Olf L, olfactory lobe; Olf N, olfactory nerve; Olf O, olfactory organ. Scale bars represent approximately 100 µm.

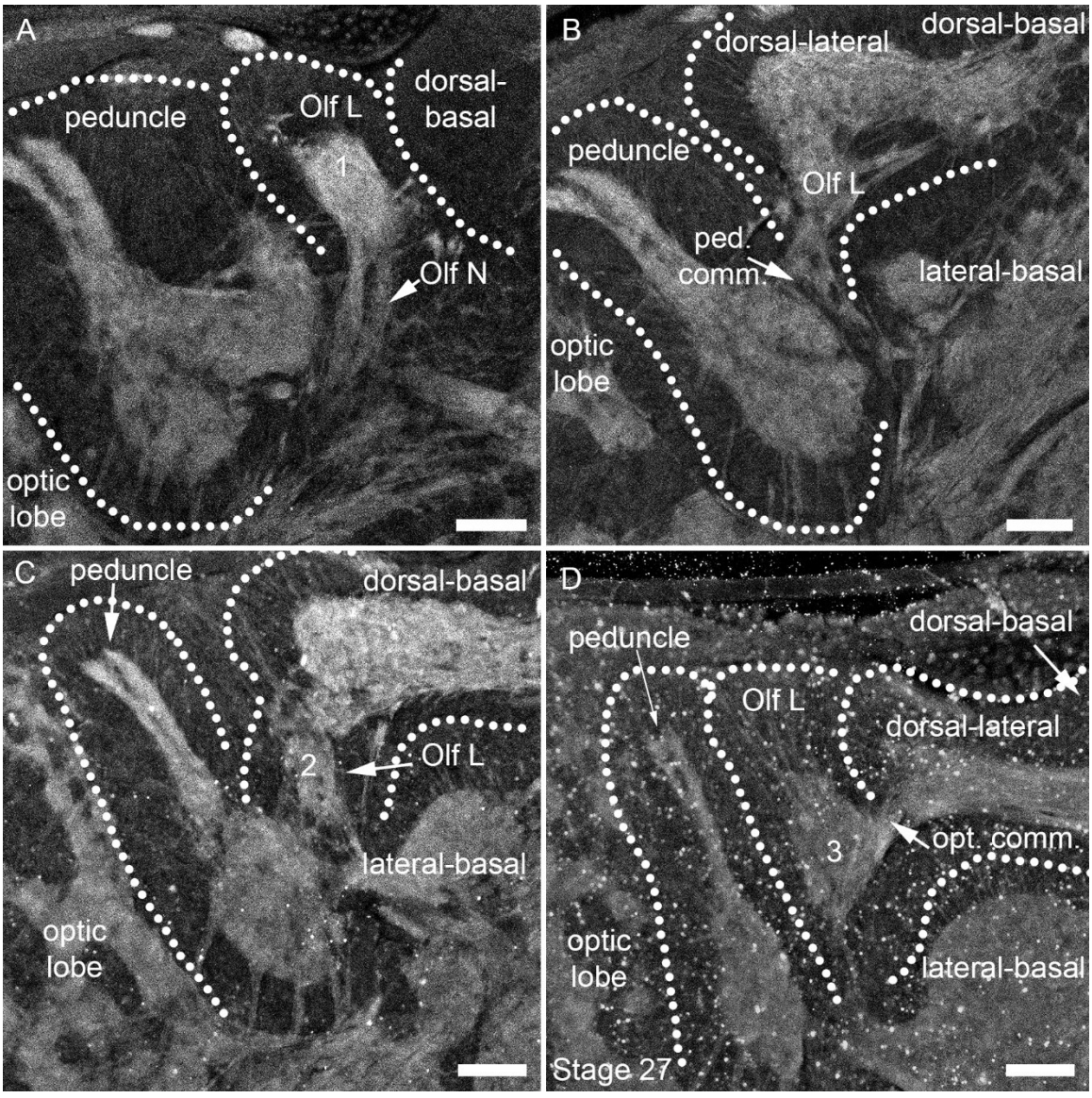
A
peduncle
Olf L
dorsal-
basal
1
Olf N
optic
lobe
B
dorsal-lateral
dorsal-basal
peduncle
Olf L
ped.
comm.
lateral-basal
optic
lobe
C
peduncle
dorsal-basal
2
Olf L
lateral-basal
optic
lobe
D
peduncle
dorsal-basal
Olf L
dorsal-lateral
3
opt. comm.
optic
lobe
lateral-basal
Stage 27

Figure 4.9 Acetylated α-tubulin (AcTub) in the olfactory lobe. Stage 27 embryo in sections from posterior to anterior. From left to right: Optic lobe, peduncle lobe, olfactory lobe, dorsal-lateral lobe, dorsal-basal lobe (up) and lateral-basal lobe (down). (A) Most posterior section shows olfactory lobule one with incoming olfactory nerve at the ventral end. (B) Olfactory lobule two connected to the peduncle lobe via the peduncle commissure (ped. comm.). (C) A more anterior section showing connectivity between olfactory lobule two and lateral-basal lobe. (D) Olfactory lobule three (ventral, connected to the dorsal-lateral lobe) and part of lobule two (projecting dorsally) in an anterior section of the CNS shows the optic commissure (opt. comm.) connecting the olfactory lobe and dorsal-basal lobe. Olf L, olfactory lobe; Olf N, olfactory nerve; Olf O, olfactory organ; ped. comm, peduncle commissure. Scale bars represent 100 μm.

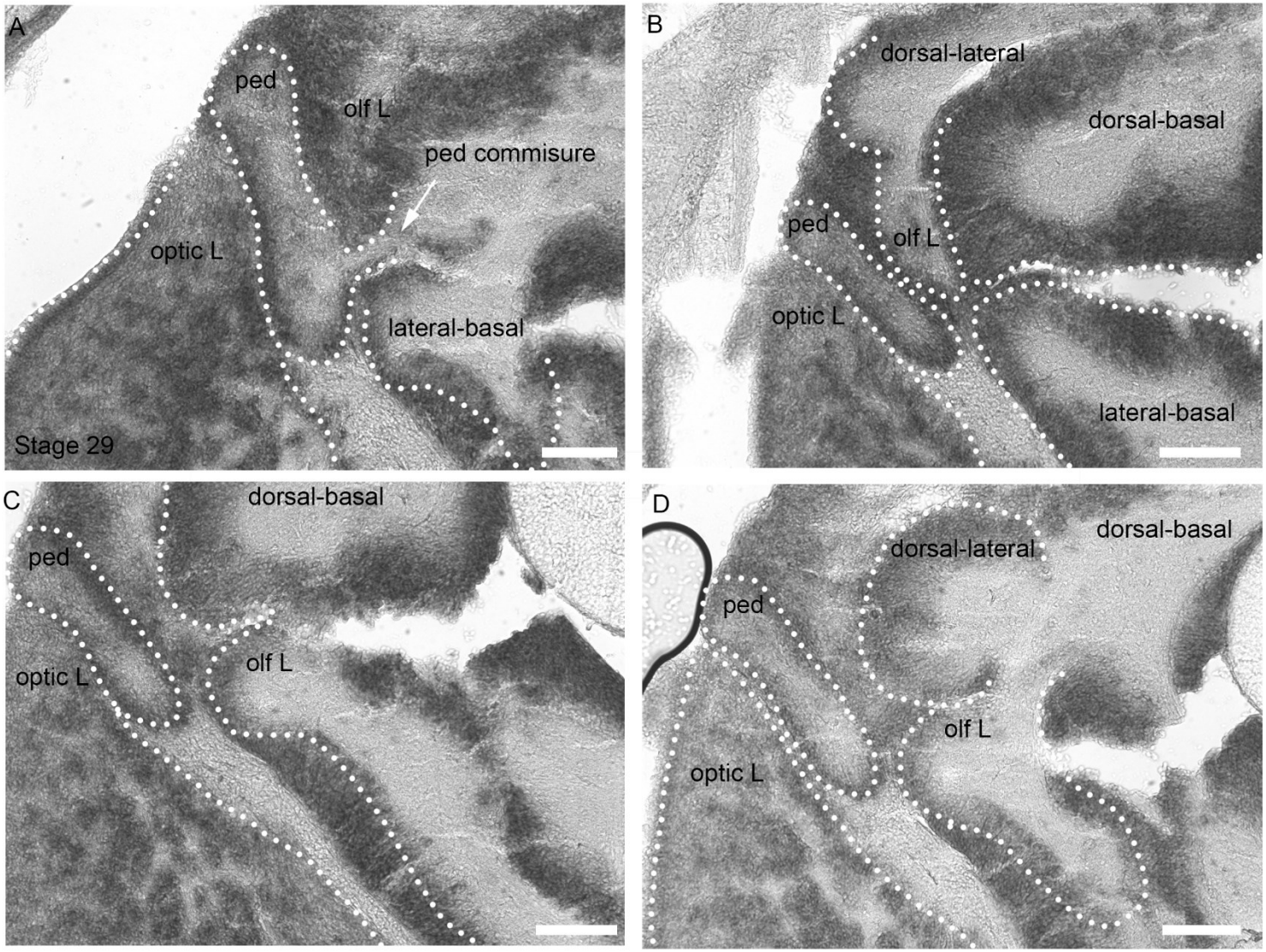
A
ped
olf L
ped commisure
optic L
lateral-basal
Stage 29
B
dorsal-lateral
dorsal-basal
ped
olf L
optic L
lateral-basal
C
dorsal-basal
ped
optic L
olf L
D
dorsal-basal
dorsal-lateral
ped
olf L
optic L

Figure 4.10 Synaptotagmin *ISH* probe in the olfactory lobe and surrounding CNS. From posterior to anterior sections (40 μm). (A) Olfactory lobe (Olf L) in stage 29 embryo. The peduncle lobe (ped) in posterior section connects to the dorsal-basal lobe via the peduncle commissure (ped. commissure). (B) The olfactory lobe is more clearly visible in a more anterior section as an extension of the dorsal-lateral lobe. (C) The olfactory lobe is a ventral extension of the dorsal-basal lobe and medial to the peduncle and optic lobes. (D) The anterior most olfactory lobe (lobules two and three) connect to the dorsal-basal lobe through the optic commissure. Olf L, olfactory lobe; Olf O, olfactory organ; optic L, optic lobe, ped, peduncle lobe. Scale bars are equal to 100 μm.

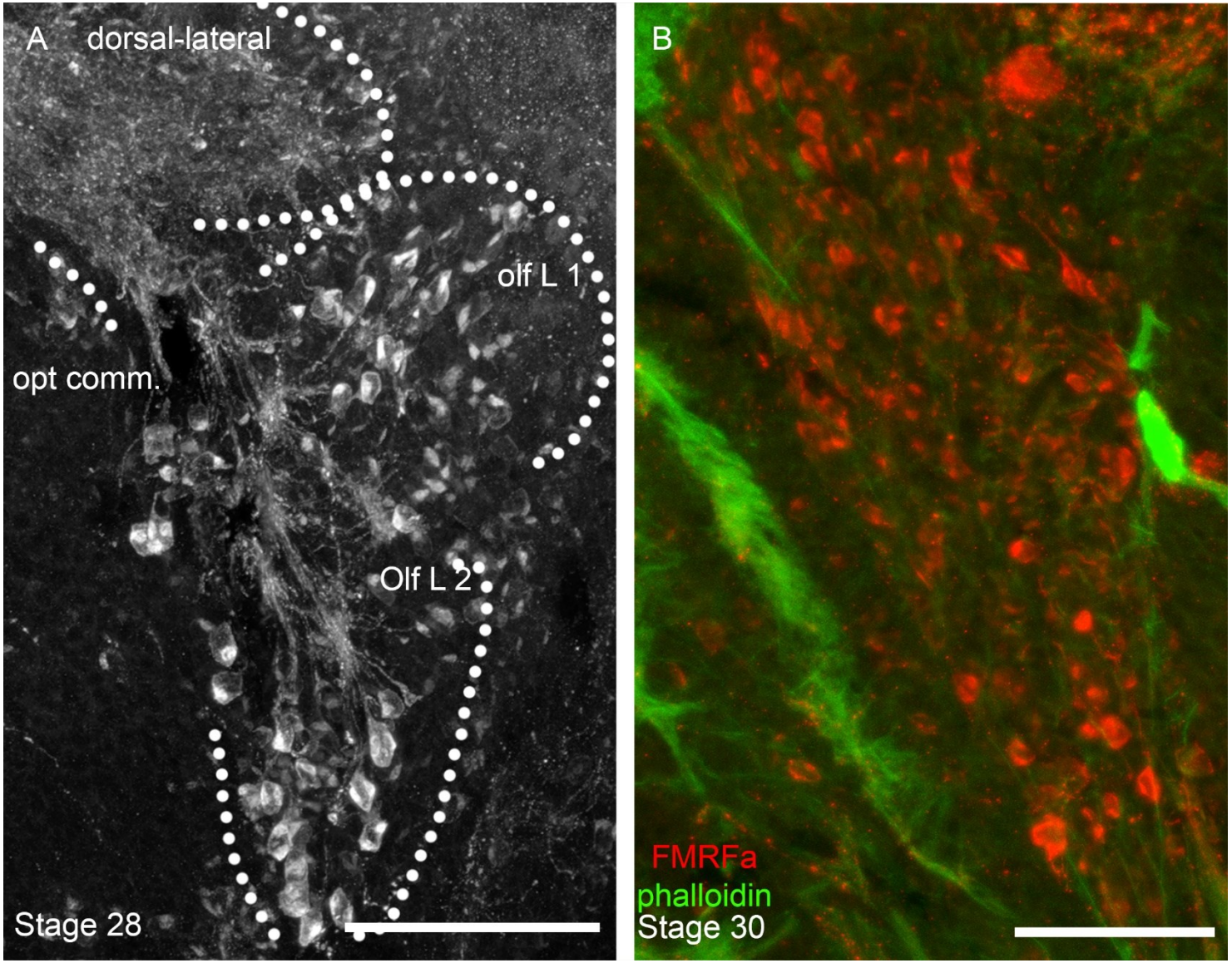
A dorsal-lateral
olf L 1
opt comm.
Olf L 2
Stage 28
B
FMRFa
phalloidin
Stage 30

Figure 4.11 FaRPs-LIR in the olfactory lobe of *S. officinalis.* (A) A medial section through the olfactory lobe in a stage 28 embryo. Cell bodies are visible in olfactory lobules one and two as well as the connecting neuropil. The optic commissure is also visible projecting into the lobe from the dorsal-lateral neuropil. (B) A posterior section of a stage 30 olfactory lobule one double-labeled with anti-FMRFa (red) and phalloidin (green) to show that the layer of cell bodies surrounding the lobule is almost completely devoid of neuropil, which is restricted to the lobe core. Olf L 1, olfactory lobule one, Olf L 2, olfactory lobule 2; Opt. comm, optic commissure. Scale bars represent 100 μm.

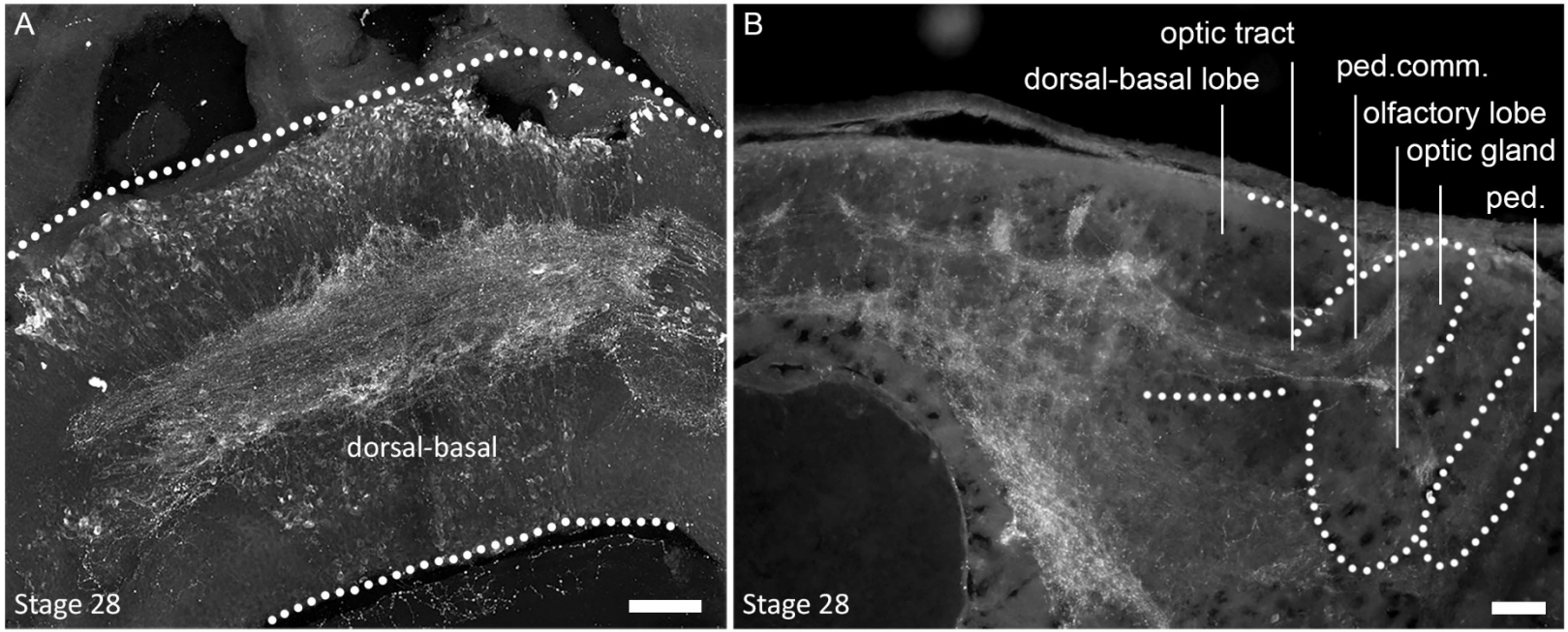
A
dorsal-basal
Stage 28
B
optic tract
dorsal-basal lobe
ped.comm.
olfactory lobe
optic gland
ped.
Stage 28

Figure 4.12 FaRP-LIR shows interconnectivity of the olfactory lobe. (A) FaRP-LIR in the supra-esophageal mass in a stage 28 embryo. Cell bodies on the dorsal edge project neurites in an anterior direction into the central neuropil of the dorsal-basal lobe. Many of the horizontal fibers project into the optic tract, some of which will innervate the olfactory lobe. (B) Anti-FMRFa staining in the dorsal-basal lobe connects via the optic commissure to the optic gland, olfactory lobe, and peduncle lobe. Ped, peduncle lobe. Scale bars represent 100 μm.

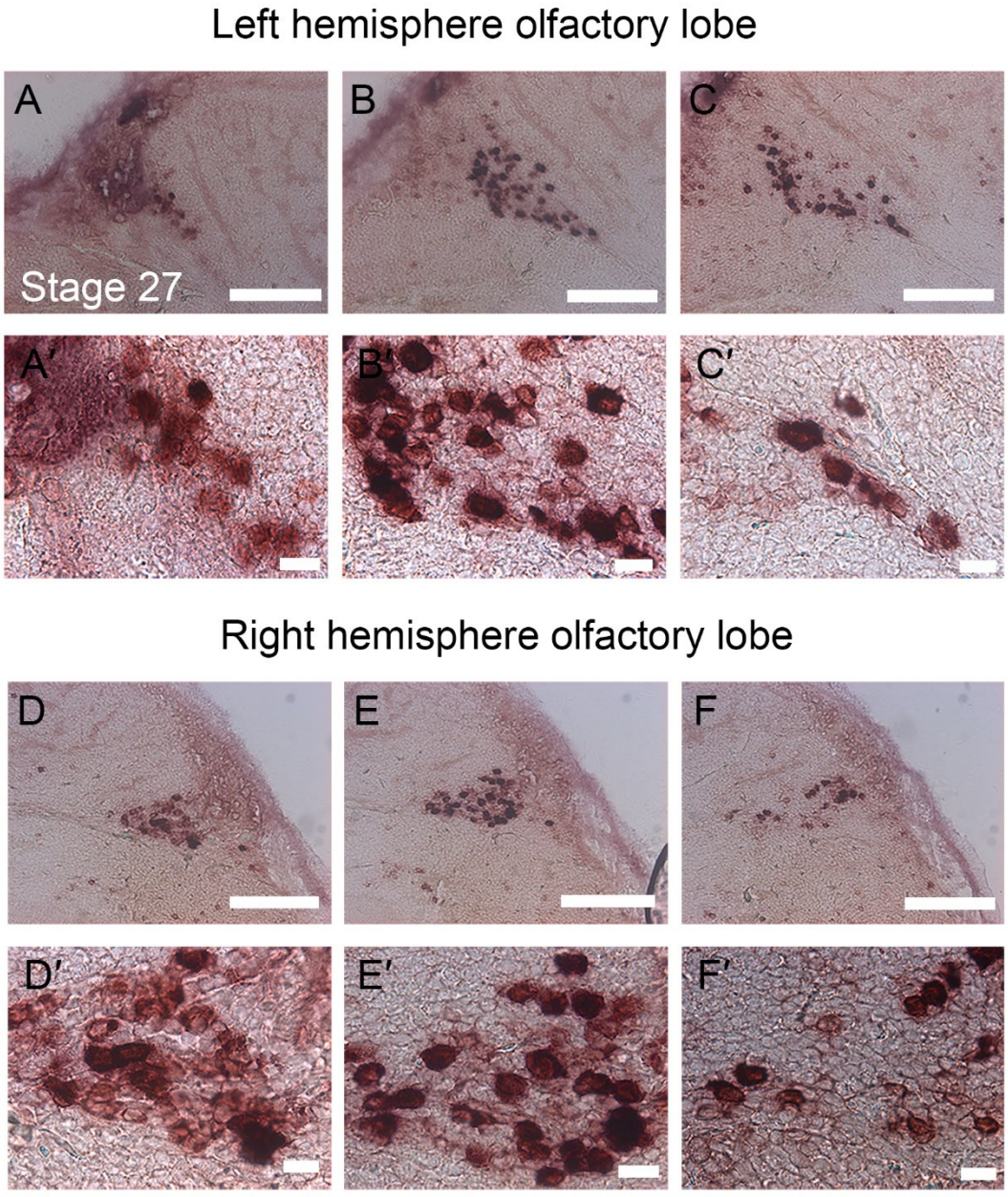
Left hemisphere olfactory lobe
A
B
C
Stage 27
A′
B′
C′
Right hemisphere olfactory lobe
D
E
F
D′
E′
F′

Figure 4.13 *ISH* in sections via FaRP mRNA antisense probe. A-F: 10x magnification; A′-F′: 40x magnification. A-C′: Left hemisphere olfactory lobe in a stage 27 embryo. (D-F′: Right hemisphere olfactory lobe. Sectioned from posterior to anterior. Scale bars in 10x represent 100 μm and in 40x represent 10 μm.

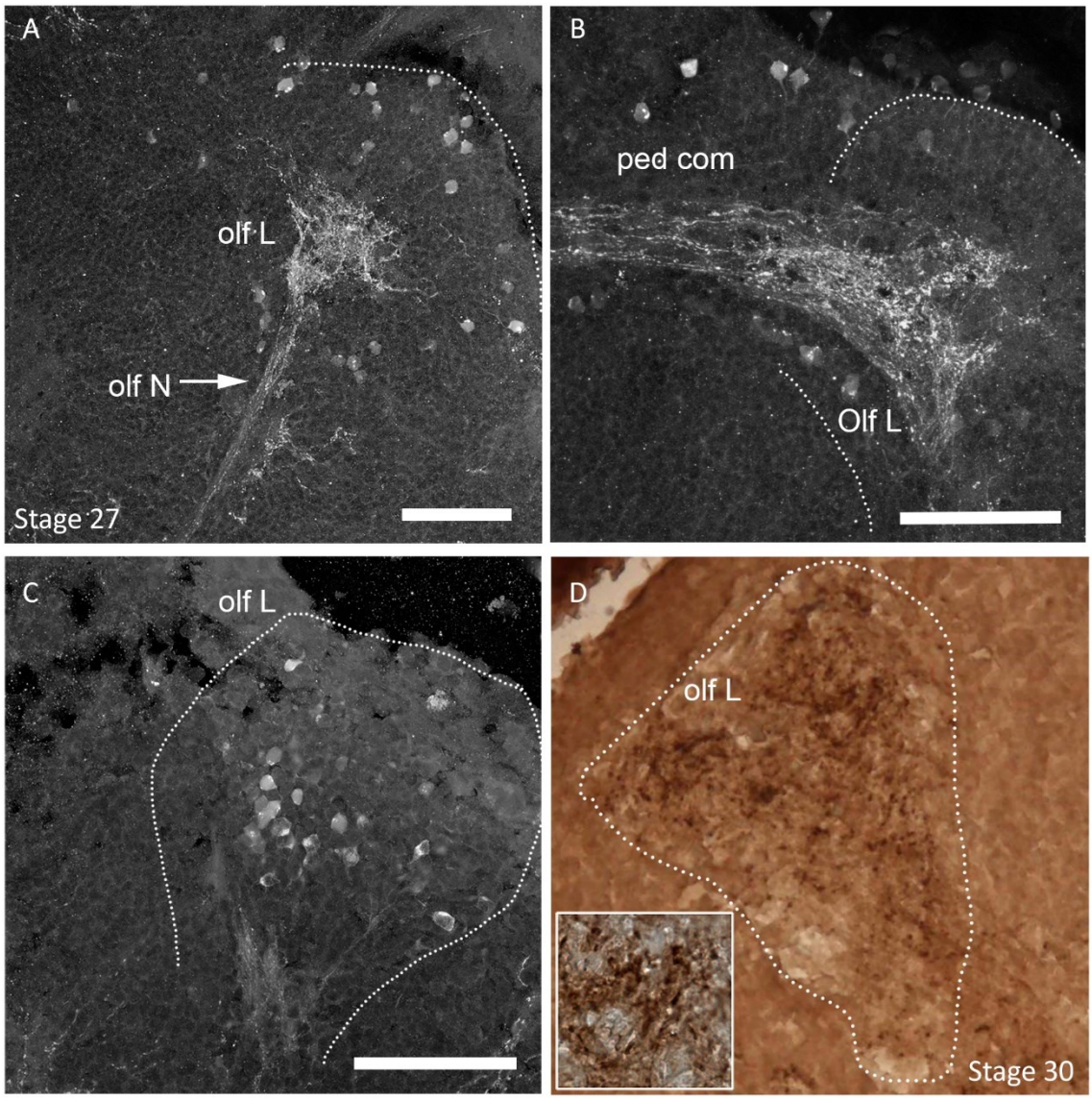
A
olf L
olf N
Stage 27
B
ped com
Olf L
C
olf L
D
olf L
Stage 30

Figure 4.14 5-HT-LIR in the olfactory lobe and surrounding CNS. Sections viewed from posterior to anterior. (A) A posterior section of the olfactory nerve in a stage 27 embryo shows the olfactory nerve innervating olfactory lobule one neuropil, with neurons around the periphery of the lobule. (B) The optic commissure connects the dorsal end of the olfactory lobule one neuropil to the dorsal-basal lobe. (C) A higher magnification picture of the 5-HT-LIR in neurons and neuropil of olfactory lobule one. (D) DAB 5-HT-LIR immunohistochemistry of the neuropil in the olfactory lobe. Insert shows a high magnification of the neuropil staining. Olf L, olfactory lobe; olf N, olfactory nerve; ped com, peduncle commissure. Scale bars represent 100 μm.

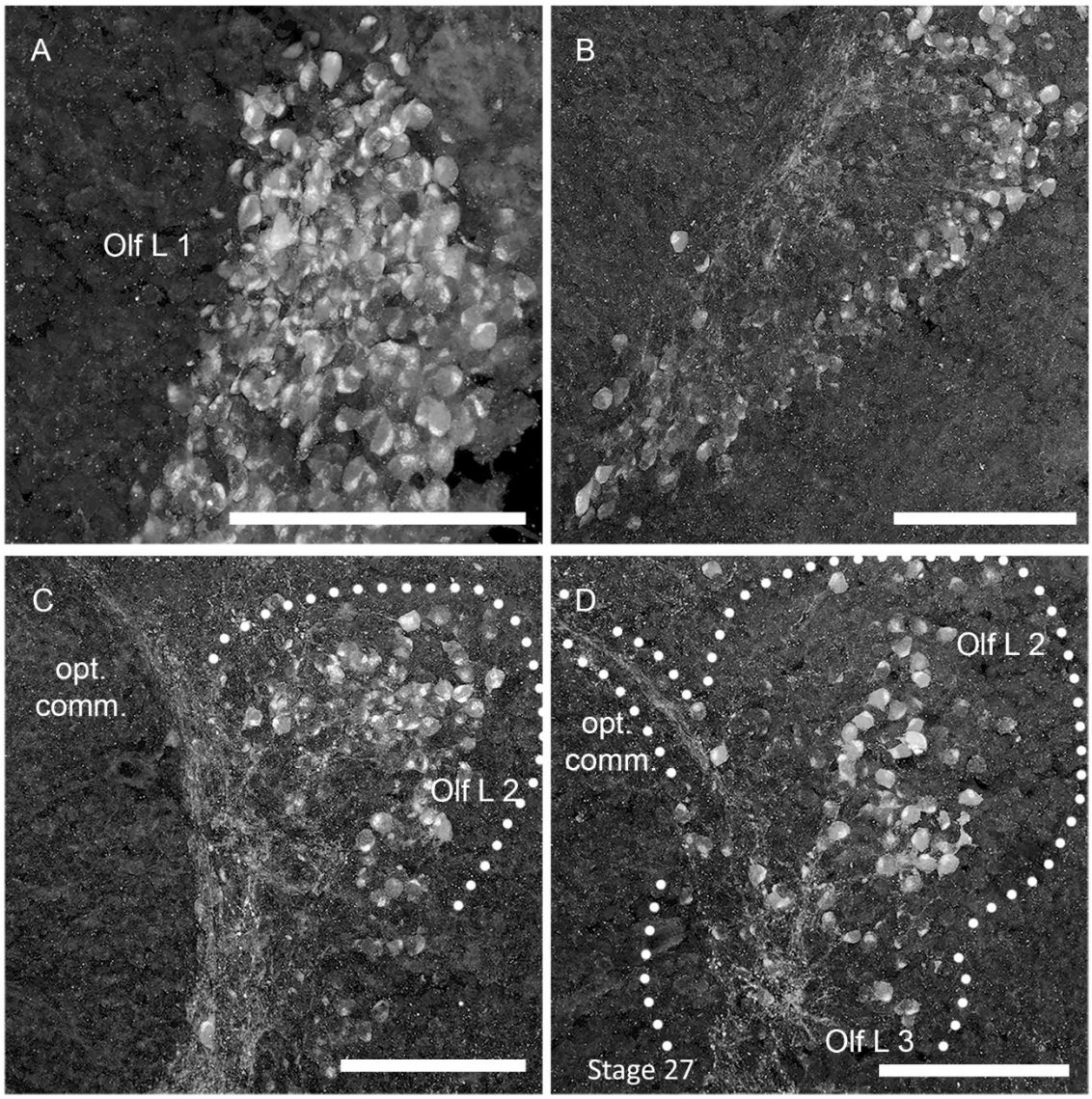
A
Olf L 1
B
C
opt.
comm.
Olf L 2
D
Olf L 2
opt.
comm.
Olf L 3
Stage 27

Figure 4.15 APGWamide in the olfactory lobe. In a stage 27 embryo. From posterior to anterior: (A) The posterior surface of olfactory lobule one is a layer of cell bodies. (B) In a more anterior section, neurons wrap around the peripheral side of the lobe whilst the interior neuropil is now visible. (C) The cell bodies of olfactory lobule two project neurites into the neuropil of lobule three. The beginnings of the optic commissure (opt. comm.) are visible in this section. (D) The anterior-most section contains neurons of olfactory lobule two and neuropil of lobule three. Olf L 1, olfactory lobule one; Olf L 2, olfactory lobule two; Olf L 3, olfactory lobule three; opt. comm, optic commissure. Scale bars represent 100 μm.

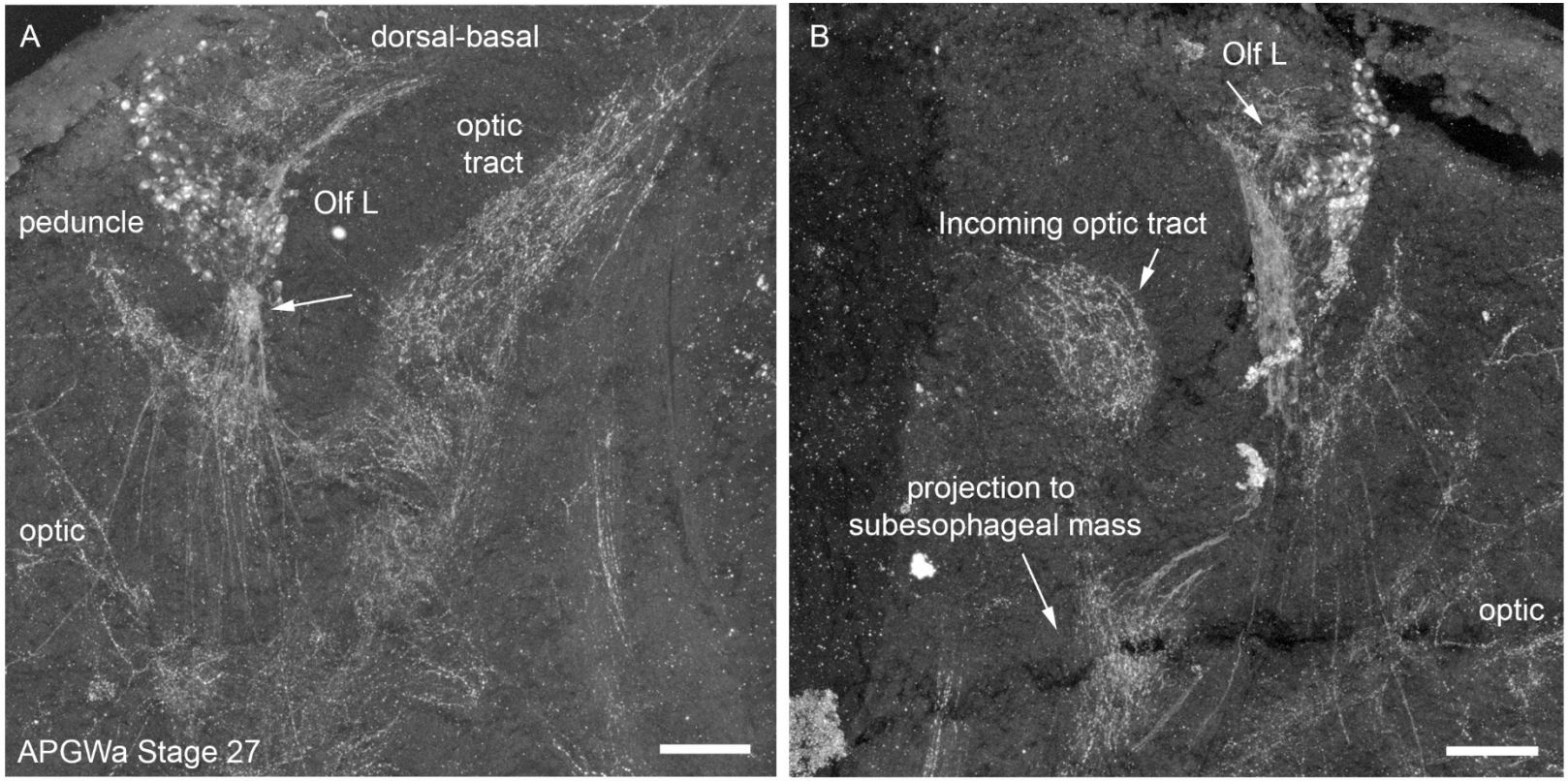
A
dorsal-basal
optic
tract
Olf L
peduncle
optic
APGWa Stage 27
B
Olf L
Incoming optic tract
projection to
subesophageal mass
optic

Figure 4.16 APGWamide-LIR shows interconnectivity of the olfactory lobe. (A) APGWa-LIR in a stage 27 embryo including the neuropil of the peduncle, olfactory lobe, optic tract, and dorsal-basal lobe. Arrow indicates termination point of olfactory nerve. (B) In a more posterior section, neuropil of the optic tract is only partly visible in this section, along with projections from the olfactory lobe down toward the sub-esophageal mass. Olf L, olfactory lobe. Scale bars equal 100 μm.

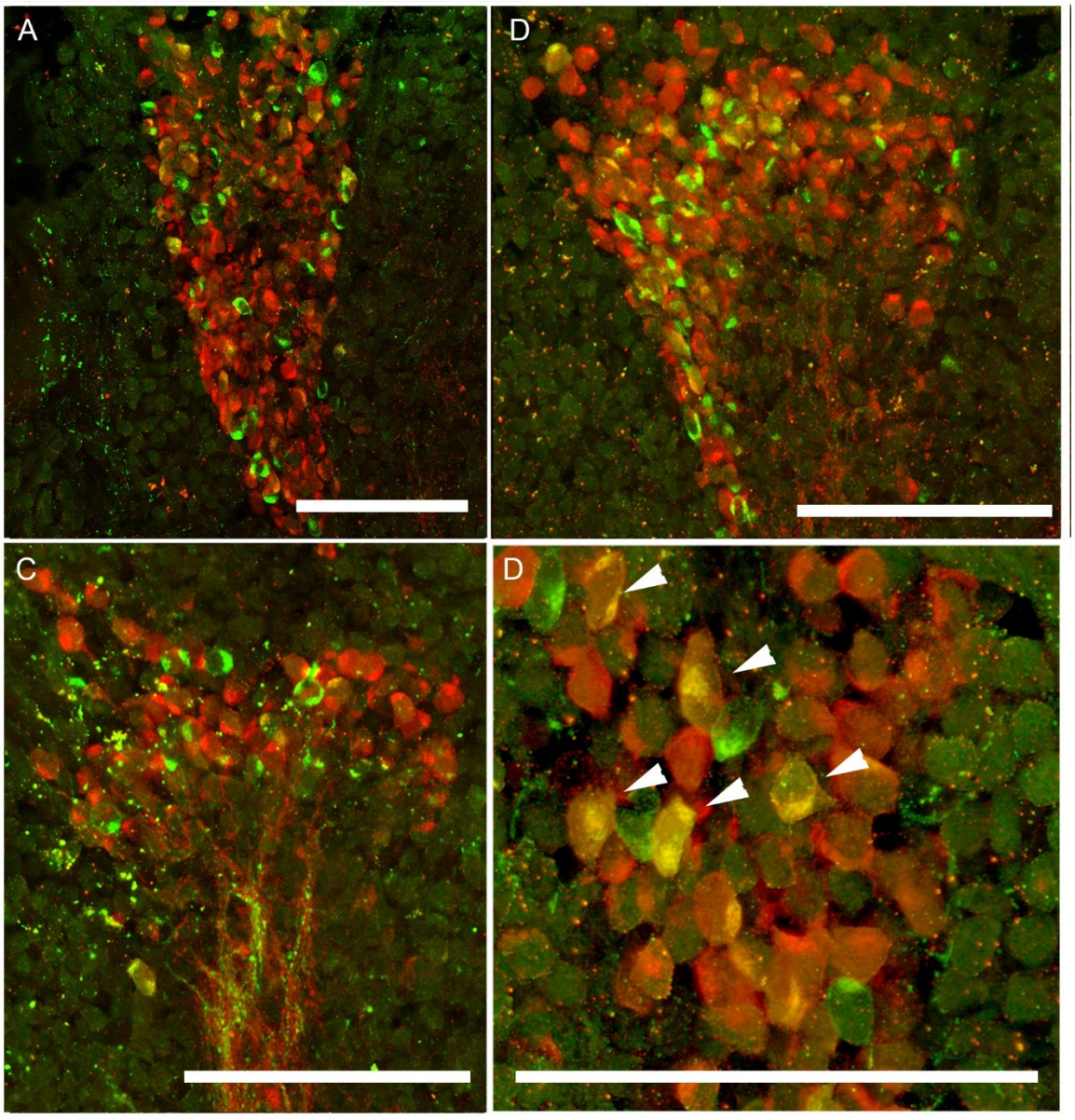
A
D
C
D

Figure 4.17 APGWamide and FMRFamide double-labelling in the olfactory lobe. (A) The cell body surface layer of olfactory lobule one in a stage 27 embryo is primarily composed of cell bodies labeled by APGWa (red) or FMRFa (green) antibodies in the medial-dorsal area of the lobule. A few cell bodies are co-labeled with APGWa and FMRFa (yellow). (B) A more anterior section of olfactory lobule one, with more of the central neuropil exposed. More FMRFa neurons are visible in the anterior area of the lobule, and more cell bodies are co-labeled. (C) The olfactory nerve projecting to the anterior tip of olfactory lobule one expresses both APGWa-positive and FMRFa-positive fibers, with no colocalization. (D) A high magnification view of the posterior cell body layer of lobule one to show individual cell bodies in the olfactory lobe. Co-labeled cell bodies identified with arrowheads. Scale bars equal 100 μm.

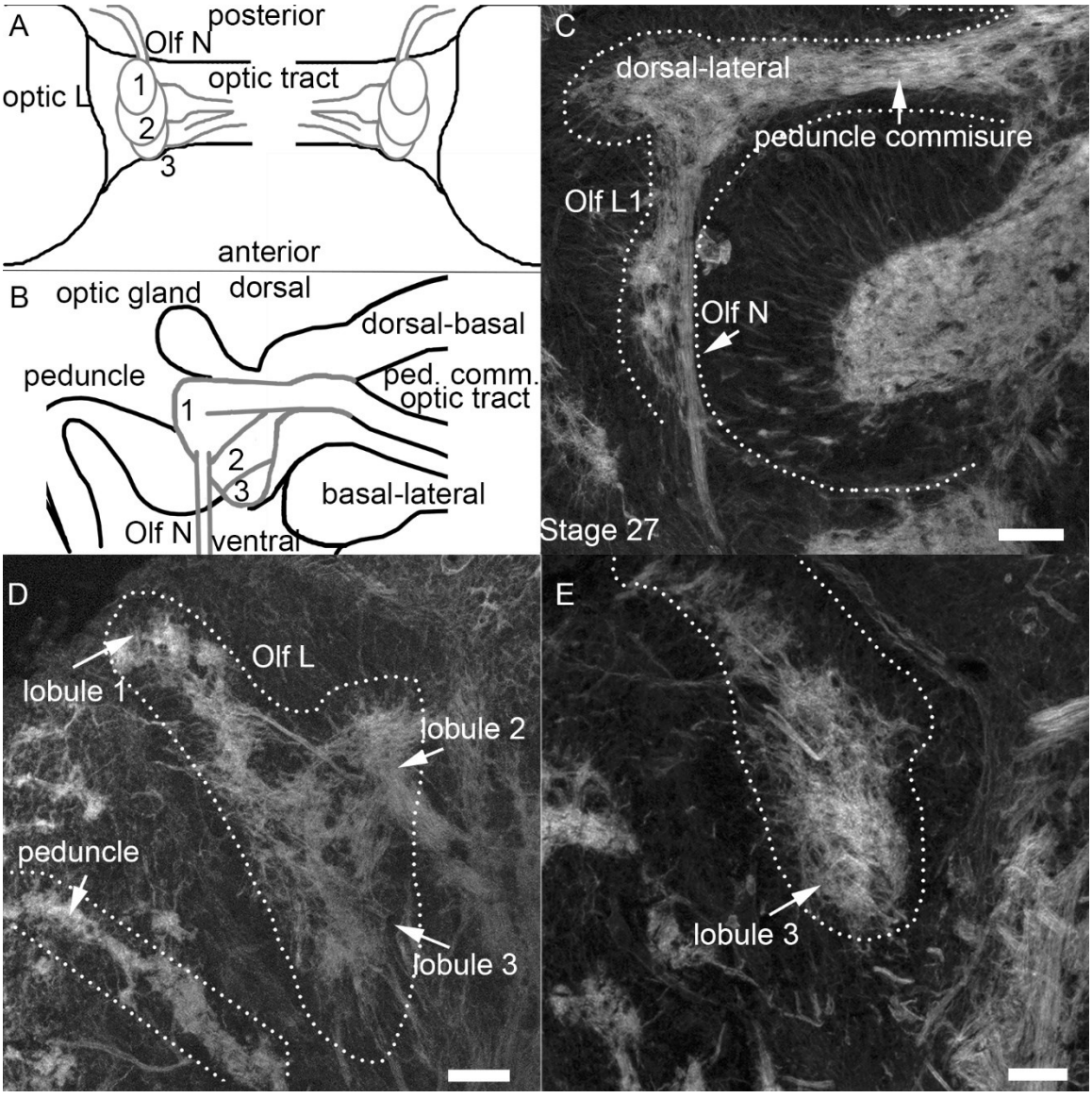
A
posterior
Olf N
optic L
1
optic tract
2
3
anterior
B
optic gland
dorsal
dorsal-basal
peduncle
ped. comm.
optic tract
1
2
3
basal-lateral
Olf N
ventral
C
dorsal-lateral
peduncle commisure
Olf L1
Olf N
Stage 27
D
Olf L
lobule 1
lobule 2
peduncle
lobule 3
E
lobule 3

Figure 4.18 Phalloidin fluorescence in the CNS of *S. officinalis*. Labeling of F-actin in a stage 27 embryo in the optic lobe, peduncle lobe, and olfactory lobe. Sections (30 μm thickness) from posterior to anterior. (A) Diagrammatic representation of the olfactory lobe (Olf L) positioned on the optic tract from the dorsal perspective. Posterior up, anterior down. Olfactory lobule one is most posterior, lobule two is the medial lobule, and olfactory lobule three is most anterior. (B) Diagrammatic representation of the olfactory lobe in transverse sections, as appears in (C-E). Dorsal up, ventral down. (C) Olfactory lobe in a posterior section shows both olfactory nerve entering the ventral end of the olfactory lobe and the peduncle commissure. (D) In a more anterior section, the olfactory lobe has its stereotypical triangular shape with the wide dorsal end. (E) Anterior section of olfactory lobule three with a narrow diameter again as it integrates with the optic tract. Olf L 1, olfactory lobule one; Olf N, olfactory nerve; Optic L, optic lobe, ped. comm., peduncle commissure. Scale bars represent 100 μm.

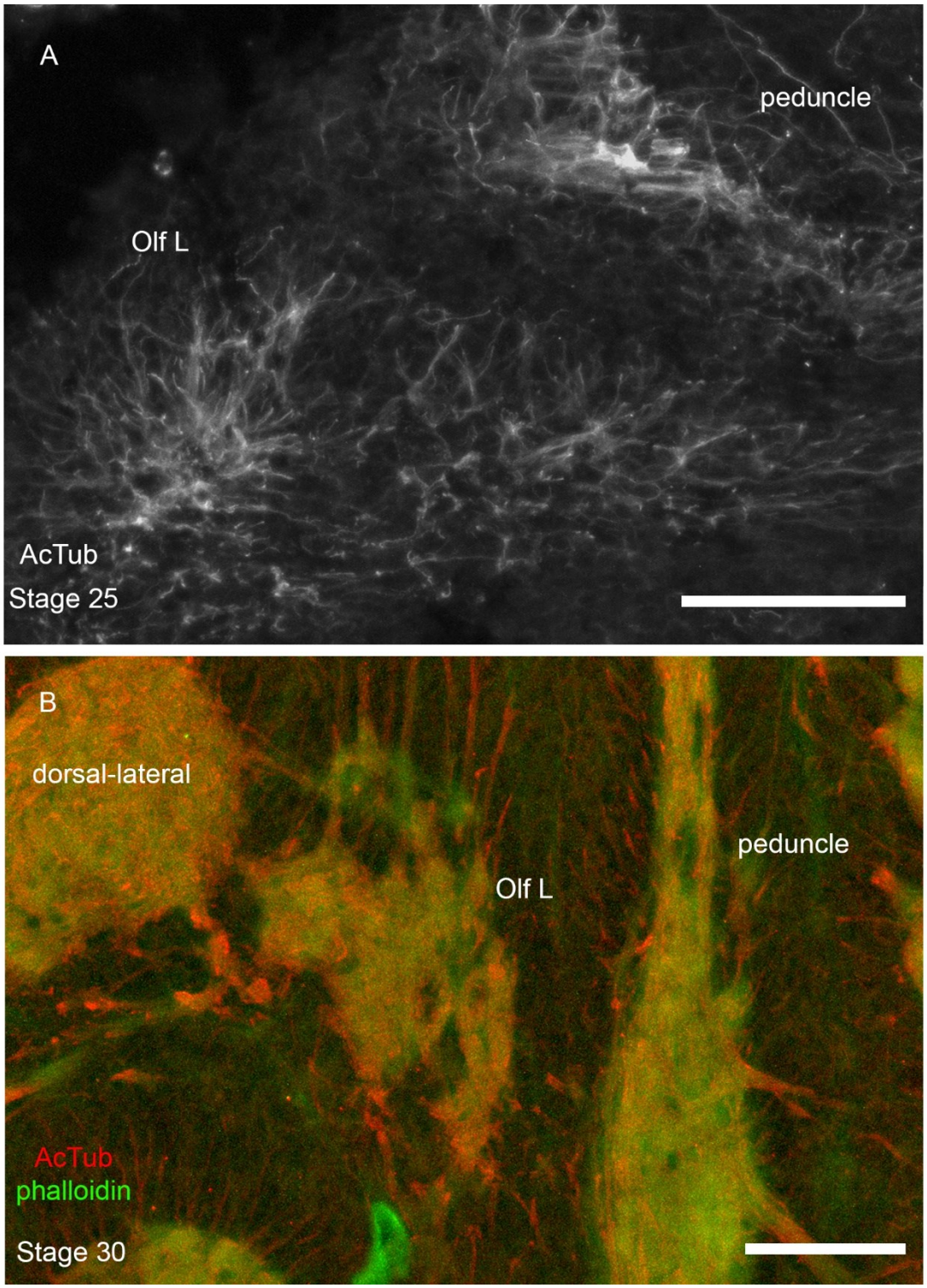
A
peduncle
Olf L
AcTub
Stage 25
B
dorsal-lateral
peduncle
Olf L
AcTub
phalloidin
Stage 30

Figure 4.19 Illustration of the development of neuropil in the olfactory lobe. (A) Loose organization of neuropil in the olfactory lobe and peduncle lobe stained with anti-AcTub at stage 25. (B) Tightly packed neuropil double-labeled with anti-AcTub (red) and phalloidin (green) at stage 30. Tubulin has more projections out of the neuropil, while F-actin seems constrained to the neuropil core. Olf L, olfactory lobe. Scale bars equal 100 μm.

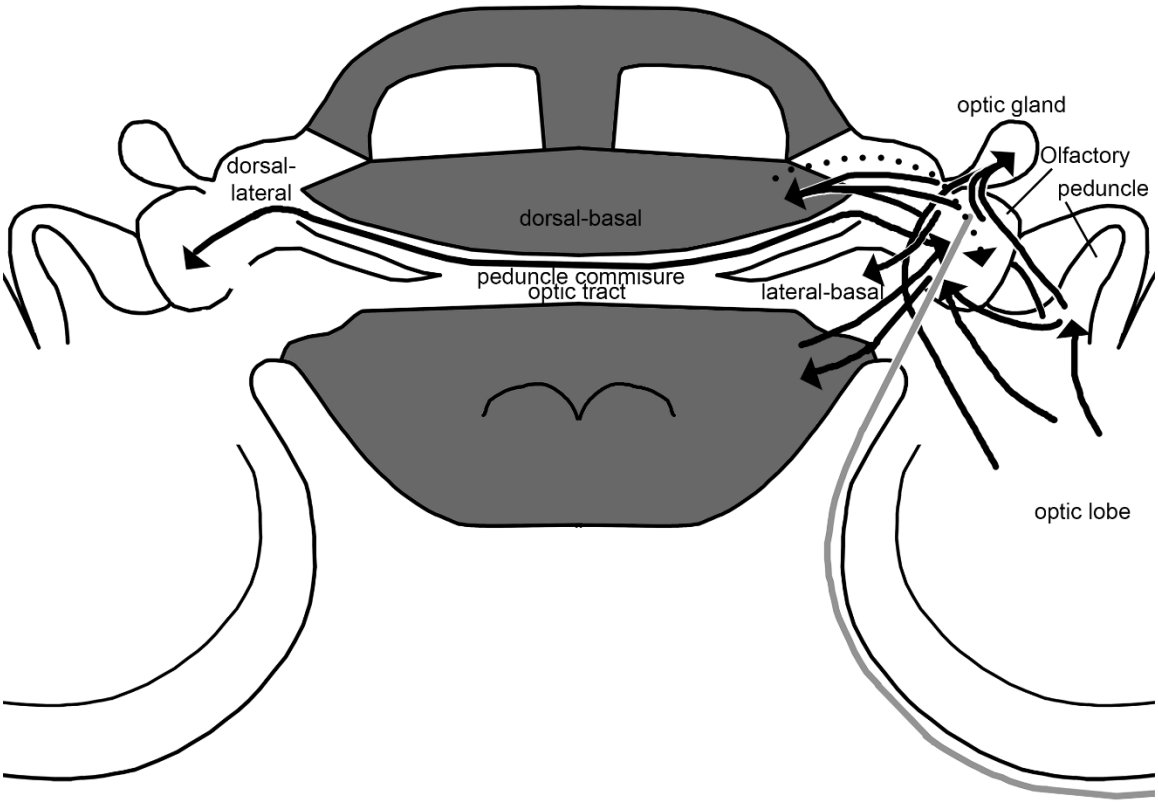

Figure 4.20 Interconnectivity of the olfactory lobe with the rest of the brain. The olfactory lobe receives input from the optic lobe, peduncle lobe, supra-esophageal mass, and peduncle commissure. There is also a connection from the dorsal-lateral lobe (dotted line) hypothesized but not proven to be efferent. The olfactory lobe projects to the optic gland, dorsal-lateral lobe, lateral-basal lobe, sub-esophageal mass, and the contralateral olfactory lobe via the peduncle commissure.

Chapter 5: Discussion

5.1 Glomeruli and Other Organizational Systems

In the previous chapter on the organization of the olfactory system, there were no structures identified that resembled the glomeruli previously described in some vertebrates, insects, crustaceans, or gastropods. I will discuss what characteristics specifically define glomeruli in an olfactory system and which features seem to be universal throughout the animal kingdom.

There are several key similarities between the olfactory glomeruli of different phyla (reviewed in Eisthen et al., 2002) that I use as a general definition to properly identify a glomerulus in cuttlefish. First, all glomeruli described thus far, except for in the snail *Achatina fulica* (Chase and Tolloczko, 1986), have been found in the central nervous system (CNS); glomeruli have been described in the olfactory bulb in vertebrates, olfactory lobe in crustaceans, antennal lobe of insects, and tentacle ganglion of snails. Second, these previously described glomeruli have an overall spherical shape, as seen in both vertebrates, insects, and crustaceans. One exception is the cone-shaped glomeruli of spiny lobster (*Panulirus argus;* Blaustein et al., 1988). Third, despite the large diversity of species, all glomeruli seem to be relatively similar in size (Table 5.1).

Table 5.1 Comparison of glomerular sizes across animals.

Organism	Diameter (μm)	Reference
Rats	50-120	Pinching and Powell, 1971
Moths	45-100	Nassel, 1999
Lobsters	40-100; 250 in length	Blaustein et al., 1988
Snails	40-100	Chase and Tolloczko, 1986

An exception is the microglomeruli found in some species of crustaceans, grasshoppers, and crickets, in which the antennal lobe contains thousands of microglomeruli that are approximately 5 μm in diameter. Although they are still innervated by olfactory sensory neurons (OSNs) and

interneurons, the purpose of these microglomeruli is unknown. Fourth, glial cells surrounded glomeruli in all animal groups, most likely to isolate individual glomeruli from each other. Any proto-glomeruli that develop in *Manduca sexta* need to be rapidly surrounded by glial cells, or else they will dissolve (Oland and Tolbert, 1988). Similarly, in rat embryos, proto-glomeruli first interact with glia to form the glomerular boundaries, then later interact with interneuron and output neurons (Treloar et al., 1999).

Vertebrates, insects, and crustaceans use glomeruli to organize their patterns of activity into an odor map. By clustering the specific types of OSN axons into collections of synapses, the glomeruli of both groups effectively organize the inputs from the olfactory epithelium. Vertebrates, insects, and crustaceans also use the second order neurons around their glomeruli to project their organized input into higher areas of the brain for olfactory learning, identification, and memory. The striking morphological similarities of the OSNs, glomeruli, interneurons, and olfactory brain centers in vertebrates, insects, and crustaceans suggest a possible optimal solution to detecting and discriminating odors (Hildebrand and Shepherd; 1997; Eisthen, 2002; Ache and Young, 2005; Kaupp, 2010).

There is some evidence to suggest that glomeruli in mammals, fish, amphibians, insects, and crustaceans might be homologous. Glomeruli have been identified in a sister group to arthropods, the velvet worms (Schurmann, 1995; Eisthen, 2002; Strausfeld et al., 2006). Eisthen attempted to visualize this pattern of glomeruli through a wide range of phyla based on previous olfactory research (Eisthen, 2002; Figure 5.1). While some aspects of olfaction, such as the ionotropic glutamate olfactory receptors, can be traced back through evolutionary history to the protostomes (such as the nematode *C. elegans*), identifying the blueprint for complex structures like glomeruli in non-cephalized animals is nearly impossible morphologically (Croset et al., 2010).

Due to the complex nature of such an organizational system across this expanse of diversity, the evolution of glomerular structures has caught the imagination of more than one scientist.

Glomeruli have been independently lost in several individual species. In vertebrates, modern toothed whales have completely lost their glomeruli, along with their entire sense of olfaction (Kishida et al., 2015). Some arthropods, such as the basal hexapods, have also lost their glomeruli (Strausfeld and Hildebrand, 1999), in addition to those arthropods without olfactory antennae, like the diving beetle, mayflies, dragonflies, and damselflies (Strausfield et al., 1998). It is harder to understand the seemingly arbitrary presence and absence of glomerular-like structures in various studied species of gastropods and their absence from *Sepia officinalis*.

5.2 Are There Glomeruli in Molluscs?

The question regarding whether there are glomerular-like structures in molluscs is an important missing piece to understanding the relationship of the olfactory system between vertebrates, insects, crustaceans, and molluscs. Their described presence in the different groups of gastropods obfuscates a clear understanding of olfactory evolutionary history.

There are two main factors that confound our understanding of glomerular-like structures in molluscs: their seemingly arbitrary presence throughout gastropods, and the limited number of species sampled (Table 5.2). The first mollusc to be observed with glomerular-like structures was the terrestrial snail *A. fulica* (Chase and Tolloczko, 1986).

Table 5.2 List of species examined for glomeruli; listed by family.

Family	Species	Habitat	Glomeruli	Reference
Stylommatophora	*Achatina fulica*	Terrestrial	Reported glomeruli	Chase and Tolloczko, 1986
	Limax marginatus	Terrestrial	No glomeruli reported	Unpublished observation, Ito et al., 2000
	Cornu aspersa	Terrestrial	No glomeruli reported	Unpublished observation, Ito et al., 2000
Nudipleura	*Phestilla sibogae*	Aquatic	Reported glomeruli	Boudko et al., 1999; Croll et al., 2001; Croll et al., 2003
	Archidoris pseudoargus	Aquatic	No glomeruli reported	Wertz et al., 2007; Faller et al., 2008
	Archidoris tornatilis	Aquatic	No glomeruli reported	Faller et al., 2008
Aplysiomorpha	*Aplysia californica*	Aquatic	Reported glomeruli	Moroz, 2006; Göbbeler and Kussman-Kolb, 2007; Cummins et al., 2014
	Aplysia punctata	Aquatic	Reported glomeruli	Wertz and Rossler, 2006

The simultaneous absence and presence of glomeruli within Nudipleura or Stylommatophora could be explained by independent loss of glomeruli within genera, but regardless demonstrates that glomeruli are not simply divided between terrestrial and aquatic species. Because so few species have been examined compared to the number of groups (Figure 5.2), other families

are needed to determine if there are any more molluscs with glomerular-like structures before conclusions can be drawn.

Glomerular structures have not been described in cephalopods. It has been suggested that they may not be present since the olfactory lobe in *Nautilus* is layered, and that of *Octopus* is smaller and has no large-scale organization (Eisthen, 2002). In this present study, the first detailed description into the organization and neurobiology of the olfactory system in cuttlefish, I confirm that cuttlefish have nothing resembling glomerular-like organization, although more olfactory systems must be described in detail to confirm this trend in cephalopods in general.

The implications of this study warrant careful consideration. It is possible that the lack of glomeruli in cuttlefish represents all of Cephalopoda have independently lost their glomerular structures. However, it is more likely that there have never been "glomeruli" in molluscs in the same sense that glomeruli have been described in insects, crustaceans, and vertebrates. After Chase and Tolloczko first described glomerular-structures in *A. fulica* in 1986, they were cited in all subsequent reports of glomeruli in other molluscan species. Thus, it is possible that all molluscan glomeruli, while homologous to each other, have no phylogenetic relationship to the glomeruli in the rest of the animal kingdom. Since there was no evidence of glomeruli in *S. officinalis*, I briefly look at what evidence would be required to conclude that glomerular structures were present for future researchers who wish to continue the work presented here.

In the tentacle of *A. fulica*, afferent OSN fibers travel down long digit extensions from the tentacle ganglion. Some of these axons are clustered into dense neuropil which is delimitated by glial cells and glial processes. These regions are identified as glomeruli (Chase and Tolloczko, 1986). Numerous small neurites are described organized in parallel down the tentacle (Figure 5.3).

The argument was that, like vertebrates, insects, and crustaceans, these glomerular regions have dense neuropil, are devoid of cell bodies, and are surrounded by glial cells. Afferent signals from the tentacles could be processed in parallel at multiple anatomical sites. However, Chase and Tolloczko acknowledge there were many differences between the glomeruli they described and those previously described in vertebrates, insects, and crustaceans (summarized in Table 5.3). While their study describes approximately 20 glomeruli in the tentacle, there are around 125 described in *Periplaneta americana,* a species of cockroach, and almost 2,000 glomeruli a rabbit (Chase and Tolloczko, 1986). The snail glomeruli only receive a small portion of olfactory afferent projections, while the rest bypass the glomeruli completely and project directly into the tentacle or cerebral ganglia. This limited input into the glomeruli is another deviation from both vertebrates, which route all their neurites through glomeruli (except for the extrabulbar pathway, which bypass the olfactory bulb to higher brain centers), and arthropods, which route most of their inputs through glomerular neurites. The irregular shapes of the snail glomeruli are also a diversion from the traditionally spherical glomeruli.

Table 5.3 Comparison of Olfactory Glomeruli in Three Diverse Animals. Adapted from Chase and Tolloczko, 1986. All data are unilateral values.

	Snail (*Achatina fulica*)	**Cockroach (*Periplaneta americana)***	**Rabbit**
Shape of glomeruli	Irregular	Spherical	Spherical
Mean volume (mm^3)	38×10^{-5}	22×10^{-5}	359×10^{-5}
Number of glomeruli	20	125	1900
Total number of olfactory receptors	1×10^5	2.8×10^5	5×10^7

	Snail (*Achatina fulica*)	Cockroach (*Periplaneta americana)*	Rabbit
Percent olfactory fibers terminating in glomeruli	10% (est.)	90% (est.)	100%
Convergence ratio, receptors: glomeruli	500	2100	26316

Chase and Tolloczko (1986) also demonstrated that there were no detectible differences in the spatial patterning of the glomerular 14-C-deoxyglucose (2 DG) labels when different odors were used as stimuli. 2 DG is a modified glucose molecule that is used as a marker for tissue glucose uptake and can identify regions of increased activity. Their experiment showed that the snail glomeruli do not operate as functionally differentiated units, unlike vertebrates, insects, and crustaceans which have a different pattern of glomerular activation depending on the stimulatory odorant (Eisthen, 2002; Nagashima and Touhara, 2010). This may be because the digits themselves impose a degree of spatial compartmentalization on the afferent projections, although this hypothesis contradicts the implied purpose of glomeruli as being spatial organizational units (Chase and Tolloczko, 1986).

Chase and Tolloczko (1986) proposed to expand the definition of glomeruli to include the snail glomeruli and all the differences they entailed. Snail glomeruli had the wrong shape, total number, and far fewer innervations. Additionally, there were no glomerular structures found in the tentacle or cerebral ganglion, just in the peripheral tissue of the tentacle itself. The organization of the glomeruli in a linear arrangement down the length of the tentacle or rhinophore also raises some questions (Wertz et a., 2006; Göbbeler and Kussman-Kolb, 2007). Such an arrangement suggests OSNs that run the length of the tentacle would project to the closest glomerulus, thereby dividing the tentacle into horizontal bands of different receptor types. This has not been previously described

or noted in any species and would be highly unlikely. Therefore, it is still unclear what the significance is of this linear chain of nodules along the tentacle.

In 1996, there was another large change to how glomeruli were identified with the advent of molecular studies. It was demonstrated that receptor cells of mammals (Vassar et al., 1994; Mombaerts et al., 1996), fish (Dynes and Ngai, 1998), and insects (Vosshall et al., 2000) all have a dispersed distribution through the peripheral epithelium; all converge their axons, organized by receptor protein, onto one or a small number of glomeruli. This common organization throughout animals suggests that not only is massive convergence fundamental to how odorants are processed in the brain, but that this type of organization may have been conserved in evolution. The consistency of this organization, despite the diversity of the animals it is found in, is a major argument against the described glomerular structures in Chase and Tolloczko, where only about 10% of the olfactory neurites terminate in glomeruli.

5.3 Conclusions

The numerous differences between glomeruli in gastropods and those found in other animals, in combination with a distinct lack of glomerular-like structures in *S. officinalis,* strongly suggests that glomerular organization of the olfactory system is not universal among cephalized animals, or at the very least may not extend throughout phyla Mollusca. There are several implications of this conclusion. With the isolation of glomerular-like structures to vertebrates, insects, and crustaceans it is highly probable that glomerular structures have independently evolved at least twice to overcome the same problem of recognizing and processing dilute chemicals. This conclusion is further supported by looking at the sister groups, where the velvet worms do exhibit glomeruli, but *C. elegans* do not. Therefore, the previously reported snail glomeruli are not homologous to vertebrate, insect, and crustacean glomeruli. To amend the previously published

phylogenetic distribution, if homologous glomeruli are removed from Gastropoda (Figure 5.4), the result is that glomeruli have independently evolved twice in evolutionary history, in Arthropoda and Vertebrata.

In the context of cephalopod olfaction, there is another possible conclusion to explain the lack of glomerular-like structures; the olfactory system in cephalopods may be reduced, like in many aquatic species (e.g. the cetaceans). Perhaps other chemosensory systems, such as those in the suckers, compensate for a reduced olfactory system. The evidence to support this conclusion includes the lack of glomeruli, the small relative size of the olfactory lobe (particularly in comparison to the optic lobes), and the seemingly unorganized patterning of neuropil in the olfactory lobe as demonstrated by phalloidin and tubulin staining. However, the same conclusion could easily be drawn for gastropods, if not for the overwhelming behavioral evidence to the contrary (Hanley et al., 2013). These behavioral studies, as well as physiological studies, are abundant in the field of gastropod chemoreception (Teyke and Gelperin, 1999; See Kiss, 2017 for a recent review of the olfactory discrimination abilities of gastropods), but the same cannot be said for cephalopods.

Although some of the fundamental behavioral research has begun (Mobley et al., 2008), the discriminatory abilities of cephalopods are still being resolved. Molecular studies including families of chemoreceptors can be used to understand discrimination abilities. It is thought that the number of receptors is correlated to the number of glomeruli, and therefore the animal's differentiation ability. For example, mammals have a large family of G-protein coupled receptors in their sensory neurons which encode a large range of odors (Hildebrand and Shepherd, 1997). Insects, with their ligand gated receptors, have a smaller range of odorants and a smaller family of receptors in their genome. The chemoreceptors of *Aplysia* have been well studied (Cummins et al, 2007; 2009; Croset et al., 2010). *Aplysia* have G-protein α subunits G_q and G_i, and G_o in addition to proteins

homologous to phospholipase C and Inisitol 1,4,5-trisphosphate receptors. They also have a family of ionotropic glutamate receptors. In particular *Aplysia* have an IR25a receptor, which is one of the oldest members of the repertoire of IR channels and its conservation in a wide variety of invertebrates suggests that it may have originated in a protostome ancestor (Croset et al., 2010). While there have been no IR receptors found in cephalopods, $G\alpha_q$ and Phospholipase C140 have been found to be coexpressed in olfactory receptor neurons (Mobley et al., 2007). Therefore, it is also recommended that in addition to behavioral studies, future studies also focus on understanding the diversity of olfactory receptors to further elucidate the differentiation abilities of cephalopods and other molluscs.

Therefore, I call for an increase in research into the behavioral and physiological study of cephalopod olfactory discriminatory ability. By understanding the degree to which cephalopods, particularly coleoids, can differentiate certain odorants, I can determine the complexity their olfactory system, and if it has been evolutionarily reduced.

5.3.1 Applications

There is another advantage to delving further into cephalopod olfaction besides postulating evolutionary hypotheses. Previous molluscan chemoreception research has targeted a variety of purposes. Molluscs have been used extensively in behavioral research, particularly as models for behavioral ecology and the neural basis of behavior (Kiss, 2017). Another area of molluscan chemosensory research is focused population control, particularly for those species of gastropods that are pests or primary hosts to tropical diseases such as schistosomiasis (Thomas et al., 1980).

There are also some practical applications to understanding a different chemosensory system organization. Biology often influences technology, as creative minds are frequently inspired by nature (Kim et al., 2013). Scientists have designed artificial intelligence on one particular animal:

humans. However, basing technology off such a complex model has its disadvantages. Sometimes a simpler model is more refined and has less complications.

Machine olfaction, the automated simulation of smell, is an emerging field of modern robotics where automatized systems are needed to measure airborne particles (Marco et al., 2012). Commonly called the e-nose, it has multiple applications including product quality assessments, detection and diagnosis of diseases, drug detection, explosives detection, and environmental monitoring (Gardner et al., 2000). Computer scientists and programmers are struggling with the issues of how to synthesize signal-preprocessing, feature extraction, feature selection, classification, clustering, and validation (Marco et al., 2012). Perhaps the final solution with be something akin to glomeruli, or maybe finally determining in how cephalopods organize their olfactory inputs will help this newly emerging field.

Understanding alternative olfactory models may also have another potential application. While humans are primarily visual, we still often use our sense of smell, and its loss greatly affects our daily life. Olfactory disorders affect approximately 1/5th of the population (Croy et al., 2014). Such disorders greatly influence quality of life and hamper food enjoyment, detection of harmful food or smoke, personal hygiene, some social situations, and working life. It may also have some impact on reproductive behavior, including inbreeding avoidance, mate selection, and emotional contagion.

A percentage of anosmics also report depression. There has been observed a correlation between olfactory function and depression in older persons (Boesveldt et al., 2011). Olfactory impairment is also an early sign of Alzheimer's disease (Nordin, 2012) and Parkinson's disease (Ponsen et al., 2004).

Therefore, by understanding every aspect of chemoreception and olfaction, particularly in other non-classical models, we can hope to better understand mechanisms of action and possibly, in the future provide, cures, prosthetics, or implants which increase quality of life for these patients. The non-glomerular organization of the cephalopod model should be considered in designing an optimal simplified solution for these applications.

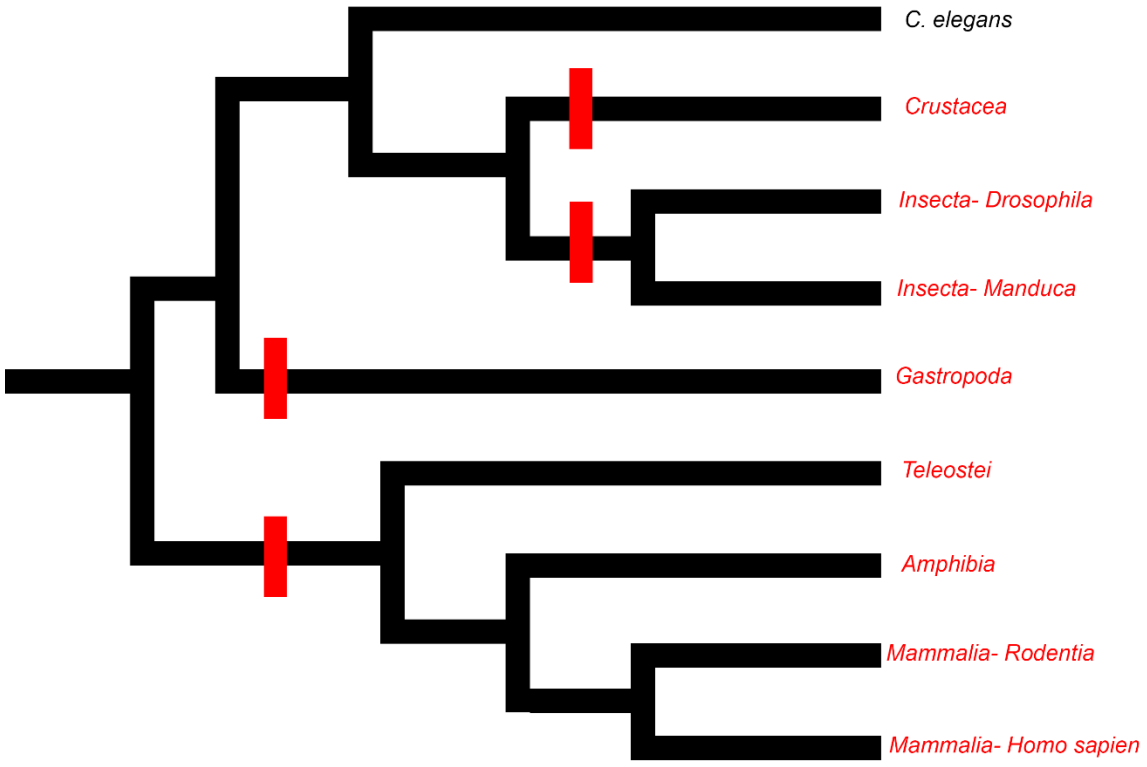

Figure 5.1 Phylogenetic distribution of glomerular structures. Based on the discussion in Eisthen, 2002. Solid red boxes indicate four hypothetical instances where glomeruli evolved independently. Based on the outgroups that lack glomeruli in the vertebrates, terrestrial insects, and lobsters, the hypothesis illustrated here suggests that glomerular structures evolved independently at least four times.

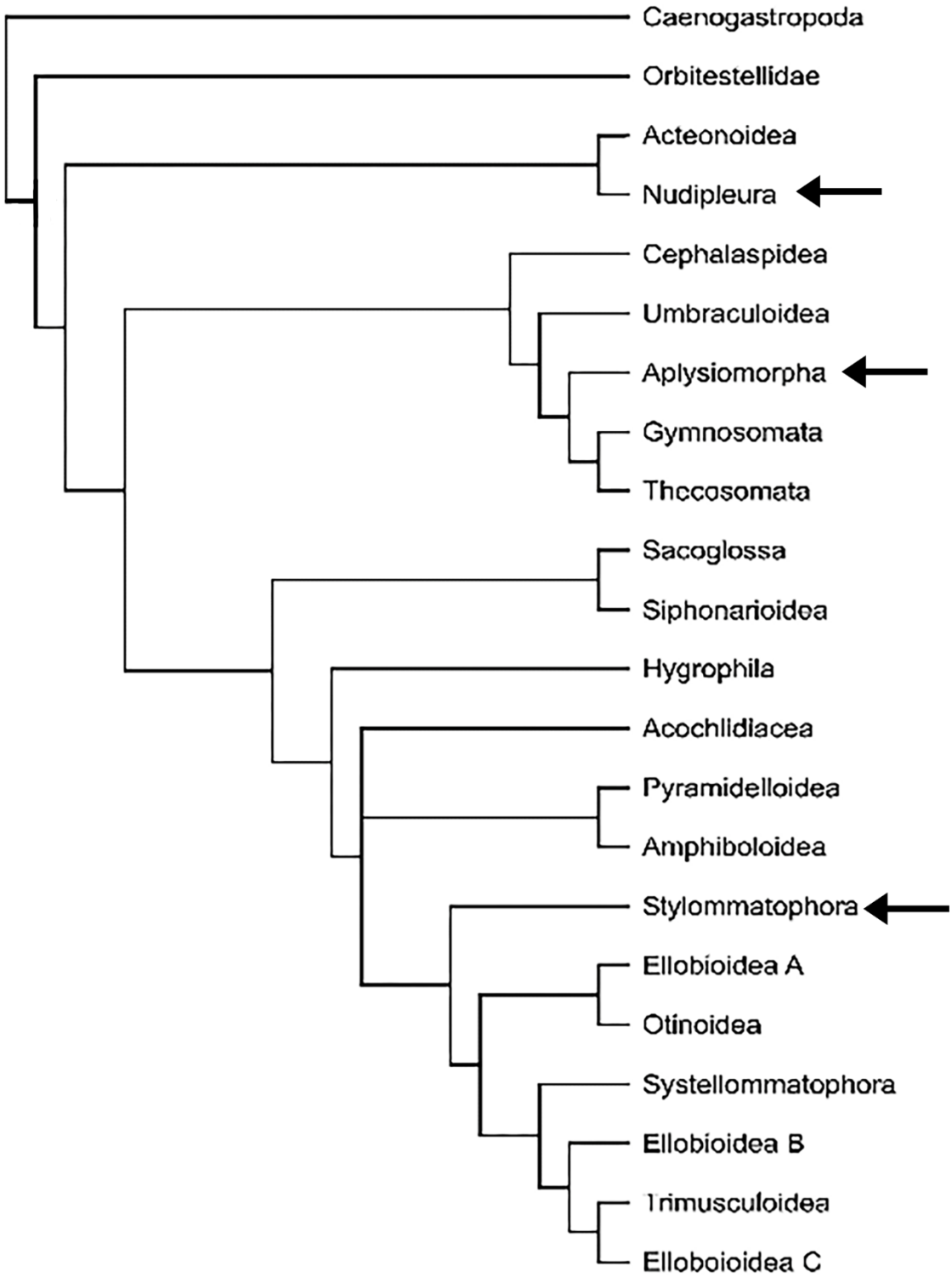
Caenogastropoda
Orbitestellidae
Acteonoidea
Nudipleura
Cephalaspidea
Umbraculoidea
Aplysiomorpha
Gymnosomata
Thecosomata
Sacoglossa
Siphonarioidea
Hygrophila
Acochlidiacea
Pyramidelloidea
Amphiboloidea
Stylommatophora
Ellobioidea A
Otinoidea
Systellommatophora
Ellobioidea B
Trimusculoidea
Elloboioidea C

Figure 5.2 Phylogenetic relationships among gastropods. Adapted from Dinapoli and Klussmann-Kolb, 2010. Arrows indicate clades in which glomerular-like structures have been reported.

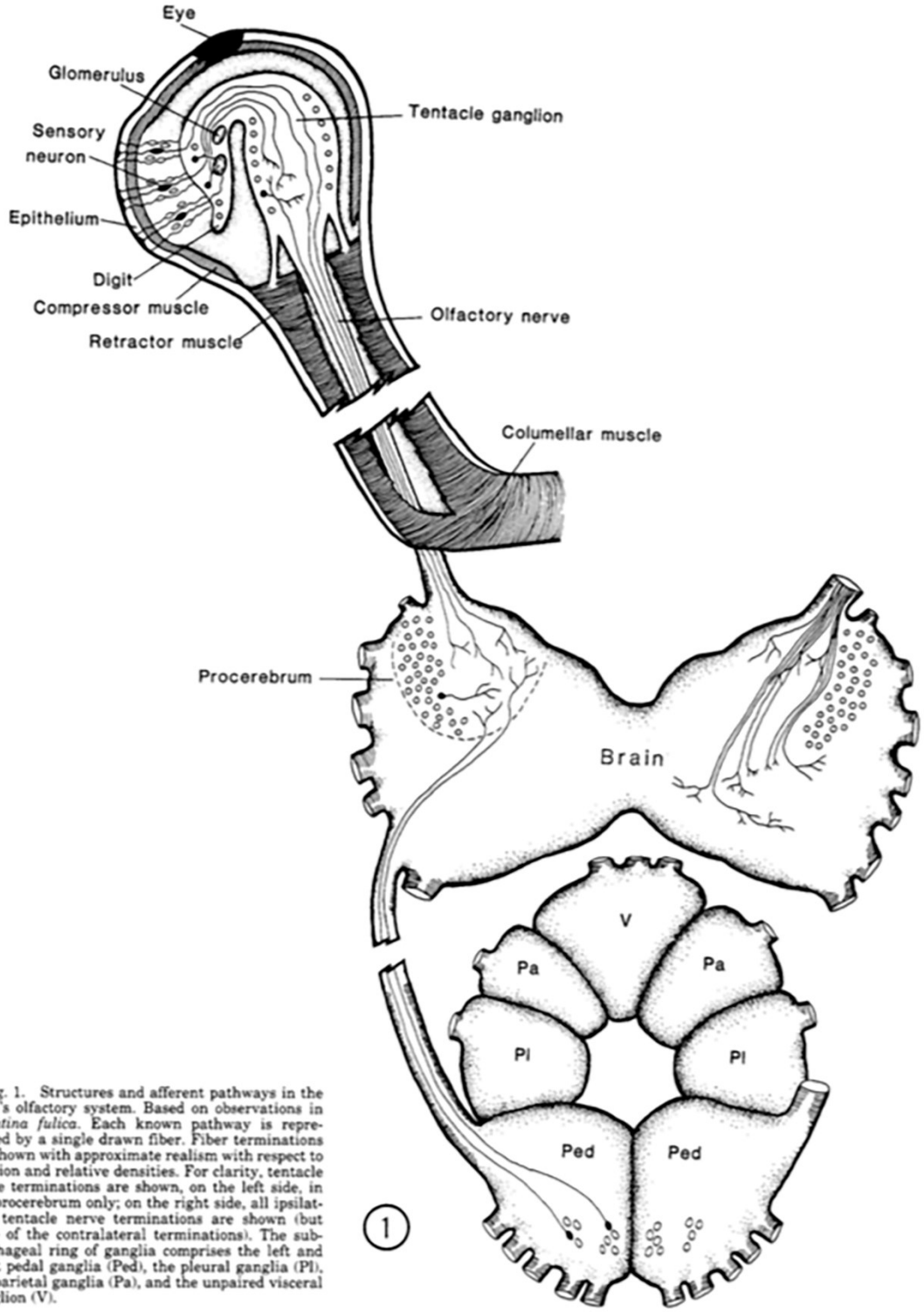

Fig. 1. Structures and afferent pathways in the snail's olfactory system. Based on observations in *Achatina fulica*. Each known pathway is represented by a single drawn fiber. Fiber terminations are shown with approximate realism with respect to position and relative densities. For clarity, tentacle nerve terminations are shown, on the left side, in the procerebrum only; on the right side, all ipsilateral tentacle nerve terminations are shown (but none of the contralateral terminations). The subesophageal ring of ganglia comprises the left and right pedal ganglia (Ped), the pleural ganglia (Pl), the parietal ganglia (Pa), and the unpaired visceral ganglion (V).

Figure 5.3 Drawing of a tentacle tip shown in sagittal view. From Chase and Tolloczko, 1993; published with permissions. The three possible projections of the receptor cell populations are each represented by a single receptor cell. The eye and its optic nerve comprise an entirely separate sensory system.

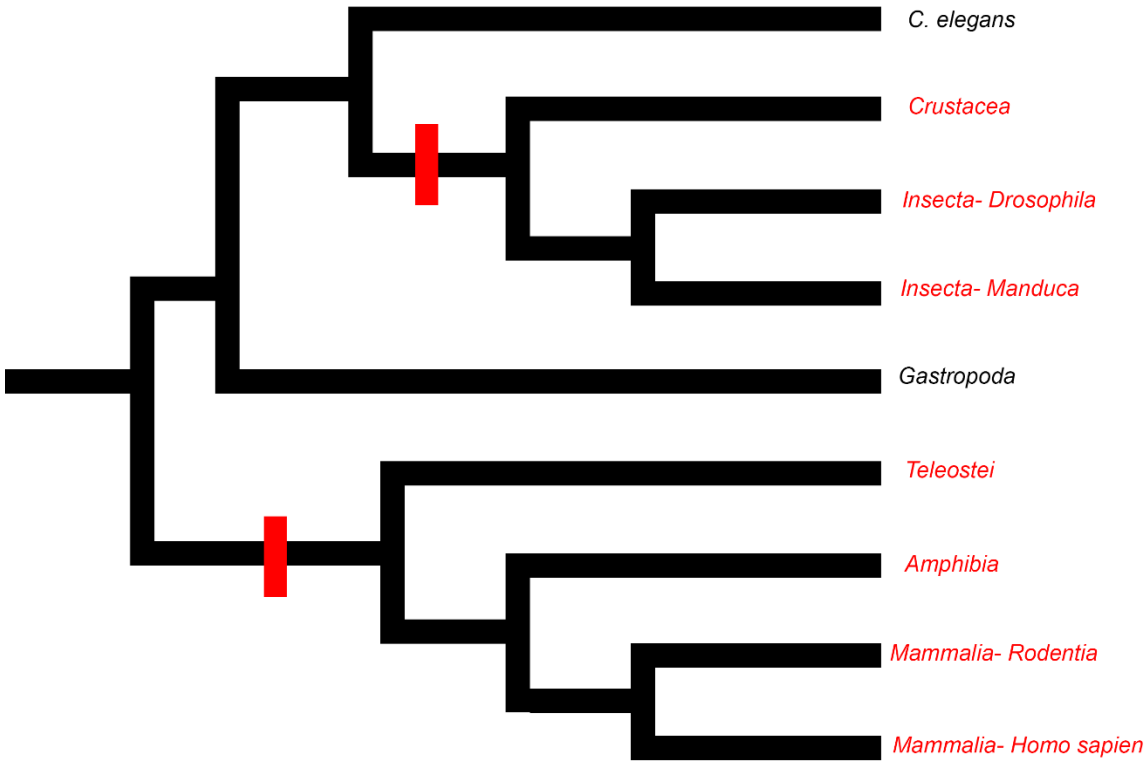

Figure 5.4 Phylogenetic distribution of glomerular structures-modified. Modified from Eisthen, 2002. Demonstration of our new phylogenetic hypothesis with the absence of glomeruli in gastropods, resulting in potentially two independent evolutions of glomeruli, one in vertebrates and one in arthropods.

References

Ache, B. W., & Young, J. M. (2005). Olfaction: Diverse species, conserved principles. *Neuron, 48*(3), 417-430.

Albertin, C. B., Simakov, O., Mitros, T., Wang, Z. Y., Pungor, J. R., Edsinger-Gonzales, E., Brenner, S., Ragsdale, C., & Rokhsar, D. S. (2015). The octopus genome and the evolution of cephalopod neural and morphological novelties. Nature, 524(7564), 220-224.

Alania, M., Sakharov, D., & Elliott, C. (2004). Multilevel inhibition of feeding by a peptidergic pleural interneuron in the mollusc *Lymnaea stagnalis*. *Journal of Comparative Physiology A, 190*(5), 379-390.

Aroua, S., Andouche, A., Martin, M., Baratte, S., & Bonnaud, L. (2011). FaRP cell distribution in the developing CNS suggests the involvement of FaRPs in all parts of the chromatophore control pathway in *Sepia officinalis* (Cephalopoda). *Zoology, 114*(2), 113-122.

Baratte, S., & Bonnaud, L. (2009). Evidence of early nervous differentiation and early catecholaminergic sensory system during *Sepia officinalis* embryogenesis. *Journal of Comparative Neurology, 517*(4), 539-549.

Barber, V., & Wright, D. (1969). The fine structure of the sense organs of the cephalopod mollusc *Nautilus*. *Cell and Tissue Research, 102*(3), 293-312.

Basil, J. A., Hanlon, R. T., Sheikh, S. I., & Atema, J. (2000). Three-dimensional odor tracking by *Nautilus pompilius*. *Journal of Experimental Biology*, 203(9), 1409-1414.

Bechtold, D. A., & Luckman, S. M. (2007). The role of RFamide peptides in feeding. *The Journal of Endocrinology, 192*(1), 3-15. doi:192/1/3 [pii]

Benton, R. (2015). Multigene family evolution: Perspectives from insect chemoreceptors. *Trends in Ecology & Evolution, 30*(10), 590-600.

Biggers, W. J., Pires, A., Pechenik, J. A., Johns, E., Patel, P., Polson, T., & Polson, J. (2012). Inhibitors of nitric oxide synthase induce larval settlement and metamorphosis of the polychaete annelid *Capitella teleta*. Invertebrate Reproduction & Development, 56(1), 1-13.

Brinkmann, N., & Wanninger, A. (2010). Capitellid connections: contributions from neuromuscular development of the maldanid polychaete *Axiothella rubrocincta* (Annelida). BMC evolutionary biology, 10(1), 168.

Blaustein, D. N., Derby, C. D., Simmons, R. B., & Beall, A. C. (1988). Structure of the brain and medulla terminalis of the spiny lobster *Panulirus argus* and the crayfish *Procambarus clarkii*, with an emphasis on olfactory centers. *Journal of Crustacean Biology,* 493-519.

Boal, J. G., Prosser, K. N., Holm, J. B., Simmons, T. L., Haas, R. E., & Nagle, G. T. (2010). Sexually mature cuttlefish are attracted to the eggs of conspecifics. *Journal of Chemical Ecology, 36*(8), 834-836.

Boal, J., & Golden, D. (1999). Distance chemoreception in the common cuttlefish, *Sepia officinalis* (mollusca, cephalopoda). *Journal of Experimental Marine Biology and Ecology, 235*(2), 307-317.

Boesveldt, S., Lindau, S. T., McClintock, M. K., Hummel, T., & Lundstrom, J. N. (2011). Gustatory and olfactory dysfunction in older adults: A national probability study. *Rhinology, 49*(3), 324-330. doi:10.4193/Rhino10.155 [doi]

Boletzky, S. (1989). Recent studies on spawning, embryonic development, and hatching in the cephalopoda. *Adv. Mar. Biol, 25*, 85-115.

Bonar, D. B. (1978). Ultrastructure of a cephalic sensory organ in larvae of the gastropod *Phestilla sibogae* (aeolidacea, nudibranchia). *Tissue and Cell, 10*(1), 153-165.

Boycott, B. (1961). The functional organization of the brain of the cuttlefish *Sepia officinalis*. *Proceedings of the Royal Society of London B: Biological Sciences, 153*(953), 503-534.

Boyle, P. (1983). Ventilation rate and arousal in the *Octopus*. *Journal of Experimental Marine Biology and Ecology, 69*(2), 129-136.

Boyle, P. (1986). Responses to water-borne chemicals by the octopus *Eledone cirrhosa* (Lamarck, 1798). *Journal of Experimental Marine Biology and Ecology, 104*(1-3), 23-30.

Boyle, P., & Rodhouse, P. (2008). Cephalopods: ecology and fisheries. John Wiley & Sons.

Budelmann, B. U. (1995). Cephalopod sense organs, nerves and the brain: Adaptations for high performance and life style. *Marine and Freshwater Behaviour and Physiology, 25*(1-3), 13-33.

Budelmann, B. U. (1996). Active marine predators: The sensory world of cephalopods. *Marine & Freshwater Behaviour & Phy, 27*(2-3), 59-75.

Buresi, A., Andouche, A., Navet, S., Bassaglia, Y., Bonnaud-Ponticelli, L., & Baratte, S. (2016). Nervous system development in cephalopods: How egg yolk-richness modifies the topology of the mediolateral patterning system. Developmental biology, 415(1), 143-156.

Buresi, A., Croll, R. P., Tiozzo, S., Bonnaud, L., & Baratte, S. (2014). Emergence of sensory structures in the developing epidermis in *Sepia officinalis* and other coleoid cephalopods. *Journal of Comparative Neurology, 522*(13), 3004-3019.

Carraher, C., Dalziel, J., Jordan, M. D., Christie, D. L., Newcomb, R. D., & Kralicek, A. V. (2015). Towards an understanding of the structural basis for insect olfaction by odorant receptors. *Insect Biochemistry and Molecular Biology, 66*, 31-41.

Chase, R., & Tolloczko, B. (1986). Synaptic glomeruli in the olfactory system of a snail, *Achatina fulica*. *Cell and Tissue Research, 246*(3), 567-573.

Chase, R., & Wells, M. (1986). Chemotactic behaviour in *Octopus*. *Journal of Comparative Physiology A, 158*(3), 375-381.

Christensen, T. A., & Hildebrand, J. G. (2002). Pheromonal and host-odor processing in the insect antennal lobe: How different? *Current Opinion in Neurobiology, 12*(4), 393-399.

Christie, A. E., Stein, W., Quinlan, J. E., Beenhakker, M. P., Marder, E., & Nusbaum, M. P. (2004). Actions of a histaminergic/peptidergic projection neuron on rhythmic motor patterns in the stomatogastric nervous system of the crab *Cancer borealis*. *Journal of Comparative Neurology, 469*(2), 153-169.

Croll, R. P. (2006). Development of embryonic and larval cells containing serotonin, catecholamines, and FMRFamide-related peptides in the gastropod mollusc *Phestilla sibogae*. *The Biological Bulletin, 211*(3), 232. doi:10.2307/4134546.

Croll, R. P., & Van Minnen, J. (1992). Distribution of the peptide Ala-Pro-Gly-Trp-NH2 (APGWamide) in the nervous system and periphery of the snail *Lymnaea stagnalis* as revealed by immunocytochemistry and *in situ* hybridization. Journal of Comparative Neurology, 324(4), 567-574.

Croset, V., Rytz, R., Cummins, S. F., Budd, A., Brawand, D., Kaessmann, H., Gibson, T. J., Benton, R. (2010). Ancient protostome origin of chemosensory ionotropic glutamate receptors and the evolution of insect taste and olfaction. *PLoS Genet, 6*(8), e1001064.

Croy, I., Nordin, S., & Hummel, T. (2014). Olfactory disorders and quality of life--an updated review. *Chemical Senses, 39*(3), 185-194. doi:10.1093/chemse/bjt072 [doi].

Cummins, S. F., Erpenbeck, D., Zou, Z., Claudianos, C., Moroz, L. L., Nagle, G. T., & Degnan, B. M. (2009). Candidate chemoreceptor subfamilies differentially expressed in the chemosensory organs of the mollusc *Aplysia*. *BMC Biology, 7*(1), 28.

Cummins, S. F., & Wyeth, R. C. (2014). Olfaction in gastropods. *Neuroecology and Neuroethology in Molluscs: The Interface between Behaviour and Environment. Edited by A. Di Cosmo and W. Winlow. Nova Science Publishers, Inc., Hauppauge, NY,* 45-72.

Cummins, S. F., Leblanc, L., Degnan, B. M., & Nagle, G. T. (2009). Molecular identification of candidate chemoreceptor genes and signal transduction components in the sensory epithelium of *Aplysia*. *The Journal of Experimental Biology, 212*(Pt 13), 2037-2044. doi:10.1242/jeb.026427 [doi].

Dancker, P., Löw, I., Hasselbach, W., & Wieland, T. (1975). Interaction of actin with phalloidin: Polymerization and stabilization of F-actin. *Biochimica Et Biophysica Acta (BBA)-Protein Structure, 400*(2), 407-414.

Darmaillacq, A., Lesimple, C., & Dickel, L. (2008). Embryonic visual learning in the cuttlefish, *Sepia officinalis*. *Animal Behaviour, 76*(1), 131-134.

D'este, L., Kimura, S., Casini, A., Matsuo, A., Bellier, J., Kimura, H., & Renda, T. G. (2008). First visualization of cholinergic cells and fibers by immunohistochemistry for choline acetyltransferase of the common type in the optic lobe and peduncle complex of *Octopus vulgaris*. *Journal of Comparative Neurology, 509*(6), 566-579.

Di Cosmo, A., & Di Cristo, C. (1998). Neuropeptidergic control of the optic gland of *Octopus vulgaris*: FMRF-amide and GnRH immunoreactivity. *Journal of Comparative Neurology, 398*(1), 1-12.

Di Cosmo, A., Di Cristo, C., Palumbo, A., d'Ischia, M., & Messenger, J. B. (2000). Nitric oxide synthase (NOS) in the brain of the cephalopod *Sepia officinalis*. *Journal of Comparative Neurology, 428*(3), 411-427.

Di Cosmo, A., Paolucci, M., & Di Cristo, C. (2004). N-methyl-D-aspartate receptor-like immunoreactivity in the brain of *Sepia* and *Octopus*. *Journal of Comparative Neurology, 477*(2), 202-219.

Dickinson, A. J., & Croll, R. P. (2003). Development of the larval nervous system of the gastropod *Ilyanassa obsoleta*. *Journal of Comparative Neurology, 466*(2), 197-218.

Dickinson, A. J., Croll, R. P., & Voronezhskaya, E. E. (2000). Development of embryonic cells containing serotonin, catecholamines, and FMRFamide-related peptides in *Aplysia californica*. *The Biological Bulletin, 199*(3), 305-315.

Dinapoli, A., & Klussmann-Kolb, A. (2010). The long way to diversity–phylogeny and evolution of the Heterobranchia (Mollusca: Gastropoda). Molecular Phylogenetics and Evolution, 55(1), 60-76.

Dynes, J. L., & Ngai, J. (1998). Pathfinding of olfactory neuron axons to stereotyped glomerular targets revealed by dynamic imaging in living zebrafish embryos. *Neuron, 20*(6), 1081-1091.

Eisthen, H. L. (2002). Why are olfactory systems of different animals so similar? *Brain, Behavior and Evolution, 59*(5-6), 273-293.

Elekes, K., & Nässel, D. (1990). Distribution of FMRFamide-like immunoreactive neurons in the central nervous system of the snail *Helix pomatia*. *Cell and Tissue Research, 262*(1), 177-190.

Elste, A., Koester, J., Shapiro, E., Panula, P., & Schwartz, J. H. (1990). Identification of histaminergic neurons in *Aplysia*. *Journal of Neurophysiology, 64*(3), 736-744.

Emery, D. G. (1975). The histology and fine structure of the olfactory organ of the squid *Lolliguncula brevis* blainville. *Tissue and Cell, 7*(2), 357-367.

Emery, D. G. (1976). Observations on the olfactory organ of adult and juvenile *Octopus joubini*. *Tissue and Cell, 8*(1), 33-46.

Enault, J., Zatylny-Gaudin, C., Bernay, B., Lefranc, B., Leprince, J., Baudy-Floc'h, M., & Henry, J. (2012). A complex set of sex pheromones identified in the cuttlefish *Sepia officinalis*. *PloS One, 7*(10), e46531.

Ennis, M., Linster, C., Aroniadou-Anderjaska, V., Ciombor, K., & Shipley, M. T. (1998). Glutamate and synaptic plasticity at mammalian primary olfactory synapses. Annals of the New York Academy of Sciences, 855(1), 457-466.

European Parliament, Council of the European Union (2010). Directive 2010/63/EU of the European Parliament and of the Council of 22 September 2010 on the

Protection of Animals Used for Scientific Purposes. Council of Europe, Strasbourg.

Faller, S., Staubach, S., & Klussmann-Kolb, A. (2008). Comparative immunohistochemistry of the cephalic sensory organs in opisthobranchia (mollusca, gastropoda). *Zoomorphology, 127*(4), 227-239.

Fan, X., Croll, R. P., Wu, B., Fang, L., Shen, Q., Painter, S. D., & Nagle, G. T. (1997). Molecular cloning of a cDNA encoding the neuropeptides APGWamide and cerebral peptide 1: Localization of APGWamide-like immunoreactivity in the central nervous system and male reproductive organs of *Aplysia*. Journal of Comparative Neurology, 387(1), 53-62.

Fiedler, A. (1992). The possible role of vena cava peptides in regulation of the branchial hearts of *Sepia officinalis* L.(cephalopoda). *Journal of Experimental Zoology Part A: Ecological Genetics and Physiology, 264*(2), 136-143.

Fioroni, P. (1990). Our recent knowledge of the development of the cuttlefish (*Sepia officinalis*). *Zoologischer Anzeiger, 224*(1-2), 1-25.

Gardner, J. W., Shin, H. W., & Hines, E. L. (2000). An electronic nose system to diagnose illness. Sensors and Actuators B: Chemical, 70(1), 19-24.

Gelperin, A. (1999). Oscillatory dynamics and information processing in olfactory systems. *The Journal of Experimental Biology, 202 (Pt 14)* (Pt 14), 1855-1864.

Gelperin, A., Flores, J., Raccuia-Behling, F., & Cooke, I. R. (2000). Nitric oxide and carbon monoxide modulate oscillations of olfactory interneurons in a terrestrial mollusk. *Journal of Neurophysiology, 83*(1), 116-127.

Gharbiah, M., Nakamoto, A., & Nagy, L. M. (2013). Analysis of ciliary band formation in the mollusc *Ilyanassa obsoleta*. Development genes and evolution, 223(4), 225-235.

Gilly, W. F., & Lucero, M. T. (1992). Behavioral responses to chemical stimulation of the olfactory organ in the squid *Loligo opalescens*. *Journal of Experimental Biology, 162*(1), 209-229.

Göbbeler, K., & Klussmann-Kolb, A. (2007). A comparative ultrastructural investigation of the cephalic sensory organs in Opisthobranchia (Mollusca, Gastropoda). Tissue and Cell, 39(6), 399-414.

Graziadei, P. (1962). Receptors in the suckers of octopus. *Nature, 195*, 57-59.

Haas, H. L., Sergeeva, O. A., & Selbach, O. (2008). Histamine in the nervous system. Physiological reviews, 88(3), 1183-1241.

Habib, M. R., Mohamed, A. H., Osman, G. Y., El-Din, A. T. S., Mossalem, H. S., Delgado, N., Torres, G., Rolon-Martinez, S., Miller, M. W., & Croll, R. P. (2015). Histamine immunoreactive elements in the central and peripheral nervous systems of the snail, *Biomphalaria spp*., intermediate host for *Schistosoma mansoni*. *PloS One, 10*(6), e0129800.

Halasz, N., & Shepherd, G. (1983). Neurochemistry of the vertebrate olfactory bulb. *Neuroscience, 10*(3), 579-619.

Hanley, M. E., Girling, R. D., Felix, A. E., Olliff, E. D., Newland, P. L., & Poppy, G. M. (2013). Olfactory selection of *Plantago lanceolata* by snails declines with seedling age. Annals of Botany, 112(4), 671-676.

Hanlon, R. T., & Messenger, J. B. (1998). *Cephalopod behaviour* Cambridge University Press.

Hansson, B. S., & Anton, S. (2000). Function and morphology of the antennal lobe: New developments. *Annual Review of Entomology, 45*(1), 203-231.

Hansson, B. (1995). Olfaction in *Lepidoptera*. *Experientia, 51*(11), 1003-1027.

Hegedűs, E., Kaslin, J., Hiripi, L., Kiss, T., Panula, P., & Elekes, K. (2004). Histaminergic neurons in the central and peripheral nervous system of gastropods (*Helix*, *Lymnaea*): An immunocytochemical, biochemical, and electrophysiological approach. *Journal of Comparative Neurology, 475*(3), 391-405.

Hildebrand, J. G., & Shepherd, G. M. (1997). Mechanisms of olfactory discrimination: Converging evidence for common principles across phyla. *Annual Review of Neuroscience, 20*(1), 595-631.

Hochberg, R., & Atherton, S. (2011). A new species of *Lepidodasys* (gastrotricha, macrodasyida) from panama with a description of its peptidergic nervous system using CLSM, anti-FMRFamide and anti-SCP B. *Zoologischer Anzeiger-A Journal of Comparative Zoology, 250*(2), 111-122.

Honkanen, T., & Ekström, P. (1990). An immunocytochemical study of the olfactory projections in the three-spined stickleback, *Gasterosteus aculeatus*, L. *Journal of Comparative Neurology, 292*(1), 65-72.

Howes, S. C., Alushin, G. M., Shida, T., Nachury, M. V., & Nogales, E. (2014). Effects of tubulin acetylation and tubulin acetyltransferase binding on microtubule structure. Molecular biology of the cell, 25(2), 257-266.

Hu, J. Y., Meng, X., & Schacher, S. (2003). Redistribution of syntaxin mRNA in neuronal cell bodies regulates protein expression and transport during synapse formation and long-term synaptic plasticity. Journal of Neuroscience, 23(5), 1804-1815.

Ito, I., Nakamura, H., Kimura, T., Suzuki, H., Sekiguchi, T., Kawabata, K., & Ito, E. (2000). Neuronal components of the superior and inferior tentacles in the terrestrial slug, *Limax marginatus*. *Neuroscience Research, 37*(3), 191-200.

Kauer, J. S., & Moulton, D. G. (1974). Responses of olfactory bulb neurones to odour stimulation of small nasal areas in the salamander. *The Journal of Physiology, 243*(3), 717-737.

Kaupp, U. B. (2010). Olfactory signaling in vertebrates and insects: Differences and commonalities. *Nature Reviews Neuroscience, 11*(3), 188-200.

Kay, L. M. (2015). Olfactory system oscillations across phyla. *Current Opinion in Neurobiology, 31*, 141-147.

Kempf, S. C., & Page, L. R. (2005). Anti-tubulin labeling reveals ampullary neuron ciliary bundles in opisthobranch larvae and a new putative neural structure associated with the apical ganglion. *The Biological Bulletin, 208*(3), 169-182.

Kim, S., Laschi, C., & Trimmer, B. (2013). Soft robotics: A bioinspired evolution in robotics. *Trends in Biotechnology, 31*(5), 287-294.

Kishida, T., Thewissen, J. G. M., Hayakawa, T., Imai, H., & Agata, K. (2015). Aquatic adaptation and the evolution of smell and taste in whales. Zoological letters, 1(1), 9.

Kiss, T. (2017). Do terrestrial gastropods use olfactory cues to locate and select food actively?. Invertebrate Neuroscience, 17(3), 9.

Komiyama, T., & Luo, L. (2006). Development of wiring specificity in the olfactory system. *Current Opinion in Neurobiology, 16*(1), 67-73.

Koueta, N., & Boucaud-Camou, E. (1999). Food intake and growth in reared early juvenile cuttlefish *Sepia officinalis* L. (Mollusca Cephalopoda). Journal of Experimental Marine Biology and Ecology, 240(1), 93-109.

Kreiling, J. A., Stephens, R. E., & Reinisch, C. L. (2005). A mixture of environmental contaminants increases cAMP-dependent protein kinase in spisula embryos. *Environmental Toxicology and Pharmacology, 19*(1), 9-18.

Kyriakides, M., & McCrohan, C. (1989). Effect of putative neuromodulators on rhythmic buccal motor output in *Lymnaea stagnalis*. *Journal of Neurobiology, 20*(7), 635-650.

Laptikhovsky, V., Salman, A., Önsoy, B., & Katagan, T. (2003). Fecundity of the common cuttlefish, *Sepia officinalis* L. (Cephalopoda, Sepiida): a new look at the old problem. Scientia Marina, 67(3), 279-284.

Le Gall, S., Féral, C., Van Minnen, J., & Marchand, C. (1988). Evidence for peptidergic innervation of the endocrine optic gland in *Sepia* by neurons showing FMRFamide-like immunoreactivity. *Brain Research, 462*(1), 83-88.

Lemaire, J. (1970). Table de développement embryonnaire de *Sepia officinalis* L. (mollusque céphalopode). *Bull Soc Zool Fr, 95*, 773-782.

LI, G., & Chase, R. (1995). Correlation of axon Projections and peptide immunoreactivity in mesocerebral neurons of the snail *Helix aspersa*. Journal of Comparative Neurology, 353(1), 9-17.

Lockyer, A. E., Spinks, J. N., Walker, A. J., Kane, R. A., Noble, L. R., Rollinson, D., Dias-Nito, E., & Jones, C. S. (2007). *Biomphalaria glabrata* transcriptome: identification of cell-signalling, transcriptional control and immune-related genes from open reading frame expressed sequence tags (ORESTES). Developmental & Comparative Immunology, 31(8), 763-782.

Li, K. W., Smit, A. B., & Geraerts, W. P. M. (1992). Structural and functional characterization of neuropeptides involved in the control of male mating behavior of *Lymnaea stagnalis*. Peptides, 13(4), 633-638.

Loi, P., Saunders, R., Young, D., & Tublitz, N. (1996). Peptidergic regulation of chromatophore function in the European cuttlefish *Sepia officinalis*. *The Journal of Experimental Biology, 199*(Pt 5), 1177-1187.

Loi, P. K., & Tublitz, N. (1997). Molecular analysis of FMRFamide- and FMRFamide-related peptides (FaRPS) in the cuttlefish *Sepia officinalis*. *The Journal of Experimental Biology, 200*(Pt 10), 1483-1489.

Mackie, G. (2008). Immunostaining of peripheral nerves and other tissues in whole-mount preparations from hatchling cephalopods. *Tissue and Cell, 40*(1), 21-29.

Marco, S., & Gutierrez-Galvez, A. (2012). Signal and data processing for machine olfaction and chemical sensing: A review. *IEEE Sensors Journal, 12*(11), 3189-3214.

Marquèze, B., Berton, F., & Seagar, M. (2000). Synaptotagmins in membrane traffic: Which vesicles do the tagmins tag? *Biochimie, 82*(5), 409-420.

Matsuo, R., Fukata, R., Kumagai, M., Kobayashi, A., Kobayashi, S., & Matsuo, Y. (2016). Distribution of histaminergic neurons and their modulatory effects on oscillatory activity in the olfactory center of the terrestrial slug *Limax*. *Journal of Comparative Neurology, 524*(1), 119-135.

Matsuo, R., Kobayashi, S., Watanabe, S., Namiki, S., Iinuma, S., Sakamoto, H., Hirose, K., & Ito, E. (2009). Glutamatergic neurotransmission in the procerebrum (olfactory center) of a terrestrial mollusk. *Journal of Neuroscience Research, 87*(13), 3011-3023.

McClintock, T. S., & Ache, B. W. (1989). Histamine directly gates a chloride channel in lobster olfactory receptor neurons. *Proceedings of the National Academy of Sciences of the United States of America, 86*(20), 8137-8141.

Messenger, J. (1971). The optic tract lobes. *The Anatomy of the Nervous System of Octopus Vulgaris. Oxford: Clarendon Press. p,* 482-506.

Messenger, J. (1979). The nervous system of *Loligo*: IV. the peduncle and olfactory lobes. *Philosophical Transactions of the Royal Society of London B: Biological Sciences, 285*(1008), 275-309.

Messenger, J. B. (1996). Neurotransmitters of cephalopods. *Invertebrate Neuroscience, 2*(2), 95-114.

Messenger, J. B. (2001). Cephalopod chromatophores: Neurobiology and natural history. *Biological Reviews, 76*(4), 473-528.

Messenger, J. B. (1967). The peduncle lobe: A visuo-motor centre in octopus. *Proceedings of the Royal Society of London. Series B, Biological Sciences, 167*(1008), 225-251.

Mobley, A. S., Mahendra, G., & Lucero, M. T. (2007). Evidence for multiple signaling pathways in single squid olfactory receptor neurons. *Journal of Comparative Neurology, 501*(2), 231-242.

Mobley, A. S., Michel, W. C., & Lucero, M. T. (2008). Odorant responsiveness of squid olfactory receptor neurons. *The Anatomical Record, 291*(7), 763-774.

Mombaerts, P., Wang, F., Dulac, C., Chao, S. K., Nemes, A., Mendelsohn, M., Edmonson, J., & Axel, R. (1996). Visualizing an olfactory sensory map. *Cell, 87*(4), 675-686.

Mori, K., Nagao, H., & Yoshihara, Y. (1999). The olfactory bulb: Coding and processing of odor molecule information. *Science (New York, N.Y.), 286*(5440), 711-715. doi:7927 [pii]

Moroz, L. L. (2006). Localization of putative nitrergic neurons in peripheral chemosensory areas and the central nervous system of *Aplysia californica*. *Journal of Comparative Neurology, 495*(1), 10-20.

Nagashima, A., & Touhara, K. (2010). Enzymatic conversion of odorants in nasal mucus affects olfactory glomerular activation patterns and odor perception. Journal of Neuroscience, 30(48), 16391-16398.

Nässel, D. R. (1999). Histamine in the brain of insects: A review. *Microscopy Research and Technique, 44*(2-3), 121-136.

Nezlin, L., & Voronezhskaya, E. (1997). GABA-immunoreactive neurones and interactions of GABA with serotonin and FMRFamide in a peripheral sensory ganglion of the pond snail *Lymnaea stagnalis*. Brain research, 772(1), 217-225.

Nixon, M., & Young, J. Z. (2003). The brains and lives of cephalopods. Oxford University Press.

Nomaksteinsky, M., Kassabov, S., Chettouh, Z., Stoeklé, H., Bonnaud, L., Fortin, G., & Brunet, J. (2013). Ancient origin of somatic and visceral neurons. *BMC Biology, 11*(1), 53.

Nordin, S., Almkvist, O., & Berglund, B. (2012). Is loss in odor sensitivity inevitable to the aging individual? A study of "successfully aged" elderly. *Chemosensory Perception, 5*(2), 188-196.

Northcutt, R. G., & Muske, L. E. (1994). Multiple embryonic origins of gonadotropin-releasing hormone (GnRH) immunoreactive neurons. *Developmental Brain Research, 78*(2), 279-290.

Novak, M. G., Ribeiro, J. M., & Hildebrand, J. G. (1995). 5-hydroxytryptamine in the salivary glands of adult female *Aedes aegypti* and its role in regulation of salivation. *The Journal of Experimental Biology, 198*(Pt 1), 167-174.

Ohsuga, K., Kurokawa, M., & Kuwasawa, K. (2000). Mosaic arrangement of SCPB-, FMRFamide-, and histamine-like immunoreactive sensory hair cells in the statocyst of the gastropod mollusc *Pleurobranchaea japonica*. *Cell and Tissue Research, 300*(1), 165-172.

Oland, L. A., & Tolbert, L. P. (1998). Glomerulus development in the absence of a set of mitral-like neurons in the insect olfactory lobe. *Journal of Neurobiology, 36*(1), 41-52.

Orona, E., Battelle, B., & Ache, B. W. (1990). Immunohistochemical and biochemical evidence for the putative inhibitory neurotransmitters histamine and GABA in lobster olfactory lobes. *Journal of Comparative Neurology, 294*(4), 633-646.

Panula, P., Häppölä, O., Airaksinen, M. S., Auvinen, S., & Virkamäki, A. (1988). Carbodiimide as a tissue fixative in histamine immunohistochemistry and its application in developmental neurobiology. *Journal of Histochemistry & Cytochemistry, 36*(3), 259-269.

Peymen, K., Watteyne, J., Frooninckx, L., Schoofs, L., & Beets, I. (2014). The FMRFamide-like peptide family in nematodes. *Frontiers in Endocrinology, 5*, 90. doi:10.3389/fendo.2014.00090 [doi]

Pinching, A. J., & Powell, T. P. (1971). The neuropil of the glomeruli of the olfactory bulb. *Journal of Cell Science, 9*(2), 347-377.

Pinelli, C., D'Aniello, B., Polese, G., & Rastogi, R. K. (2004). Extrabulbar olfactory system and nervus terminalis FMRFamide immunoreactive components in *Xenopus laevis* ontogenesis. *Journal of Chemical Neuroanatomy, 28*(1), 37-46.

Piper, M., & Holt, C. (2004). RNA translation in axons. Annu. Rev. Cell Dev. Biol., 20, 505-523.

Polese, G., Bertapelle, C., & Di Cosmo, A. (2015). Role of olfaction in *Octopus vulgaris* reproduction. *General and Comparative Endocrinology, 210*, 55-62.

Polese, G., Bertapelle, C., & Di Cosmo, A. (2016). Olfactory organ of *Octopus vulgaris*: Morphology, plasticity, turnover and sensory characterization. *Biology Open, 5*(5), 611-619. doi:10.1242/bio.017764 [doi].

Ponsen, M. M., Stoffers, D., Booij, J., van Eck-Smit, B. L., Wolters, E. C., & Berendse, H. W. (2004). Idiopathic hyposmia as a preclinical sign of Parkinson's disease. *Annals of Neurology, 56*(2), 173-181.

Raikova, O. I., Reuter, M., Kotikova, E. A., & Gustafsson, M. K. (1998). A commissural brain! the pattern of 5-HT immunoreactivity in *Acoela* (plathelminthes). *Zoomorphology, 118*(2), 69-77.

Rawlinson, K. A. (2010). Embryonic and post-embryonic development of the polyclad flatworm *Maritigrella crozieri*; implications for the evolution of spiralian life history traits. Frontiers in Zoology, 7(1), 12.

Reuter, M., Raikova, O., & Gustafsson, M. (1998). An endocrine brain? the pattern of FMRF-amide immunoreactivity in *Acoela* (plathelminthes). *Tissue and Cell, 30*(1), 57-63.

Romagny, S., Darmaillacq, A. S., Guibe, M., Bellanger, C., & Dickel, L. (2012). Feel, smell and see in an egg: Emergence of perception and learning in an immature invertebrate, the cuttlefish embryo. *The Journal of Experimental Biology, 215*(Pt 23), 4125-4130. doi:10.1242/jeb.078295 [doi].

Rossler, W., Kuduz, J., Schurmann, F. W., & Schild, D. (2002). Aggregation of f-actin in olfactory glomeruli: A common feature of glomeruli across phyla. *Chemical Senses, 27*(9), 803-810.

Röszer, T., Jenei, Z., Gáll, T., Nagy, O., Czimmerer, Z., Serfözö, Z., ... & Bánfalvi, G. (2004). A possible stimulatory effect of FMRFamide on neural nitric oxide production in the central nervous system of Helix lucorum L. Brain, behavior and evolution, 63(1), 23-33.

Ruth, P., Schmidtberg, H., Westermann, B., & Schipp, R. (2002). The sensory epithelium of the tentacles and the rhinophore of *Nautilus pompilius* L. (cephalopoda, nautiloidea). *Journal of Morphology, 251*(3), 239-255.

Saleuddin, S. (2017). Physiology of molluscs.

Schindelin, J., Arganda-Carreras, I., Frise, E., Kaynig, V., Longair, M., Pietzsch, T., Schmid, B. (2012). Fiji: An open-source platform for biological-image analysis. *Nature Methods, 9*(7), 676-682.

Schürmann, F. W. (1995). Common and special features of the nervous system of Onychophora: a comparison with Arthropoda, Annelida and some other invertebrates. EXPERIENTIA-BASEL-SUPPLEMENTUM-, 72, 139-139.Schwartz, J. C., Pollard, H., & Quach, T. T. (2006). Histamine as a neurotransmitter in mammalian brain: Neurochemical evidence. *Journal of Neurochemistry, 35*(1), 26-33.

Serizawa, S., Miyamichi, K., Nakatani, H., Suzuki, M., Saito, M., Yoshihara, Y., & Sakano, H. (2003). Negative feedback regulation ensures the one receptor-one olfactory neuron rule in mouse. *Science (New York, N.Y.), 302*(5653), 2088-2094. doi:10.1126/science.1089122 [doi].

Shigeno, S., Kidokoro, H., Tsuchiya, K., Segawa, S., & Yamamoto, M. (2001). Development of the brain in the oegopsid squid, *Todarodes pacificus*: An atlas up to the hatching stage. *Zoological Science, 18*(4), 527-541.

Shigeno, S., Tsuchiya, K., & Segawa, S. (2001). Embryonic and paralarval development of the central nervous system of the loliginid squid *Sepioteuthis lessoniana*. *Journal of Comparative Neurology, 437*(4), 449-475.

Shigeno, S., & Yamamoto, M. (2002). Organization of the nervous system in the pygmy cuttlefish, *Idiosepius paradoxus* Ortmann (idiosepiidae, cephalopoda). *Journal of Morphology, 254*(1), 65-80.

Smit, A. B., Jiménez, C. R., Dirks, R. W., Croll, R. P., & Geraerts, W. P. (1992). Characterization of a cDNA clone encoding multiple copies of the neuropeptide APGWamide in the mollusk *Lymnaea stagnalis*. Journal of Neuroscience, 12(5), 1709-1715.

Smith, S., Nason, J., & Croll, R. (1997). Detection of APGWamide-like immunoreactivity in the sea scallop, *Placopecten magellanicus*. *Neuropeptides, 31*(2), 155-165.

Soinila, S., Mpitsos, G. J., & Panula, P. (1990). Comparative study of histamine immunoreactivity in nervous systems of *Aplysia* and *Pleurobranchaea*. *Journal of Comparative Neurology, 298*(1), 83-96.

Speca, D. J., Lin, D. M., Sorensen, P. W., Isacoff, E. Y., Ngai, J., & Dittman, A. H. (1999). Functional identification of a goldfish odorant receptor. *Neuron, 23*(3), 487-498.

Strausfeld, N. J., Hansen, L., Li, Y., Gomez, R. S., & Ito, K. (1998). Evolution, discovery, and interpretations of arthropod mushroom bodies. Learning & memory, 5(1), 11-37.

Strausfeld, N. J., & Hildebrand, J. G. (1999). Olfactory systems: common design, uncommon origins?. Current opinion in neurobiology, 9(5), 634-639.

Strausfeld, N. J., Strausfeld, C. M., Loesel, R., Rowell, D., & Stowe, S. (2006). Arthropod phylogeny: Onychophoran brain organization suggests an archaic relationship with a chelicerate stem lineage. *Proceedings. Biological Sciences, 273*(1596), 1857-1866. doi:267G8Q8T5Q577562 [pii].

Stuart, A. E. (1999). From fruit flies to barnacles, histamine is the neurotransmitter of arthropod photoreceptors. *Neuron, 22*(3), 431-433.

Sundermann-Meister, G. (1978). A new type of ciliated cells in the epidermis of late embryonic stages and juveniles of *Loligo vulgaris* (mollusca, cephalopoda). *Zool Jb Anat, 99*, 493-499.

Susaki, E. A., Tainaka, K., Perrin, D., Yukinaga, H., Kuno, A., & Ueda, H. R. (2015). Advanced CUBIC protocols for whole-brain and whole-body clearing and imaging. *Nature Protocols, 10*(11), 1709-1727.

Suzuki, H., Kimura, T., Sekiguchi, T., & Mizukami, A. (1997). FMRF amide-like-immunoreactive primary sensory neurons in the olfactory system of the terrestrial mollusc, *Limax marginatus*. *Cell and Tissue Research, 289*(2), 339-345.

Tansey, E. (1979). Neurotransmitters in the cephalopod brain. *Comparative Biochemistry and Physiology Part C: Comparative Pharmacology, 64*(2), 173-182.

Thomas, J., Assefa, B., Cowley, C., & Ofosu-Barko, F. (1980). Behavioural responses to amino acids and related compounds, including propionic acid, by adult *Biomphalaria glabrata* (say), a snail host of *Schistosoma mansoni*. *Comparative Biochemistry and Physiology Part C: Comparative Pharmacology, 66*(1), 17-27.

Todt, C., Büchinger, T., & Wanninger, A. (2008). The nervous system of the basal mollusk *Wirenia argentea* (Solenogastres): a study employing immunocytochemical and 3D reconstruction techniques. Marine Biology Research, 4(4), 290-303.

Treloar, H. B., Miller, A. M., Ray, A., & Greer, C. A. (2010). Development of the olfactory system. In A. Menini (Ed.), *The neurobiology of olfaction* (). Boca Raton (FL): by Taylor and Francis Group, LLC. doi: NBK55972 [bookaccession].

van Golen, F. A., Li, K. W., de Lange, R. P., Jespersen, S., & Geraerts, W. P. (1995). Mutually exclusive neuronal expression of peptides encoded by the FMRFa gene underlies a differential control of copulation in *Lymnaea*. Journal of Biological Chemistry, 270(47), 28487-28493.

Vassar, R., Chao, S. K., Sitcheran, R., Nun, J. M., Vosshall, L. B., & Axel, R. (1994). Topographic organization of sensory projections to the olfactory bulb. *Cell, 79*(6), 981-991.

Vosshall, L. B., Wong, A. M., & Axel, R. (2000). An olfactory sensory map in the fly brain. *Cell, 102*(2), 147-159.

Wachowiak, M., Cohen, L. B., & Ache, B. W. (2002). Presynaptic inhibition of olfactory receptor neurons in crustaceans. *Microscopy Research and Technique, 58*(4), 365-375.

Wachowiak, M., & Cohen, L. B. (1999). Presynaptic inhibition of primary olfactory afferents mediated by different mechanisms in lobster and turtle. *The Journal of Neuroscience: The Official Journal of the Society for Neuroscience, 19*(20), 8808-8817.

Wachowiak, M., Diebel, C., & Ache, B. (1997). Local interneurons define functionally distinct regions within lobster olfactory glomeruli. *The Journal of Experimental Biology, 200*(Pt 6), 989-1001.

Walderon, M. D., Nolt, K. J., Haas, R. E., Prosser, K. N., Holm, J. B., Nagle, G. T., & Boal, J. G. (2011). Distance chemoreception and the detection of conspecifics in *Octopus bimaculoides*. *Journal of Molluscan Studies.*

Wells, M. (1963). Taste by touch: Some experiments with octopus. *Journal of Experimental Biology, 40*(1), 187-193.

Wells, M. J., Freeman, N. H., & Ashburner, M. (1965). Some experiments on the chemotactile sense of octopuses. *The Journal of Experimental Biology, 43*(3), 553-563.

Wertz, A., Rössler, W., Obermayer, M., & Bickmeyer, U. (2006). Functional neuroanatomy of the rhinophore of *Aplysia punctata*. *Frontiers in Zoology, 3*(1),6.

Wertz, A., Rössler, W., Obermayer, M., & Bickmeyer, U. (2007). Functional neuroanatomy of the rhinophore of *Archidoris pseudoargus*. *Helgoland Marine Research, 61*(2), 135-142.

Weth, F., Nadler, W., & Korsching, S. (1996). Nested expression domains for odorant receptors in zebrafish olfactory epithelium. Proceedings of the National Academy of Sciences, 93(23), 13321-13326.

Wildenburg, G., & Fioroni, P. (1989). Ultrastructure of the olfactory organ during embryonic development and at the hatching stage of *Loligo vulgaris* lam. (cephalopoda). *J. Ceph. Biol, 1*(1), 56-70.

Williamson, R., & Chrachri, A. (2004). Cephalopod neural networks. *Neuro-Signals, 13*(1-2), 87-98. doi:10.1159/000076160 [doi].

Wirsig-Wiechmann, C. R., & Oka, Y. (2002). The terminal nerve ganglion cells project to the olfactory mucosa in the dwarf gourami. *Neuroscience Research, 44*(3), 337-341.

Wollesen, T., Loesel, R., & Wanninger, A. (2009). Pygmy squids and giant brains: Mapping the complex cephalopod CNS by phalloidin staining of vibratome sections and whole-mount preparations. *Journal of Neuroscience Methods, 179*(1), 63-67.

Wollesen, T., Cummins, S. F., Degnan, B. M., & Wanninger, A. (2010)a. FMRFamide gene and peptide expression during central nervous system development of the cephalopod mollusk, *Idiosepius notoides*. *Evolution & Development, 12*(2), 113-130.

Wollesen, T., Degnan, B. M., & Wanninger, A. (2010)b. Expression of serotonin (5-HT) during CNS development of the cephalopod mollusk, *Idiosepius notoides*. *Cell and Tissue Research, 342*(2), 161-178.

Wollesen, T., Loesel, R., & Wanninger, A. (2008). FMRFamide-like immunoreactivity in the central nervous system of the cephalopod mollusc, *Idiosepius notoides*. *Acta Biologica Hungarica, 59*(Supplement 2), 111-116.

Wollesen, T., Sukhsangchan, C., Seixas, P., Nabhitabhata, J., & Wanninger, A. (2012). Analysis of neurotransmitter distribution in brain development of benthic and pelagic octopod cephalopods. *Journal of Morphology, 273*(7), 776-790.

Woodhams, M. P., & Messenger, J. (1974). A note on the ultrastructure of the octopus olfactory organ. *Cell and Tissue Research, 152*(2), 253-258.

Wyeth, R. C., & Croll, R. P. (2011). Peripheral sensory cells in the cephalic sensory organs of *Lymnaea stagnalis*. *Journal of Comparative Neurology, 519*(10), 1894-1913.

Yamamoto, M., Shimazaki, Y., & Shigeno, S. (2003). Atlas of the embryonic brain in the pygmy squid, *Idiosepius paradoxus*. *Zoological Science, 20*(2), 163-179.

Yasuda-Kamatani, Y., & Yasuda, A. (2006). Characteristic expression patterns of allatostatin-like peptide, FMRFamide-related peptide, orcokinin, tachykinin-related peptide, and SIFamide in the olfactory system of crayfish *Procambarus clarkii*. *Journal of Comparative Neurology, 496*(1), 135-147.

Yee, C. L., Yang, R., Böttger, B., Finger, T. E., & Kinnamon, J. C. (2001). “Type III” cells of rat taste buds: Immunohistochemical and ultrastructural studies of neuron-specific enolase, protein gene product 9.5, and serotonin. *Journal of Comparative Neurology, 440*(1), 97-108.

Young, J. Z. (1965). The central nervous system of nautilus. *Philosophical Transactions of the Royal Society of London B: Biological Sciences, 249*(754), 1-25.

Young, J. Z. (1971). Anatomy of the nervous system of octopus vulgaris.

Young, J. Z. (1972). The organization of a cephalopod ganglion. *Philosophical Transactions of the Royal Society of London. Series B, Biological Sciences,* 409-429.

Zatylny, C., Gagnon, J., Boucaud-Camou, E., & Henry, J. (2000). ILME: A waterborne pheromonal peptide released by the eggs of *Sepia officinalis*. *Biochemical and Biophysical Research Communications, 275*(1), 217-222.

Zatylny-Gaudin, C., & Favrel, P. (2014). Diversity of the RFamide peptide family in mollusks. *Frontiers in Endocrinology, 5*, 178. doi:10.3389/fendo.2014.00178 [doi].

Zhang, X., Mao, Y., Huang, Z., Qu, M., Chen, J., Ding, S., Hong, J., & Sun, T. (2012). Transcriptome analysis of the octopus vulgaris central nervous system. *PloS One, 7*(6), e40320.

Appendix A: Unpublished Results

A1.1 Tested Antibodies

Often, when doing immunohistochemistry on a molluscan model, the specificity of the antibody being tested is not close enough to the evolved molluscan protein of interest, resulting either in total prevention of binding or dim and faint staining. These results are often "thrown out" and unpublished, because in the mind of the scientist, the antibody in question "did not work." However, testing new antibodies and different procedures are a part of the scientific method. A problem arises when these antibodies that have been tested and "failed" remain unpublished and obsolete. When another scientist also gets the same idea to test that antibody, there is no information in the literature to reference.

Some journals and databases have attempted to overcome this issue by starting a journal such as *New Negatives in Plant Science*. However, not all journals are as accepting of negative results, suggesting that they are not high impact enough or just not interesting.

Therefore, one of the few remaining places that people can report failed antibody testing for publication is in thesis. Here, I mention some methods and antibodies that were tested during the last several years of exploring the olfactory system of *Sepia officinalis* that did not make it to final publication and the reasons behind these decisions.

Table A1.1 Table of Unpublished Results. Including target antigen, producer, and the reason the results were discounted or excluded from this study.

Target Antigen	Producer(s)	Reasons for excluding
Tyrosine hydroxylase	Immunostar, Hudson WI, USA	No consistent staining between fluorescence, DAB, or *ISH*
GABA	Immunostar, Hudson, WI, USA	Stained epithelial cells and blood vessels
Glutamate	Sigma Aldrich, Mississauga, ON, Canada	No consistent staining
Homer	Synaptic Systems, Goettingen, Germany	No consistent staining except lateral lines
Bassoon	Enzo Life Science, Farmingdale, NY	No consistent staining
Vesicular acetylcholine transporter protein	EMD Milipore, Billerica, MA, USA	No consistent staining
Vesicular glutamate transporter protein	Synaptic Systems, Goettingen, Germany and Sigma Aldrich, Mississauga, ON, Canada	No consistent staining except lateral lines
Synaptotagmin 1E11	Custom antibody	No consistent staining
Synaptotagmin V	Santa Cruz Biotechnology, Dallas, TX, USA	No staining
Synaptotagmin I	Santa Cruz Biotechnology, Dallas, TX, USA	No staining

A1.2 Tested Fixation Procedures

In addition, I attempted many different protocols for fixation of *S. officinalis* in whole-mount that did not succeed in complete fixation through the central nervous system. I record which protocols were attempted as well as if peripheral or central fixation was successful for future studies who are interested in immunohistochemistry or *in situ* hybridization on *S. officinalis* in whole-mount.

Table A1.2 Fixation Methods that were Tested from 2014-2017. * = peripheral fixation but no CNS fixation; ** = both peripheral and CNS fixed; N/A = not applicable.

	2014	2015	2016	2017
PFA 4%	*12 hrs whole	*24 hrs whole	**48 hrs head and mantle severed	**72 hrs head and mantle severed; arms removed
	*12 hrs eyes removed	**36 hrs whole	N/A	N/A
	*12 hrs 3 holes punctured on each side	** 48 hrs whole	N/A	N/A
	*12 hrs head and mantle severed	** 5 hrs then severed head from mantle then additional 1 hr PFA 4% then head cut down anterior-posterior axis then 36 hrs PFA 4%	N/A	N/A
	12 hrs 0.025% collagenase II for 1 hr before fixation	** 12 hrs brain completely dissected out	N/A	N/A
	12 hrs 0.025% collagenase II for 0.5 hrs before fixation	N/A	N/A	N/A
Methanol	12 hrs whole	N/A	24 hrs mantle and head severed	N/A

	2014	2015	2016	2017
	12 hrs eyes removed	N/A	N/A	N/A
	12 hrs 3 holes punctured on each side	N/A	N/A	N/A
	12 hrs head and mantle severed	N/A	N/A	N/A
	12 hrs eyes removed and constant agitation	N/A	N/A	N/A
	12 hrs 3 holes punctured on each side and constant agitation	N/A	N/A	N/A
	12 hrs head and mantle severed and constant agitation	N/A	N/A	N/A
EDAC	EDAC 3 hrs PFA 4% 12 hrs Eyes removed Head and mantle severed	12 hrs EDAC then 12 hrs PFA 2% whole	*12 hrs EDAC then PFA 4% 24 hrs mantle and head severed	**24 hrs EDAC then 48 hrs 4% PFA; mantle and head severed after 12 hrs; arms removed
	12 hrs EDAC then 12 hrs PFA 4% whole 0.05% collagenase II for 1.5 hrs before fixation	12 hrs. mix of EDAC 2% and 0.4% PFA then PFA 2% 12 hrs whole	N/A	**24 hrs EDAC then 48 hrs 4% PFA; mantle and head severed after 12 hrs; arms removed; EDAC injected in perfusion style into brain

	2014	2015	2016	2017
	N/A	12 hrs EDAC then PFA 2% 24 hrs whole	N/A	N/A
	N/A	12 hrs mix of EDAC 2% and 0.4% PFA then PFA 2% 24 hrs whole	N/A	N/A
	N/A	12 hrs EDAC then PFA 2% 12 hrs head and mantle severed	N/A	N/A
	N/A	*12 hrs EDAC then PFA 4% 48 hrs	N/A	N/A
Glutaraldehyde	4 hrs Glutaraldehyde 0.5% in 4% PFA solution eyes removed and head and mantle severed	N/A	24 hrs glutaraldehyde 0.5% in 4% PFA solution mantle and head severed	N/A
Paraformaldehyde /lysine/periodate	N/A	N/A	*24 hrs	N/A

A1.3 Tested Blocking Solutions

Finally, to optimize immunohistochemistry results, I tested four alternative blocking solutions with each fixative type. Reported below are the blocking solutions tested that did not result in better staining than reported in my final results above.

Table A1.3 Different Blocking Buffers Tested. To determine optimal immunohistochemical staining for each fixation procedure.

Blocking buffers tested
TRIS-HCL (pH 8.0)
PBS-T (2% Triton X-100, 1% DMSO, 1% BSA)
EDTA then PBS-T

Appendix B: Control Experiments

A2.1 *In situ Hybridization* Controls

In situ hybridization (*ISH*) staining was confirmed with a sense single strand mRNA probe that is the same sequence as the endogenous single strand mRNA and therefore will not bind, resulting in no staining. This was demonstrated using the antisense mRNA probe had the complementary sequence and was therefore specific to the targeted endogenous mRNA (Figure A2.1).

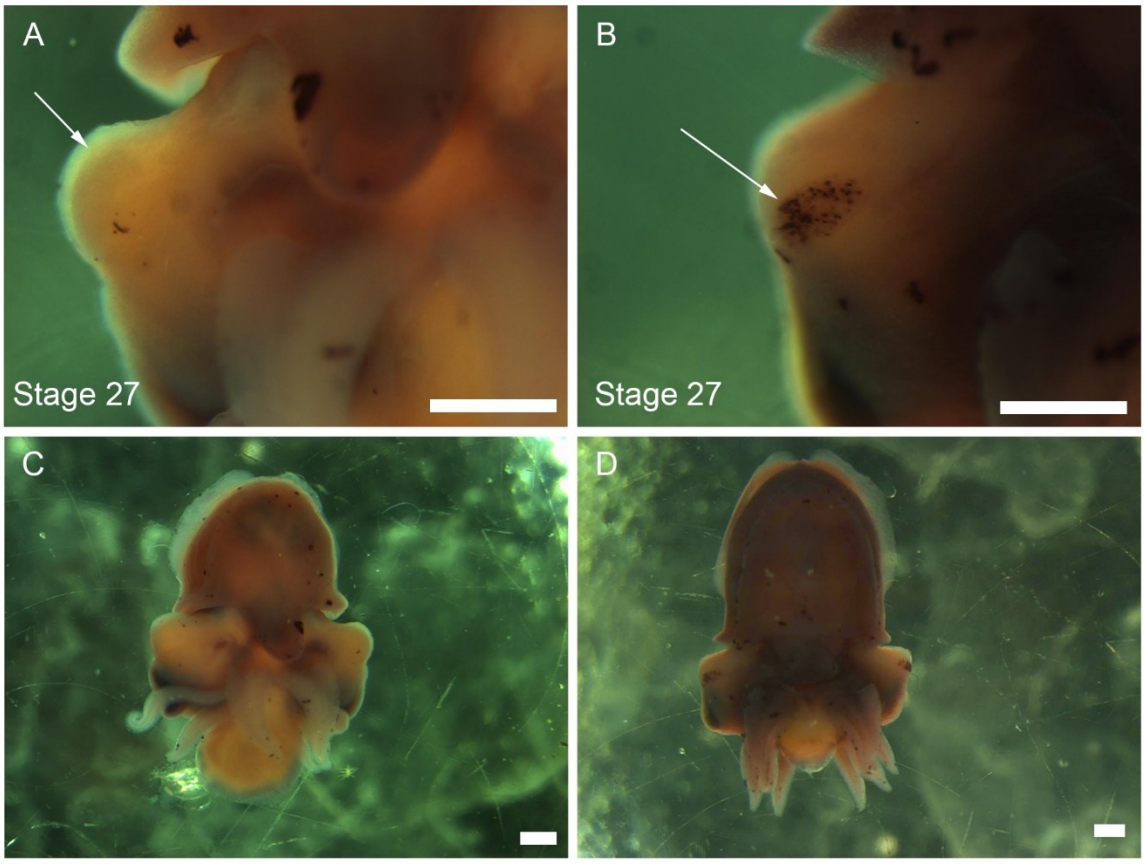
A
Stage 27
B
Stage 27
C
D

Figure A2.1 FMRFamide sense versus antisense mRNA probe. FMRFamide (FMRFa) mRNA sense probe in a stage 27 embryo. (A) No visible staining in the olfactory region, or anywhere else on the mantle, head, or arms. (B) After incubating in the same exact conditions for the same amount of time, staining was isolated to that region of epithelium. (C) A low magnification of the entire embryo demonstrating no FMRFa expression. (D) Same conditions, FMRFa expression in the olfactory organs. Scale bars are equal to 1 mm.

A2.2 Endogenous Tissue Fluorescence Controls

An additional concern was the natural autofluorescence of *S. officinalis* tissue. It has often been reported that iridophores in the skin naturally reflect light at certain wavelengths, so I wanted to confirm that the staining reported in this study was due to the immunohistochemistry protocol and was not affected by natural reflection. I sampled several sections of central nervous system (CNS) and mantle tissue and exposed them to different wavelengths under the fluorescent microscope to observe natural autofluorescence of untreated tissue. No autofluorescence was detected under 555 nm (Supplementary Figure A2.2 B) or 488 nm (Supplementary Figure A2.2 C) wavelengths, and incredibly minimal fluorescence in the epithelium was observed under UV light (Supplementary Figure A2.2 A).

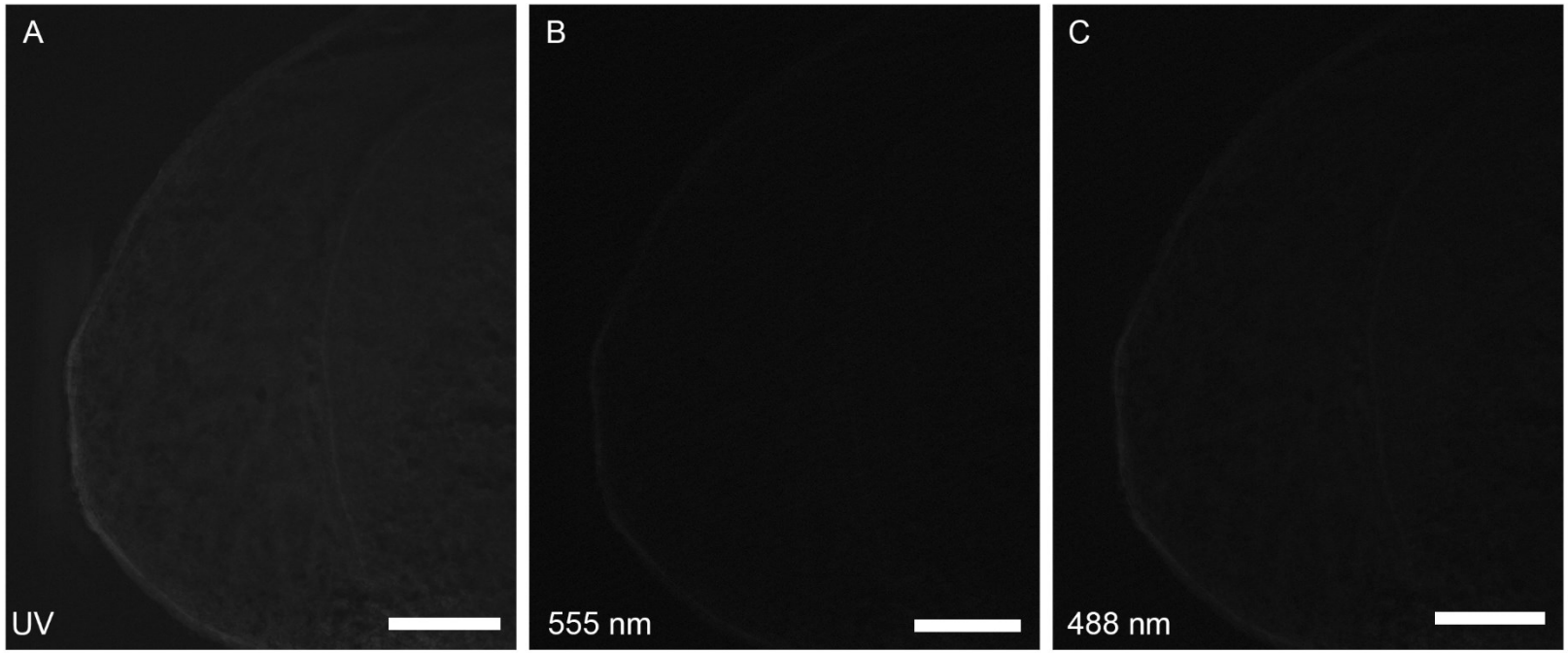
A
UV
B
555 nm
C
488 nm

Figure A2.2 Demonstration of natural autofluorescence of CNS. Tissue after Sectioning in a stage 27 embryo fixed with 4% PFA (A) Slight autofluorescence of tissue under UV light. UV light was used for DAPI label of nuclei, and any experimental results at this intensity would have been discounted. (B) No fluorescence of natural tissue under 555 nm wavelength at the same intensity of UV (C) No natural fluorescence of natural tissue under 488 nm wavelength of same intensity as (A) and (B).

A2.3 Omission of Primary Antibody Controls

The next control experiment I conducted was to observe the amount of fluorescence due to the secondary antibody by omitting the primary antibody in the usual immunohistochemistry experiments. Control experiments (without primary antibody) were conducted on one section while the rest of the series was treated under normal experimental conditions (with primary antibody) so that the control section (40 μm thick) could be easily compared. The non-primary antibody control sections resulted in a general light hazy staining throughout the tissue, without any specific pattern or strong labeling of cells or neurites, which directly contradicted the experimental sections in the subsequent section which demonstrated the usual pattern of staining as described in the results. As an additional precaution, I only focused on those areas of the CNS that had demonstrated consistent staining. For example, my control experiment omitting anti-serotonin was conducted in the olfactory lobe so that the experimental condition showed both neurons and neuropil, while the control showed no specific staining (Figure A2.3 A). Anti-APGWamide (APGWa) was consistent in the neuropil of the optic lobe, and was expressed in the experimental section next to the control section, but no staining was observed in the control (Figure A2.3 B). Likewise, FMRFa and histamine (HA) antibody omissions were all conducted on sections of the olfactory organ, as there was the most consistent staining throughout my experiments (Figure A2.3 C-D).

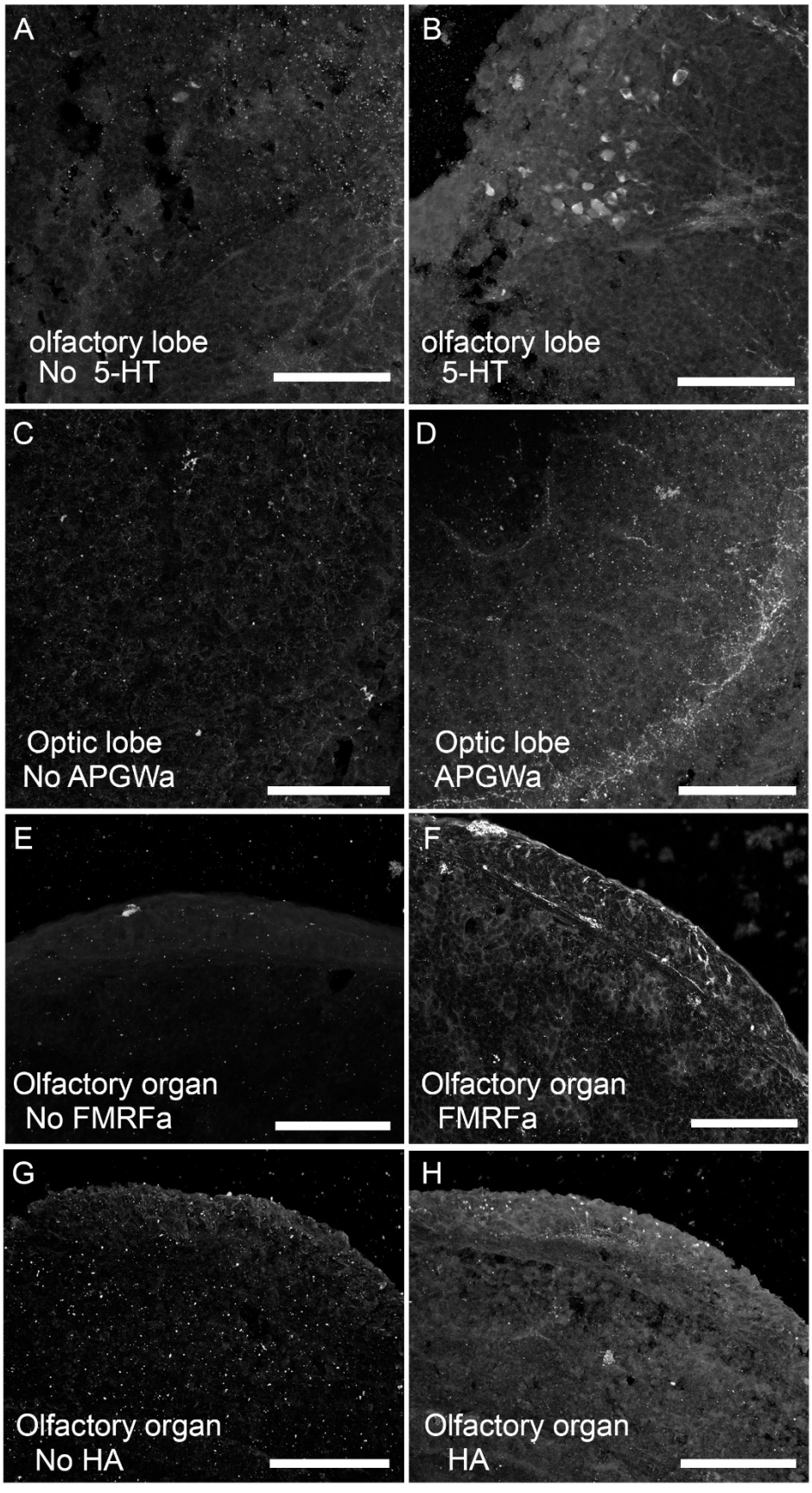
A
olfactory lobe
No 5-HT
B
olfactory lobe
5-HT
C
Optic lobe
No APGWa
D
Optic lobe
APGWa
E
Olfactory organ
No FMRFa
F
Olfactory organ
FMRFa
G
Olfactory organ
No HA
H
Olfactory organ
HA

Figure A2.3 Immunohistochemical controls with primary antibody. On sequential sections of stage 27 embryos (40 µm thickness) to demonstrate staining with (right) and without (left) primary antibody in regions in which the antibody is expressed strongly. (A) No serotonin (5-HT)-LIR in the dorsal-basal lobe without primary antibody, (B) but the subsequent section demonstrated strong immunofluorescence in cell bodies and neuropil. (C) No APGWa-LIR in the neuropil of the optic lobe, however all other sections (D) show intensely labeled neuropil with APGWa-antibody. (E) No immunofluorescence in the olfactory organ without anti-FMRFa, (F) yet there are fibers, cell bodies, and neuropil visible with the antibody present. (G) No staining in the olfactory organ without primary HA antibody, (H) but the stereotypical bright elements and neuropil staining are visible in the control section.

A2.4 Histamine-conjugate Pre-absorption Controls

Histamine conjugated to bovine serum albumin was used to quench activity of the primary antibody to demonstrate the specificity of the anti-histamine. In a similar experiment to the previous controls, the histamine conjugate was incubated with primary anti-histamine for 24 hrs before being applied to one section of the olfactory organ while the sequential section on the slide was treated with normal anti-histamine. The remaining procedure was conducted as described in the Chapter 2: Material and Methods. Figure A2.4 demonstrates the results from the preabsorbed-antibody (Figure A2.4 A) and the experimental condition (Figure A2.4 B) in which no conjugate was added to the primary antibody beforehand.

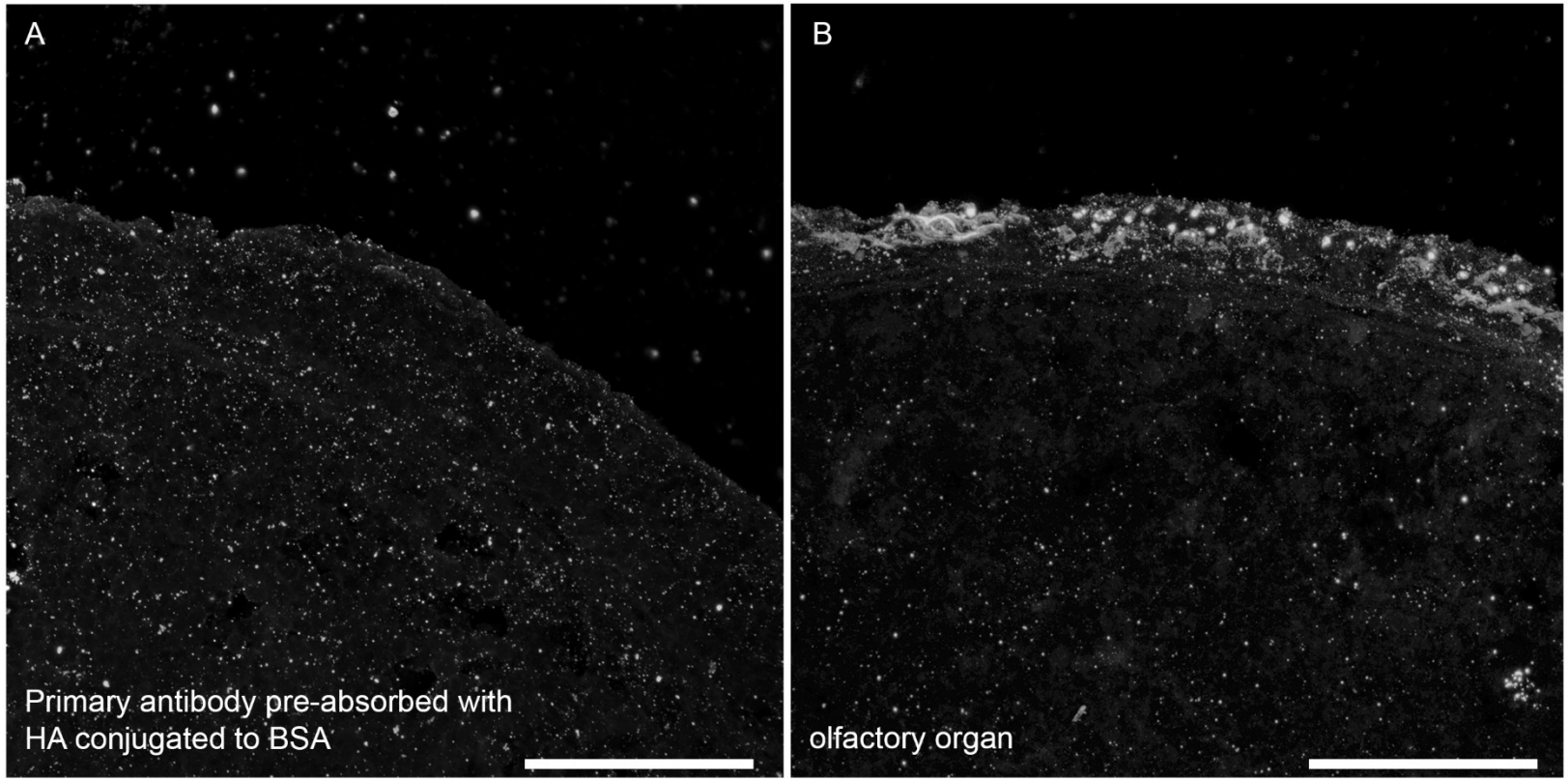
A
Primary antibody pre-absorbed with
HA conjugated to BSA
B
olfactory organ

Figure A2.4 Pre-absorption control experiment. (A) Histamine was conjugated to bovine serum albumin (BSA) and incubated with 1:200 primary antibody overnight, and applied to one section. (B) Immunohistochemistry was performed as on a stage 27 embryo as normal with experimental conditions observed on surrounding sections. Scale bars are equal to 100 μm.

Appendix C: Histidine Decarboxylase mRNA NCBI Blast Results

A3.1 Histidine Decarboxylase BLASTp Results in Invertebrates

Results from the NCBI BLASTp query of *S. officinalis* histidine decarboxylase mRNA within the non-redundant protein sequences database were used for the creation of the phylogenetic tree. Identity was between 82-71% similar, with E-values at a minimum of E^{-56}. Results are displayed in phylogenetic tree in Figure 3.9.

Table A3.1 Raw data from BLASTp query for *S. officinalis* HDC. From the non-redundant protein sequences database for *S. officinalis* HDC peptide sequence used for the creation of the phylogenetic tree (Figure 3.9).

Accession Number	Identity %	Max Score	E-value	Total Score
XP_019926970.1	82.051	89.74	2.00E-62	211
EKC37654.1	81.081	89.19	4.82E-58	197
XP_014666248.1	77.778	87.18	4.59E-59	202
NP_001191536.1	77.778	86.32	3.17E-57	199
XP_019932773.1	77.778	86.32	6.77E-56	191
XP_014297826.1	76.923	86.32	2.55E-58	199
XP_011308066.1	76.923	86.32	4.12E-58	199
XP_011308065.1	76.923	86.32	4.70E-58	199
XP_015127352.1	76.923	86.32	4.98E-58	199
XP_013070812.1	76.923	84.62	9.33E-56	191
JAN41888.1	76.068	86.32	4.52E-59	199
KZS17607.1	76.068	86.32	2.59E-58	199
XP_018918112.1	76.068	87.18	4.52E-58	197
KPM10342.1	76.068	86.32	9.97E-58	196

Accession Number	Identity %	Max Score	E-value	Total Score
XP_011494806.1	76.068	85.47	1.25E-57	196
XP_008179690.1	76.068	86.32	2.06E-57	196
XP_011155866.1	76.068	85.47	2.23E-57	197
XP_011153941.1	76.068	85.47	2.45E-57	197
XP_011155865.1	76.068	85.47	2.48E-57	197
XP_015372399.1	76.068	86.32	3.63E-57	196
XP_012264934.1	76.068	84.62	3.70E-57	195
XP_011688458.1	76.068	85.47	4.77E-57	197
XP_011494797.1	76.068	85.47	4.78E-57	196
XP_012059444.1	76.068	84.62	5.03E-57	196
XP_014474476.1	76.068	85.47	5.24E-57	196
XP_014275441.1	76.068	85.47	6.48E-57	195
KYN08025.1	76.068	84.62	1.12E-56	196
EGI58389.1	76.068	84.62	1.12E-56	196
XP_018399133.1	76.068	84.62	1.15E-56	196
KYN20262.1	76.068	84.62	1.24E-56	196
KYN35038.1	76.068	84.62	1.25E-56	196

Accession Number	Identity %	Max Score	E-value	Total Score
XP_011065790.1	76.068	84.62	1.25E-56	196
XP_018348285.1	76.068	84.62	1.26E-56	196
XP_018399126.1	76.068	84.62	1.29E-56	196
XP_018362421.1	76.068	84.62	1.29E-56	196
XP_018050596.1	76.068	84.62	1.29E-56	196
XP_012536885.1	76.068	84.62	1.46E-56	195
KYQ55866.1	76.068	84.62	2.62E-56	194
XP_018302816.1	76.068	84.62	3.01E-56	194
KYM81151.1	76.068	84.62	5.40E-56	196
OTF71062.1	75.214	86.32	9.57E-59	198
XP_011865708.1	75.214	85.47	4.62E-58	195
XP_015430117.1	75.214	85.47	1.06E-57	196
XP_015519147.1	75.214	85.47	1.32E-57	196
XP_011865703.1	75.214	85.47	2.01E-57	195
XP_014236666.1	75.214	85.47	2.07E-57	197
XP_014236665.1	75.214	85.47	2.10E-57	197
XP_016768642.1	75.214	85.47	3.26E-57	197

Accession Number	Identity %	Max Score	E-value	Total Score
XP_016921370.1	75.214	85.47	3.59E-57	197
XP_016768640.1	75.214	85.47	3.64E-57	197
XP_016921368.1	75.214	85.47	3.73E-57	197
XP_006621119.1	75.214	85.47	3.73E-57	197
KZC08499.1	75.214	85.47	3.77E-57	196
XP_006570903.1	75.214	85.47	3.77E-57	197
XP_006621116.1	75.214	85.47	3.86E-57	197
XP_012168299.1	75.214	85.47	3.93E-57	197
XP_012245142.1	75.214	85.47	3.93E-57	197
XP_003393425.1	75.214	85.47	4.07E-57	197
XP_012348090.1	75.214	85.47	4.54E-57	197
KDR23540.1	75.214	86.32	7.31E-57	194
XP_015589121.1	75.214	85.47	9.31E-57	196
XP_012147916.1	75.214	85.47	1.01E-56	196
XP_017762045.1	74.359	85.47	6.38E-57	196
XP_017762038.1	74.359	85.47	6.46E-57	196
XP_016841713.1	74.359	85.47	9.59E-57	195

Accession Number	Identity %	Max Score	E-value	Total Score
XP_016841712.1	74.359	85.47	1.03E-56	195
XP_017881211.1	74.359	85.47	1.17E-56	195
XP_017881210.1	74.359	85.47	1.22E-56	195
XP_016841711.1	74.359	85.47	1.98E-56	195
XP_008202389.1	74.359	85.47	2.10E-56	195
JAT15827.1	74.359	82.05	2.75E-56	182
XP_014212796.1	74.359	84.62	3.05E-56	193
XP_014212795.1	74.359	84.62	3.67E-56	193
XP_012234480.1	74.359	84.62	6.48E-56	193
XP_014212794.1	74.359	84.62	8.82E-56	193
XP_014212793.1	74.359	84.62	1.03E-55	193
XP_014212792.1	74.359	84.62	1.05E-55	193
XP_014614571.1	73.504	84.62	1.89E-57	184
XP_013401543.1	73.504	88.89	9.06E-57	195
XP_015930081.1	73.504	88.89	4.80E-56	191
XP_014245782.1	71.795	87.18	9.92E-57	192
XP_019622539.1	71.795	86.32	3.44E-56	193

A3.2 Histidine Decarboxylase BLASTp Results in Model Species

To confirm that our *S. officinalis* histidine decarboxylase (HDC) mRNA sequence was not restricted to invertebrates, I report results from the NCBI BLASTp query of *S. officinalis* HDC mRNA within the model organisms (landmark) database that were used for the creation of the phylogenetic tree of comparisons to well-studied model organisms. Identity was between 65-29% similar. Results are displayed in phylogenetic tree in Figure 3.10.

Table A3.2 Raw data from BLASTp query for *S. officinalis* HDC. From the Model Organisms (landmark) Database for *S. officinalis* HDC peptide sequence used for the creation of the phylogenetic tree (Figure 3.10).

Accession Number	Identity %	Max Score	E-value	Total Score
NP_523679.2	65.812	88.03	2.93E-55	187
NP_001260856.1	65.812	88.03	4.75E-55	184
XP_016877587.1	62.393	81.2	5.36E-50	169
NP_032256.3	62.393	82.05	1.05E-49	170
XP_006498847.1	62.393	82.05	1.27E-49	170
XP_016877586.1	62.393	81.2	1.28E-49	169
XP_016877585.1	62.393	81.2	1.33E-49	169
NP_002103.2	62.393	81.2	2.07E-49	169
XP_016877583.1	62.393	81.2	2.87E-49	169

Accession Number	Identity %	Max Score	E-value	Total Score
NP_724489.1	59.292	77.88	1.82E-41	147
NP_001096063.1	55.556	82.05	2.03E-44	155
XP_005169965.1	54.701	81.2	7.30E-44	153
NP_610226.2	53.448	72.41	6.39E-38	137
NP_495744.1	52.137	72.65	1.33E-38	139
NP_495743.1	52.137	72.65	2.99E-38	139
NP_724163.1	52.137	66.67	2.50E-37	135
NP_724164.1	52.137	66.67	2.61E-37	134
NP_057881.1	51.724	72.41	2.67E-39	139
XP_006514549.1	51.724	72.41	4.93E-39	139
NP_476592.1	50.435	65.22	2.01E-34	127
NP_724162.1	50.435	65.22	5.05E-34	125
NP_001229818.1	50	73.28	6.39E-39	137
NP_001229816.1	50	73.28	1.18E-38	137
XP_011513463.2	50	73.28	1.55E-38	137
NP_000781.1	50	73.28	2.72E-38	137
NP_001229817.1	50	73.28	7.57E-38	134

Accession Number	Identity %	Max Score	E-value	Total Score
NP_001229815.1	50	73.28	1.72E-37	134
XP_005271802.1	50	73.28	1.72E-37	134
NP_998507.1	50	68.97	6.70E-37	133
XP_003521317.1	41.803	58.2	1.76E-27	107
NP_001324415.1	40.984	58.2	1.53E-24	99.8
NP_849999.1	40.984	58.2	1.75E-24	99.8
NP_502265.2	40.196	60.78	2.76E-20	88.2
NP_001293075.1	40.171	54.7	5.75E-21	90.1
XP_016877584.1	40.171	54.7	5.80E-21	90.1
XP_003547319.1	39.85	57.14	3.49E-24	99
NP_001190862.1	39.474	62.28	1.76E-22	94.4
NP_194597.1	39.474	62.28	1.79E-22	94.4
NP_001190861.1	39.474	62.28	1.80E-22	94.4
NP_001078461.1	39.474	62.28	1.89E-22	94.4
NP_498210.1	38.462	64.96	4.01E-23	95.9
NP_001021151.1	37.607	61.54	1.41E-22	94.4
NP_001021150.1	37.607	61.54	1.42E-22	94.4

Accession Number	Identity %	Max Score	E-value	Total Score
XP_003535055.2	37.594	54.14	3.65E-23	95.9
XP_003529905.1	35.461	50.35	2.22E-21	91.3
NP_001329473.1	31.69	50	3.48E-17	79.3
NP_001285910.1	30.189	49.06	0.74	32.3
NP_476788.1	29.63	48.15	0.32	33.5

Appendix D: Copyright Permissions

ELSEVIER LICENSE
TERMS AND CONDITIONS

Jun 22, 2017

This Agreement between Ms. Alexia Scaros ("You") and Elsevier ("Elsevier") consists of your license details and the terms and conditions provided by Elsevier and Copyright Clearance Center.

License Number	4134280855913
License date	Jun 22, 2017
Licensed Content Publisher	Elsevier
Licensed Content Publication	Tissue and Cell
Licensed Content Title	The histology and fine structure of the olfactory organ of the squid Lolliguncula brevis blainville
Licensed Content Author	Dennis G. Emery
Licensed Content Date	Jan 1, 1975
Licensed Content Volume	7
Licensed Content Issue	2
Licensed Content Pages	11
Start Page	357
End Page	367
Type of Use	reuse in a thesis/dissertation
Portion	figures/tables/illustrations
Number of figures/tables/illustrations	1
Format	both print and electronic
Are you the author of this Elsevier article?	No
Will you be translating?	No
Order reference number	
Original figure numbers	Figure 16
Title of your thesis/dissertation	The Olfactory System of the Embryonic Common Cuttlefish, Sepia officinalis (Linnaeus, 1758)
Expected completion date	Aug 2017
Estimated size (number of pages)	150
Elsevier VAT number	GB 494 6272 12
Requestor Location	Ms. Alexia Scaros 5850 College Street PO BOX 15000 Halifax, NS B3H 4R2 Canada Attn: Ms. Alexia Scaros
Total	0.00 CAD

Terms and Conditions

INTRODUCTION

1. The publisher for this copyrighted material is Elsevier. By clicking "accept" in connection with completing this licensing transaction, you agree that the following terms and conditions apply to this transaction (along with the Billing and Payment terms and conditions established by Copyright Clearance Center, Inc. ("CCC"), at the time that you opened your Rightslink account and that are available at any time at http://myaccount.copyright.com).

GENERAL TERMS

2. Elsevier hereby grants you permission to reproduce the aforementioned material subject to the terms and conditions indicated.
3. Acknowledgement: If any part of the material to be used (for example, figures) has appeared in our publication with credit or acknowledgement to another source, permission must also be sought from that source. If such permission is not obtained then that material may not be included in your publication/copies. Suitable acknowledgement to the source must be made, either as a footnote or in a reference list at the end of your publication, as follows:
"Reprinted from Publication title, Vol /edition number, Author(s), Title of article / title of chapter, Pages No., Copyright (Year), with permission from Elsevier [OR APPLICABLE SOCIETY COPYRIGHT OWNER]." Also Lancet special credit - "Reprinted from The Lancet, Vol. number, Author(s), Title of article, Pages No., Copyright (Year), with permission from Elsevier."
4. Reproduction of this material is confined to the purpose and/or media for which permission is hereby given.
5. Altering/Modifying Material: Not Permitted. However figures and illustrations may be altered/adapted minimally to serve your work. Any other abbreviations, additions, deletions and/or any other alterations shall be made only with prior written authorization of Elsevier Ltd. (Please contact Elsevier at permissions@elsevier.com). No modifications can be made to any Lancet figures/tables and they must be reproduced in full.
6. If the permission fee for the requested use of our material is waived in this instance, please be advised that your future requests for Elsevier materials may attract a fee.
7. Reservation of Rights: Publisher reserves all rights not specifically granted in the combination of (i) the license details provided by you and accepted in the course of this licensing transaction, (ii) these terms and conditions and (iii) CCC's Billing and Payment terms and conditions.
8. License Contingent Upon Payment: While you may exercise the rights licensed immediately upon issuance of the license at the end of the licensing process for the transaction, provided that you have disclosed complete and accurate details of your proposed use, no license is finally effective unless and until full payment is received from you (either by publisher or by CCC) as provided in CCC's Billing and Payment terms and conditions. If full payment is not received on a timely basis, then any license preliminarily granted shall be deemed automatically revoked and shall be void as if never granted. Further, in the event that you breach any of these terms and conditions or any of CCC's Billing and Payment terms and conditions, the license is automatically revoked and shall be void as if never granted. Use of materials as described in a revoked license, as well as any use of the materials beyond the scope of an unrevoked license, may constitute copyright infringement and publisher reserves the right to take any and all action to protect its copyright in the materials.
9. Warranties: Publisher makes no representations or warranties with respect to the licensed material.
10. Indemnity: You hereby indemnify and agree to hold harmless publisher and CCC, and their respective officers, directors, employees and agents, from and against any and all claims arising out of your use of the licensed material other than as specifically authorized pursuant to this license.

11. No Transfer of License: This license is personal to you and may not be sublicensed, assigned, or transferred by you to any other person without publisher's written permission.
12. No Amendment Except in Writing: This license may not be amended except in a writing signed by both parties (or, in the case of publisher, by CCC on publisher's behalf).
13. Objection to Contrary Terms: Publisher hereby objects to any terms contained in any purchase order, acknowledgment, check endorsement or other writing prepared by you, which terms are inconsistent with these terms and conditions or CCC's Billing and Payment terms and conditions. These terms and conditions, together with CCC's Billing and Payment terms and conditions (which are incorporated herein), comprise the entire agreement between you and publisher (and CCC) concerning this licensing transaction. In the event of any conflict between your obligations established by these terms and conditions and those established by CCC's Billing and Payment terms and conditions, these terms and conditions shall control.
14. Revocation: Elsevier or Copyright Clearance Center may deny the permissions described in this License at their sole discretion, for any reason or no reason, with a full refund payable to you. Notice of such denial will be made using the contact information provided by you. Failure to receive such notice will not alter or invalidate the denial. In no event will Elsevier or Copyright Clearance Center be responsible or liable for any costs, expenses or damage incurred by you as a result of a denial of your permission request, other than a refund of the amount(s) paid by you to Elsevier and/or Copyright Clearance Center for denied permissions.

LIMITED LICENSE

The following terms and conditions apply only to specific license types:
15. **Translation**: This permission is granted for non-exclusive world **English** rights only unless your license was granted for translation rights. If you licensed translation rights you may only translate this content into the languages you requested. A professional translator must perform all translations and reproduce the content word for word preserving the integrity of the article.
16. **Posting licensed content on any Website**: The following terms and conditions apply as follows: Licensing material from an Elsevier journal: All content posted to the web site must maintain the copyright information line on the bottom of each image; A hyper-text must be included to the Homepage of the journal from which you are licensing at http://www.sciencedirect.com/science/journal/xxxxx or the Elsevier homepage for books at http://www.elsevier.com; Central Storage: This license does not include permission for a scanned version of the material to be stored in a central repository such as that provided by Heron/XanEdu.
Licensing material from an Elsevier book: A hyper-text link must be included to the Elsevier homepage at http://www.elsevier.com . All content posted to the web site must maintain the copyright information line on the bottom of each image.

Posting licensed content on Electronic reserve: In addition to the above the following clauses are applicable: The web site must be password-protected and made available only to bona fide students registered on a relevant course. This permission is granted for 1 year only. You may obtain a new license for future website posting.
17. **For journal authors:** the following clauses are applicable in addition to the above:
Preprints:
A preprint is an author's own write-up of research results and analysis, it has not been peer-reviewed, nor has it had any other value added to it by a publisher (such as formatting, copyright, technical enhancement etc.).
Authors can share their preprints anywhere at any time. Preprints should not be added to or enhanced in any way in order to appear more like, or to substitute for, the final versions of articles however authors can update their preprints on arXiv or RePEc with their Accepted Author Manuscript (see below).

If accepted for publication, we encourage authors to link from the preprint to their formal publication via its DOI. Millions of researchers have access to the formal publications on ScienceDirect, and so links will help users to find, access, cite and use the best available version. Please note that Cell Press, The Lancet and some society-owned have different preprint policies. Information on these policies is available on the journal homepage.
Accepted Author Manuscripts: An accepted author manuscript is the manuscript of an article that has been accepted for publication and which typically includes author-incorporated changes suggested during submission, peer review and editor-author communications.
Authors can share their accepted author manuscript:

- immediately
  - via their non-commercial person homepage or blog
  - by updating a preprint in arXiv or RePEc with the accepted manuscript
  - via their research institute or institutional repository for internal institutional uses or as part of an invitation-only research collaboration work-group
  - directly by providing copies to their students or to research collaborators for their personal use
  - for private scholarly sharing as part of an invitation-only work group on commercial sites with which Elsevier has an agreement
- After the embargo period
  - via non-commercial hosting platforms such as their institutional repository
  - via commercial sites with which Elsevier has an agreement

In all cases accepted manuscripts should:

- link to the formal publication via its DOI
- bear a CC-BY-NC-ND license - this is easy to do
- if aggregated with other manuscripts, for example in a repository or other site, be shared in alignment with our hosting policy not be added to or enhanced in any way to appear more like, or to substitute for, the published journal article.

Published journal article (JPA): A published journal article (PJA) is the definitive final record of published research that appears or will appear in the journal and embodies all value-adding publishing activities including peer review co-ordination, copy-editing, formatting, (if relevant) pagination and online enrichment.
Policies for sharing publishing journal articles differ for subscription and gold open access articles:
Subscription Articles: If you are an author, please share a link to your article rather than the full-text. Millions of researchers have access to the formal publications on ScienceDirect, and so links will help your users to find, access, cite, and use the best available version.
Theses and dissertations which contain embedded PJAs as part of the formal submission can be posted publicly by the awarding institution with DOI links back to the formal publications on ScienceDirect.
If you are affiliated with a library that subscribes to ScienceDirect you have additional private sharing rights for others' research accessed under that agreement. This includes use for classroom teaching and internal training at the institution (including use in course packs and courseware programs), and inclusion of the article for grant funding purposes.
Gold Open Access Articles: May be shared according to the author-selected end-user license and should contain a CrossMark logo, the end user license, and a DOI link to the formal publication on ScienceDirect.
Please refer to Elsevier's posting policy for further information.
18. **For book authors** the following clauses are applicable in addition to the above:
Authors are permitted to place a brief summary of their work online only. You are not

allowed to download and post the published electronic version of your chapter, nor may you scan the printed edition to create an electronic version. **Posting to a repository:** Authors are permitted to post a summary of their chapter only in their institution's repository.
19. **Thesis/Dissertation**: If your license is for use in a thesis/dissertation your thesis may be submitted to your institution in either print or electronic form. Should your thesis be published commercially, please reapply for permission. These requirements include permission for the Library and Archives of Canada to supply single copies, on demand, of the complete thesis and include permission for Proquest/UMI to supply single copies, on demand, of the complete thesis. Should your thesis be published commercially, please reapply for permission. Theses and dissertations which contain embedded PJAs as part of the formal submission can be posted publicly by the awarding institution with DOI links back to the formal publications on ScienceDirect.

Elsevier Open Access Terms and Conditions
You can publish open access with Elsevier in hundreds of open access journals or in nearly 2000 established subscription journals that support open access publishing. Permitted third party re-use of these open access articles is defined by the author's choice of Creative Commons user license. See our open access license policy for more information.
Terms & Conditions applicable to all Open Access articles published with Elsevier:
Any reuse of the article must not represent the author as endorsing the adaptation of the article nor should the article be modified in such a way as to damage the author's honour or reputation. If any changes have been made, such changes must be clearly indicated.
The author(s) must be appropriately credited and we ask that you include the end user license and a DOI link to the formal publication on ScienceDirect.
If any part of the material to be used (for example, figures) has appeared in our publication with credit or acknowledgement to another source it is the responsibility of the user to ensure their reuse complies with the terms and conditions determined by the rights holder.
Additional Terms & Conditions applicable to each Creative Commons user license:
CC BY: The CC-BY license allows users to copy, to create extracts, abstracts and new works from the Article, to alter and revise the Article and to make commercial use of the Article (including reuse and/or resale of the Article by commercial entities), provided the user gives appropriate credit (with a link to the formal publication through the relevant DOI), provides a link to the license, indicates if changes were made and the licensor is not represented as endorsing the use made of the work. The full details of the license are available at http://creativecommons.org/licenses/by/4.0.
CC BY NC SA: The CC BY-NC-SA license allows users to copy, to create extracts, abstracts and new works from the Article, to alter and revise the Article, provided this is not done for commercial purposes, and that the user gives appropriate credit (with a link to the formal publication through the relevant DOI), provides a link to the license, indicates if changes were made and the licensor is not represented as endorsing the use made of the work. Further, any new works must be made available on the same conditions. The full details of the license are available at http://creativecommons.org/licenses/by-nc-sa/4.0.
CC BY NC ND: The CC BY-NC-ND license allows users to copy and distribute the Article, provided this is not done for commercial purposes and further does not permit distribution of the Article if it is changed or edited in any way, and provided the user gives appropriate credit (with a link to the formal publication through the relevant DOI), provides a link to the license, and that the licensor is not represented as endorsing the use made of the work. The full details of the license are available at http://creativecommons.org/licenses/by-nc-nd/4.0.
Any commercial reuse of Open Access articles published with a CC BY NC SA or CC BY NC ND license requires permission from Elsevier and will be subject to a fee.
Commercial reuse includes:

- Associating advertising with the full text of the Article
- Charging fees for document delivery or access

- Article aggregation
- Systematic distribution via e-mail lists or share buttons

Posting or linking by commercial companies for use by customers of those companies.

20. **Other Conditions**:

v1.9

Questions? customercare@copyright.com or +1-855-239-3415 (toll free in the US) or +1-978-646-2777.

SPRINGER LICENSE
TERMS AND CONDITIONS

Jun 22, 2017

This Agreement between Ms. Alexia Scaros ("You") and Springer ("Springer") consists of your license details and the terms and conditions provided by Springer and Copyright Clearance Center.

License Number	4134281095654
License date	Jun 22, 2017
Licensed Content Publisher	Springer
Licensed Content Publication	Cell and Tissue Research
Licensed Content Title	Synaptic glomeruli in the olfactory system of a snail, Achatina fulica
Licensed Content Author	Ronald Chase
Licensed Content Date	Jan 1, 1986
Licensed Content Volume	246
Licensed Content Issue	3
Type of Use	Thesis/Dissertation
Portion	Figures/tables/illustrations
Number of figures/tables/illustrations	1
Author of this Springer article	No
Order reference number	
Original figure numbers	Figure 1
Title of your thesis / dissertation	The Olfactory System of the Embryonic Common Cuttlefish, Sepia officinalis (Linnaeus, 1758)
Expected completion date	Aug 2017
Estimated size(pages)	150
Requestor Location	Ms. Alexia Scaros 5850 College Street PO BOX 15000 Halifax, NS B3H 4R2 Canada Attn: Ms. Alexia Scaros
Billing Type	Invoice
Billing Address	Ms. Alexia Scaros 5850 College Street PO BOX 15000 Halifax, NS B3H 4R2 Canada Attn: Ms. Alexia Scaros
Total	0.00 CAD
Terms and Conditions	

Introduction

The publisher for this copyrighted material is Springer. By clicking "accept" in connection with completing this licensing transaction, you agree that the following terms and conditions apply to this transaction (along with the Billing and Payment terms and conditions established by Copyright Clearance Center, Inc. ("CCC"), at the time that you opened your Rightslink account and that are available at any time at http://myaccount.copyright.com).

Limited License

With reference to your request to reuse material on which Springer controls the copyright, permission is granted for the use indicated in your enquiry under the following conditions:

- Licenses are for one-time use only with a maximum distribution equal to the number stated in your request.
- Springer material represents original material which does not carry references to other sources. If the material in question appears with a credit to another source, this permission is not valid and authorization has to be obtained from the original copyright holder.
- This permission
• is non-exclusive
• is only valid if no personal rights, trademarks, or competitive products are infringed.
• explicitly excludes the right for derivatives.
- Springer does not supply original artwork or content.
- According to the format which you have selected, the following conditions apply accordingly:
• **Print and Electronic:** This License include use in electronic form provided it is password protected, on intranet, or CD-Rom/DVD or E-book/E-journal. It may not be republished in electronic open access.
• **Print:** This License excludes use in electronic form.
• **Electronic:** This License only pertains to use in electronic form provided it is password protected, on intranet, or CD-Rom/DVD or E-book/E-journal. It may not be republished in electronic open access.

For any electronic use not mentioned, please contact Springer at permissions.springer@spi-global.com.

- Although Springer controls the copyright to the material and is entitled to negotiate on rights, this license is only valid subject to courtesy information to the author (address is given in the article/chapter).
- If you are an STM Signatory or your work will be published by an STM Signatory and you are requesting to reuse figures/tables/illustrations or single text extracts, permission is granted according to STM Permissions Guidelines: http://www.stm-assoc.org/permissions-guidelines/

For any electronic use not mentioned in the Guidelines, please contact Springer at permissions.springer@spi-global.com. If you request to reuse more content than stipulated in the STM Permissions Guidelines, you will be charged a permission fee for the excess content.

Permission is valid upon payment of the fee as indicated in the licensing process. If permission is granted free of charge on this occasion, that does not prejudice any rights we might have to charge for reproduction of our copyrighted material in the future.

-If your request is for reuse in a Thesis, permission is granted free of charge under the following conditions:

This license is valid for one-time use only for the purpose of defending your thesis and with a maximum of 100 extra copies in paper. If the thesis is going to be published, permission needs to be reobtained.

- includes use in an electronic form, provided it is an author-created version of the thesis on his/her own website and his/her university's repository, including UMI (according to the definition on the Sherpa website: http://www.sherpa.ac.uk/romeo/);
- is subject to courtesy information to the co-author or corresponding author.

Geographic Rights: Scope
Licenses may be exercised anywhere in the world.
Altering/Modifying Material: Not Permitted
Figures, tables, and illustrations may be altered minimally to serve your work. You may not alter or modify text in any manner. Abbreviations, additions, deletions and/or any other alterations shall be made only with prior written authorization of the author(s).
Reservation of Rights
Springer reserves all rights not specifically granted in the combination of (i) the license details provided by you and accepted in the course of this licensing transaction and (ii) these terms and conditions and (iii) CCC's Billing and Payment terms and conditions.
License Contingent on Payment
While you may exercise the rights licensed immediately upon issuance of the license at the end of the licensing process for the transaction, provided that you have disclosed complete and accurate details of your proposed use, no license is finally effective unless and until full payment is received from you (either by Springer or by CCC) as provided in CCC's Billing and Payment terms and conditions. If full payment is not received by the date due, then any license preliminarily granted shall be deemed automatically revoked and shall be void as if never granted. Further, in the event that you breach any of these terms and conditions or any of CCC's Billing and Payment terms and conditions, the license is automatically revoked and shall be void as if never granted. Use of materials as described in a revoked license, as well as any use of the materials beyond the scope of an unrevoked license, may constitute copyright infringement and Springer reserves the right to take any and all action to protect its copyright in the materials.
Copyright Notice: Disclaimer
You must include the following copyright and permission notice in connection with any reproduction of the licensed material:
"Springer book/journal title, chapter/article title, volume, year of publication, page, name(s) of author(s), (original copyright notice as given in the publication in which the material was originally published) "With permission of Springer"
In case of use of a graph or illustration, the caption of the graph or illustration must be included, as it is indicated in the original publication.
Warranties: None
Springer makes no representations or warranties with respect to the licensed material and adopts on its own behalf the limitations and disclaimers established by CCC on its behalf in its Billing and Payment terms and conditions for this licensing transaction.
Indemnity
You hereby indemnify and agree to hold harmless Springer and CCC, and their respective officers, directors, employees and agents, from and against any and all claims arising out of your use of the licensed material other than as specifically authorized pursuant to this license.
No Transfer of License
This license is personal to you and may not be sublicensed, assigned, or transferred by you without Springer's written permission.
No Amendment Except in Writing
This license may not be amended except in a writing signed by both parties (or, in the case of Springer, by CCC on Springer's behalf).
Objection to Contrary Terms
Springer hereby objects to any terms contained in any purchase order, acknowledgment, check endorsement or other writing prepared by you, which terms are inconsistent with these terms and conditions or CCC's Billing and Payment terms and conditions. These terms and conditions, together with CCC's Billing and Payment terms and conditions (which are incorporated herein), comprise the entire agreement between you and Springer (and CCC) concerning this licensing transaction. In the event of any conflict between your obligations

established by these terms and conditions and those established by CCC's Billing and Payment terms and conditions, these terms and conditions shall control.

Jurisdiction

All disputes that may arise in connection with this present License, or the breach thereof, shall be settled exclusively by arbitration, to be held in the Federal Republic of Germany, in accordance with German law.

Other conditions:

V 12AUG2015